AD-A134 843 VARIABLE AREA EJECTOR-DIFFUSER MODEL TESTS(U) NAVAL POSTGRADUATE SCHOOL MONTEREY CA T H WALSH SEP 83 1/2

UNCLASSIFIED F/G 21/5 NL

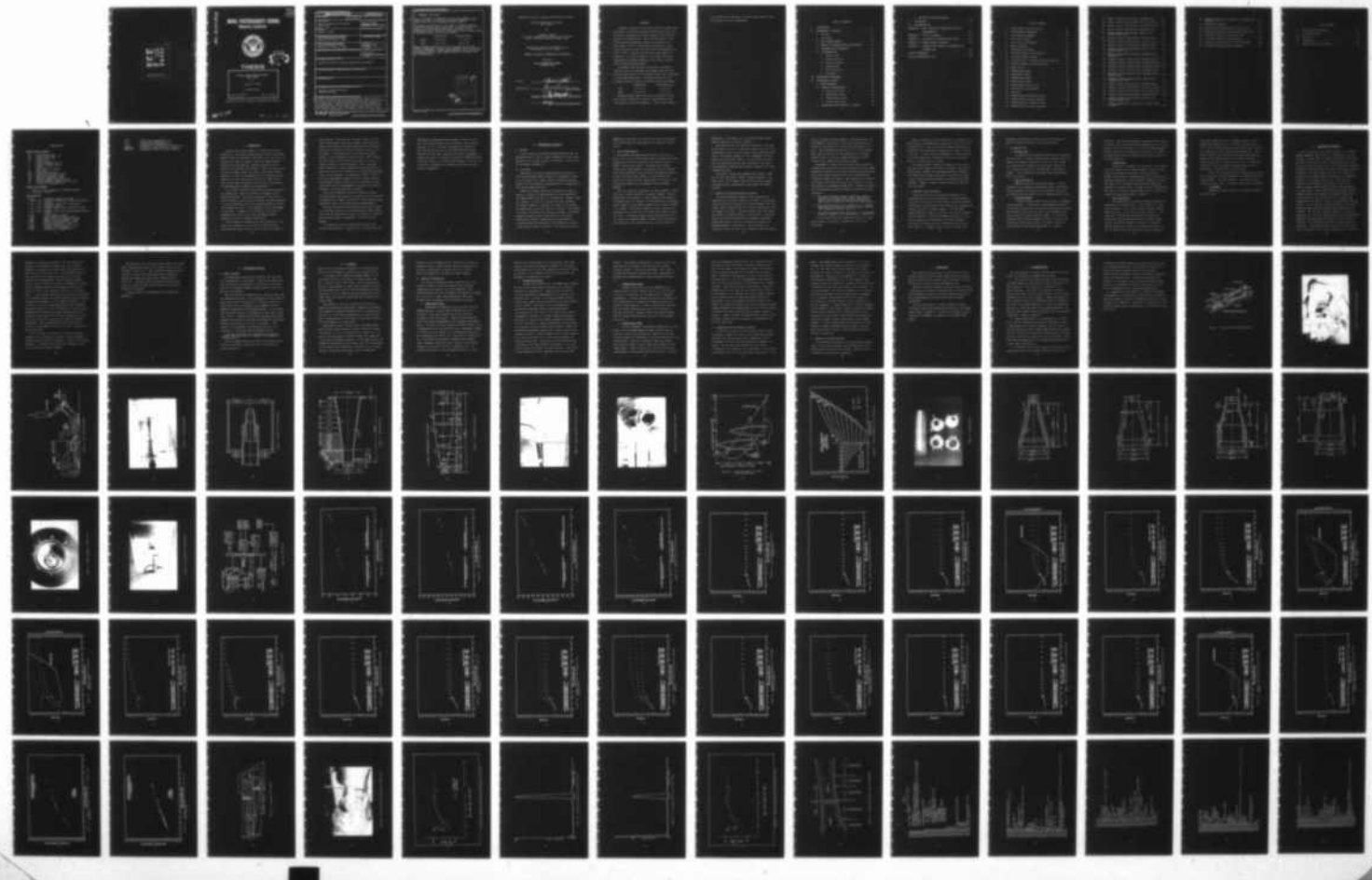

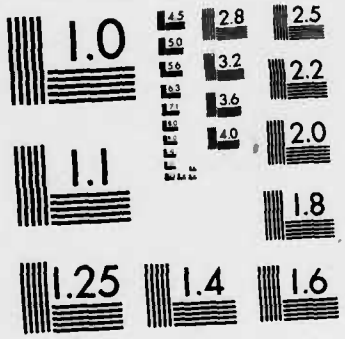

MICROCOPY RESOLUTION TEST CHART
NATIONAL BUREAU OF STANDARDS-1963-A

AD-A134843

(2)

NAVAL POSTGRADUATE SCHOOL
Monterey, California

DTIC
ELECTE
NOV 18 1983
S D
B

THESIS

VARIABLE AREA EJECTOR-DIFFUSER
MODEL TESTS

by

Thomas H. Walsh

September 1983

Thesis Advisor: Paul F. Pucci

Approved for public release; distribution unlimited.

DTIC FILE COPY

83 11 18 063

SECURITY CLASSIFICATION OF THIS PAGE (When Data Entered)

REPORT DOCUMENTATION PAGE		READ INSTRUCTIONS BEFORE COMPLETING FORM
1. REPORT NUMBER	2. GOVT ACCESSION NO. AD-A134843	3. RECIPIENT'S CATALOG NUMBER
4. TITLE (and Subtitle) Variable Area Ejector-Diffuser Model Tests		5. TYPE OF REPORT & PERIOD COVERED Master's Thesis September 1983
		6. PERFORMING ORG. REPORT NUMBER
7. AUTHOR(s) Thomas H. Walsh		8. CONTRACT OR GRANT NUMBER(s)
9. PERFORMING ORGANIZATION NAME AND ADDRESS Naval Postgraduate School Monterey, California 93943		10. PROGRAM ELEMENT, PROJECT, TASK AREA & WORK UNIT NUMBERS
11. CONTROLLING OFFICE NAME AND ADDRESS Naval Postgraduate School Monterey, California 93943		12. REPORT DATE September 1983
		13. NUMBER OF PAGES 121
14. MONITORING AGENCY NAME & ADDRESS(if different from Controlling Office)		15. SECURITY CLASS. (of this report) Unclassified
		15a. DECLASSIFICATION/DOWNGRADING SCHEDULE

16. DISTRIBUTION STATEMENT (of this Report)

Approved for public release; distribution unlimited.

17. DISTRIBUTION STATEMENT (of the abstract entered in Block 20, if different from Report)

18. SUPPLEMENTARY NOTES

19. KEY WORDS (Continue on reverse side if necessary and identify by block number)

Supersonic Ejector-Diffuser
Pressure Recovery

20. ABSTRACT (Continue on reverse side if necessary and identify by block number)

A modular variable area ejector-diffuser was constructed and tested to establish baseline characteristics that could be used for comparison of results obtained from potential geometric reconfiguration. F404 and TF30 engines (afterburning and non-afterburning modes) were modeled with a scale factor of 22.1. The diffuser-ejector had a cylindrical inlet duct (3.47 inch dia.) which transitioned at an L/D of 1.33 to a conical section —> cont'd

DD FORM 1 JAN 73 1473 EDITION OF 1 NOV 65 IS OBSOLETE
S/N 0102-LF-014-6601

SECURITY CLASSIFICATION OF THIS PAGE (When Data Entered)

20. ABSTRACT (Continued)

with a half angle of 8 degrees for an overall length of 24.0 inches, and with a translating centerbody composed of four conical sections with differing included angles.

Performance was evaluated on the basis of pressure recovery across the diffuser with primary mass flow only, and with the injection of 5% secondary mass flow in addition to the primary mass flow. Tests were conducted in the following ranges of pressure recovery across the diffuser.

	Afterburning	Nonafterburning
F404	1.2 to 2.0	1.1 to 1.6
TF30	2.1 to 3.8	1.2 to 2.5

Maximum primary mass flow and total pressure for the F404 without afterburner (smallest engine modeled) were 0.43 lbm/sec. and 2.95 atmospheres. These same parameters for the TF30 with afterburner (largest engine modeled) were 1.74 lbm/sec. and 2.57 atmospheres.

Accession For
NTIS GRA&I
DTIC TAB
Unannounced
Justification
By
Distribution/
Availability Codes
Dist | Avail and/or Special
A-1

DTIC COPY INSPECTED

Approved for public release; distribution unlimited.

Variable Area Ejector-Diffuser Model Tests

by

Thomas H. Walsh
Lieutenant Commander, United States Coast Guard
B.S., California Maritime Academy, 1966

Submitted in partial fulfillment of the
requirements for the degree of

MASTER OF SCIENCE IN MECHANICAL ENGINEERING

from the

NAVAL POSTGRADUATE SCHOOL
September 1983

Author: Thomas H. Walsh

Approved by: James L. Lucas
Thesis Advisor

D. J. Marto
Chairman, Department of Mechanical Engineering

J. M. Dyer
Dean of Science and Engineering

ABSTRACT

A modular variable area ejector-diffuser was constructed and tested to establish baseline characteristics that could be used for comparison of results obtained from potential geometric reconfiguration. F404 and TF30 engines (afterburning and nonafterburning modes) were modeled with a scale factor of 22.1. The diffuser-ejector had a cylindrical inlet duct (3.47 inch dia.) which transitioned at an L/D of 1.33 to a conical section with a half angle of 8 degrees for an overall length of 24.0 inches, and with a translating centerbody composed of four conical sections with differing included angles.

Performance was evaluated on the basis of pressure recovery across the diffuser with primary mass flow only, and with the injection of 5% secondary mass flow in addition to the primary mass flow. Tests were conducted in the following ranges of pressure recovery across the diffuser.

	Afterburning	Nonafterburning
F404	1.2 to 2.0	1.1 to 1.6
TF30	2.1 to 3.8	1.2 to 2.5

Maximum primary mass flow and total pressure for the F404 without afterburner (smallest engine modeled) were 0.43 lbm/sec. and 2.95 atmospheres. These same parameters

for the TF30 with afterburner (largest engine modeled) were 1.74 lbm/sec. and 2.57 atmospheres.

TABLE OF CONTENTS

LIST OF FIGURES

LIST OF TABLES

NOMENCLATURE

English Letter Symbols

AB - Afterburning mode
Ast - Second throat area, in^2
A* - Throat area, in^2
D - Diameter, in
d* - Throat diameter, in
E - Young's Modulus, Lbf/in^2
I - Moment of inertia, in^4
L - Length, in
$\dot{m}$ - Mass Flow rate, Lbm/sec
M - Mass, Lbm
NAB - Nonafterburning mode
Po - Stagnation pressure, Lbf/ft^2
Pcell - Test cell pressure, in H_2O
Pd - Diffuser pressures, in H_2O
Pex - Exhaust chamber pressure, in H_2O
Pt - Total pressure at nozzle inlet, in H_2O
To - Stagnation temperature, °R

Greek Letter Symbols

β - Ratio of throat diameter to entrance diameter
ω - Frequency, rad/sec

Tabulated Data

P ATM - Atmospheric pressure, in Hg
P 01S, P 02S - Secondary; ASME orifice upstream pressure, in H_2O
P 03S, P 04S - Secondary; ASME orifice downstream pressure, in H_2O
P 01P, P 02P - Primary; ASME orifice upstream pressure, in H_2O
P 03P, P 04P - Primary; ASME orifice downstream pressure, in H_2O
P TOT - Total pressure, in H_2O
P TST - Inlet static pressure, in H_2O
P CEL - Engine test cell pressure, in H_2O
P THS - Nozzle entrance pressure, in H_2O
P THT - Nozzle throat pressures, in H_2O
P D - Diffuser pressures, in H_2O
P EXH - Exhaust chamber pressure, in H_2O
T PRI - Primary air temperature, °R
T SEC - Secondary air temperature, °r

T TOT	- Nozzle inlet temperature, °R
T C	- Centerbody temperatures, °R
T D	- Diffuser wall temperatures, °R
C POS	- Centerbody tip position from reference, in
MDOT PRI	- Primary air mass flow rate, Lbm/sec
MDOT SEC	- Secondary air mass flow rate, Lbm/sec

I. INTRODUCTION

Aircraft gas turbine engines are routinely tested in ground level cells under simulated high altitude conditions. High altitude (low pressure) conditions in the test cell are achieved by using air pumps to remove the engine exhaust products and simultaneously maintain the specified low pressure in the engine test chamber. Given the large physical size and power output of today's aircraft gas turbine engines it is easy to comprehend that the construction and operation of this type of test facility is rather costly. One of the largest operational cost factors is the expense of operating the air pumps or air exhausters.

In a typical facility of this type the kinetic energy of the exhaust gas stream is converted to pressure in the diffusion process. This rise in pressure at the inlet to the air exhauster system directly reduces the power required to run the exhausters since the required pressure differential between the inlet to the exhauster and the environment is now lower. A measure of the diffuser's efficiency in performing this task is the ratio of exhaust chamber pressure to test cell pressure (Pex/Pcell).

Copious amounts of research have been conducted in the search for improving the efficiency of these diffusers. Unfortunately, engine tests of this type are not normally a

static process. The test facility must be able to effectively handle power transients, changes in operating mode between afterburning and nonafterburning, and the amount of secondary air injected to effect cooling of the test cell and engine. The maintenance of cell pressure requires removal of the secondary air from the cell. This requires that the diffuser also perform as an ejector, or as it is commonly termed, an ejector-diffuser. Due to the major capital expense of initial construction or modification of these test facilities, flexibility in testing various engine sizes is also necessary. As discussed in Taylor [Ref. 1] the above requirements negate the idea of using a single fixed geometry ejector-diffuser for all engines and conditions and has led to development of variable area ejector-diffusers of the type depicted in Figure 1.

Analytically modeling the entire diffusion process including shocks and mixing in a variable area cross section is mathematically complex and subject to many idealizations. Consequently work in this area has been experiemental.

The major objective of this project was to test a model of an existing variable area ejector-diffuser under laboratory cold flow conditions in order to establish a reference which could be used for comparison of results for new designs.

In conjunction with the design and testing of the ejector-diffuser model, a goal was set of interfacing a new

NPS Mechanical Engineering microcomputer (Digital LSI-11 with tape storage medium) with the Hewlett Packard instrumentation in use at the NPS Turbopropulsion Laboratory. This goal was not met as the new IEEE 488-1975 Standard interface circuit board purchased from Digital Equipment Corporation would not respond to read/write commands and was returned to Digital for repair under warranty. Specifics of work done in attempting to accomplish this goal are contained in Appendix A.

II. EXPERIMENTAL APPARATUS

A. SCALING

A scale factor of 22.139 was determined based upon the characteristics of the air supply compressor and the throat diameter of the largest engine to be modeled. Calculations are included in Appendix B.

B. AIR SUPPLY

Compressed air from the Turbopropulsion Laboratory's (TPL) Allis-Chalmers twelve-stage axial compressor (Figure 2) was utilized in all model testing. Maximum discharge pressure of this machine is approximately 3.0 atmospheres at 15.0 lbm/sec mass flow rate.

Supply and exhaust piping was configured as shown in Figure 3. Primary air and secondary air were supplied to the engine model and test cell, respectively, through 3 inch I.D. piping. A 6 inch I.D. suction line was attached to the exhaust chamber to simulate the effect of the exhaust air pumps used in the full scale test facility. For greater efficiency in adjusting the primary, secondary, and exhaust pressure throttle valves, three Fisher Co. 9-15 PSIG, differential pressure transmitters were purchased and installed inside TPL building No. 215 immediately adjacent to the pressure scanner controller. The installation of an

ASME-type orifice [Ref. 2] in each of the two 3 inch supply lines facilitated the calculation of air mass flow coefficients.

C. TEST SYSTEM MODULES

This project was conducted concurrently with one by Molloy [Ref. 3] with each project based on separate existing geometries installed at the Naval Air Propulsion Center (NAPC), Trenton, New Jersey. A variable area ejector-diffuser was investigated in this project while a straight tube ejector-diffuser with variations was studied by Molloy. As the two projects were similar, it was decided that a single test system would be constructed to be shared by the two projects simply by interchanging ejector-diffuser modules.

The test system was comprised of 3 major modules: engine test cell, ejector-diffuser, and exhaust chamber. Figure 4 shows these three modules in their assembled configuration. The engine test cell (Figure 5), was constructed of aluminum, with a nominal 12 inch inside diameter and an overall length of 15 inches. The exhaust chamber was also constructed of aluminum with a 3 foot by 3 foot cross section and a length of 4 feet. A removable rubber gasketed plexiglass cover on the side of the exhaust chamber allowed visual monitoring of the centerbody drive mechanism as well as easy access for

adjustments. The engine test cell with attendant engine support assemblies is shown in Figure 5.

The foundation for the modules was slotted at the base of the engine test cell to allow the engine test cell to be clamped down at any of a wide range of axial positions relative to the exhaust chamber so as to accommodate various length ejector-diffuser models. As the primary and secondary PVC piping was made up with couplings it was easily reconfigured by substituting different lengths of the lower straight sections.

The exhaust chamber was assembled with machine screws and silicone caulking to ensure airtight integrity. All other joints on the engine test cell and ejector diffuser were made up with studs and nuts and sealed with rubber O-rings.

D. MODELS OF EJECTOR-DIFFUSER AND ENGINES

The ejector-diffuser (Figure 6) was fabricated of aluminum with an overall length of 24 inches. Its entrance cross section was cylindrical (3.47 inch diameter) for 4.61 inches, thence transitioning to a conical cross section with an 8 degree half-angle. The exit diameter was 8.92 inches. The length to entrance diameter ratio was 6.92. Installed within the ejector-diffuser was an aluminum translating centerbody (Figure 7 and 8) of length 16.46 inches and maximum diameter of 4.29 inches. The centerbody was constructed with a conical tip, followed by three truncated

conical sections with half-angles of 19.80, 10.78, 8.80, and 2.60 degrees, respectively. The third truncated conical section was followed by a 4.31 inch long cylindrical tail-piece. The centerbody was mounted on a 0.75 inch diameter steel shaft which was in turn supported by an aluminum spider (Figure 9) that was clamped between the ejector-diffuser exit flange and the exhaust chamber.

The geometry of the ejector-diffuser with translating centerbody was such that an annular second throat was formed between the surfaces of the ejector-diffuser and centerbody. This second throat became smaller as the centerbody was translated towards the engine. The method used to determine this annular cross sectional area as a function of centerbody position is discussed in Appendix C. Figure 10 depicts the cross sectional area in the ejector-diffuser for three conditions:

a. The ejector-diffuser without centerbody installed, labelled as "diffuser alone" (ABD). The discontinuity on this curve (B) marks the diffuser transition from a cylindrical to a conical cross section.

b. The ejector-diffuser with centerbody at its forwardmost position (as set up for this project), labelled "with centerbody forward" (AB'C'D).

c. The ejector-diffuser with centerbody at its aftermost position, labelled "with centerbody aft" (ABA"B"C"D).

It can be seen from this figure that there is a large step increase in flow area following the tail of the centerbody.

Figure 11 shows this area decreasing to a minimum at the second throat and subsequently expanding to the area at the centerbody tail. Each curve on this figure represents one position of the centerbody, beginning at the axial location of the tip. If the tip of the centerbody is retracted past the ejector-diffuser's cylindrical to conical transition point, no second throat is formed.

Four engine models (Figure 12 through 16) were tested. Two models were based on the TF30 jet engine in the afterburning mode (TF30AB) and nonafterburning mode (TF30NAB). The remaining two models were based on the F404 jet engine in the afterburning made (404AB) and nonafterburning mode (404NAB). Figure 17 shows an engine installed inside the test cell module.

E. CENTERBODY DRIVE MECHANISM

To provide facility in varying the position of the centerbody within the ejector-diffuser, a drive mechanism (Figure 18) utilizing an electric motor, reduction gearing, fine-pitched lead screw and travelling yoke was designed and installed inside the exhaust chamber. The centerbody support shaft was locked to the travelling yoke with double nuts and washers. This drive mechanism provided a 6 inch travel stroke of the centerbody. The drive mechanism controller utilized a ten-turn potentiometer (giving very fine control), a feedback control loop for accurate and

repeatable positioning, and fore and aft limit switches to prevent stalling or burnout of the electric motor.

F. INSTRUMENTATION

1. Pressure Taps

All pressure taps (Figure 6) were sized in accordance with Reference 2. Static pressures were recorded across the primary and secondary metering orifices (for use in mass flow calculations), engine inlet and throat, engine test cell, ejector-diffuser wall (24 locations), and exhaust chamber. Total pressure at the engine inlet was measured with a Kiel probe.

2. Metering Orifices

ASME-type metering orifices with beta = .7 were installed in the primary and secondary lines. After determining discharge coefficients for each engine the orifice was removed from the primary line to reduce pressure losses.

3. Pressure Scanner

A 48 port pressure scanner was utilized in recording system pressures. The pressure scanner measures differential pressure between the selected port and a known reference One pressure scanner port was open to the atmosphere and zeroed against an input reference signal. All other port pressures were referenced against this port, giving a precise gage pressure which became a transducer output for conditioning and subsequent measurement by a digital

voltmeter. Two dedicated pressure transducers were connected in parallel with the tubing from the pressure scanner to the pressure taps for the engine test cell and exhaust chamber. Outputs from these two transducers were fed to two digital voltmeters which allowed continual monitoring of these two critical parameters.

4. Thermocouples

Primary air, secondary air, and engine inlet temperatures were measured with copper-constantan (Type T) thermocouples, utilizing an electronic ice point reference. Primary and secondary air thermocouples were located 6 pipe diameters downstream of their respective ASME-type orifices. The engine inlet thermocouple was installed immediately adjacent to the Kiel probe. Voltages from the thermocouples were input to a Hewlett Packard 3495A Scanner and thence to a Hewlett Packard 3455 Digital Voltmeter.

5. Data Acquisition

An integrated data acquisition system designed and implemented by Geopfarth [Ref. 4] was employed to record fluid properties. The system utilizes a Hewlett Packard 9830A Calculator as the system and bus controller. Also connected to the Hewlett Packard HP-IB interface bus (Figure 19) are the pressure scanner multiplexer which selects the pressure scanner to be used, the HP-3495A Scanner which steps through the thermocouple channels as well as causing the forty-eight port pressure scanner to

step under program control. A computer program (Table I) adapted from Geopfarth [Ref. 4] was modified and executed on the Hewlett Packard 9830A to control the scanner and print out a hard copy of the pressures and temperatures. Atmospheric pressure read from a Wallace and Tiernan gage was manually input when prompted by the computer program. A second manual input for each test point was a voltage level read from a digital voltmeter which was reduced by the program to a tip position of the centerbody.

There were no feasible means of transferring the raw data collected by the above system to the NPS IBM 3033 mainframe computer. The data transfer to the IBM was accomplished by manual input, utilizing a simple Fortran program.

6. Instruments

Appendix D contains a list of pertinent instrument specifications.

III. EXPERIMENTAL PROCEDURE

Prior to each run, a test matrix (Table II) of exhaust chamber pressures versus test cell pressures was laid out in order to ensure that all desired test points were covered and also to ascertain the most time-effective test agenda. To arrive at the first test point, the differential pressure transmitters were utilized to regulate the exhauster eductor and primary air supply valves such that full suction was applied to the exhaust chamber followed by full compressor pressure to the primary supply line. This typically resulted in approximately -100 inches of water on the exhaust chamber and 250 inches of water total pressure at the engine model. While maintaining this minimum exhaust chamber pressure, the compressor atmospheric bypass was closed down until the total pressure at the engine was approximately 400 inches of water. The centerbody was then driven in slowly from the retracted position to the fully-projected position while monitoring the engine test cell pressure. The test cell pressure dropped off, reached a minimum value, and then climbed rapidly after the centerbody passed the optimum point of projection into the ejector-diffuser. The centerbody controller voltage was noted at this point. The centerbody was retracted and then driven back in using very slow, small increments until the point of

minimum cell pressure was reached. The data acquisition program on the HP-9830A calculator was then activated, sampling all pressures and temperatures and printing out a hard copy of the collected data. The centerbody was then fully retracted, the exhaust pressure was set halfway between full and atmospheric, and the process repeated. The full matrix covered the ranges of atmospheric, one-half, and full exhaust pressures and minimum, one-third, two-thirds, and full total pressures delivered to the engine model. In this manner each engine was tested over the range of deliverable pressure and mapped against exhaust pressures ranging from atmospheric to full exhauster capacity. The test points of the above-mentioned matrix were conducted using only primary air with the exception of the last point (maximum total pressure and exhaust pressure) which was repeated six more times with discrete increments of secondary flow injection to determine the effects on ejector performance. The centerbody was retracted and used to search for the optimum location at only one of these secondary test points.

Great care must be exercised in setting the exhaust pressure as it is possible to adjust it above atmospheric pressure rather than below atmospheric, which is the desired condition. A pressure very much above atmospheric would likely rupture the exhaust chamber.

Following the runs, the raw data was entered in the IBM 3033, formatted and printed out in tabular form (one run included in Table III). A data reduction program was then utilized to compute and output mass flows, stagnation pressure and temperature and several pressure ratios (Table IV). Pressure ratios and pressure distributions along the ejector-diffuser were plotted and displayed in Figures 20 through 44.

A prerun checklist was developed and is detailed in Appendix D.

IV. EXPERIMENTAL RESULTS

A. MODEL RESPONSE

The experimental results were obtained from four runs, one corresponding to each engine. Each run was broken down into test points corresponding to a particular total pressure (Pt) and exhaust chamber pressure (Pex) as laid out in the run's test matrix.

Each test point was commenced with a fixed Pt, Pexh, and the centerbody retracted. The centerbody was then driven in slowly while Pcell was monitored. Initially, there was a rapid drop in Pcell, followed by what appeared to be an asymptotic approach to the minimum pressure. If the centerbody was driven in past the optimum point there was a rapid rise in Pcell. Regaining the previous minimum value always required retracting the centerbody approximately halfway and driving it in carefully so as not to overshoot. This behavior is in agreement with Reference 1 which in its discussion of centerbody ejector-diffusers states:

> "...the best performance is obtained for the smallest second throat area that will maintain the minimum cell pressure ratio."

The relationship between the area of the second throat (Ast) and the nozzle throat area (A*) for an adiabatic system is given by:

$$Ast = \frac{A^*}{(Poy/Pox)}$$

where Pox is the stagnation pressure at the nozzle throat and Poy is the stagnation pressure at the second throat.

If the nozzle flow (using the 404NAB) expands to the inlet duct area and is followed by a normal shock, then Ast = .638 A* or Ast = 6.03 in**2. For any discontinuity, such as oblique shocks, for which Poy is greater than Poy for the normal shock, Ast will be correspondingly reduced. Conversely, if Ast is smaller than the predicted Ast for a normal shock, Poy must be higher than that predicted for a normal shock.

This appears to have been borne out in testing the models as the smallest engine model (404NAB) at maximum Pt and minimum Pex achieved minimum Pcell at a centerbody tip position of -4.37 inches corresponding to a second throat area of approximately 5 in**2 which is less than the Ast of 6.03 in**2 based on a normal shock.

Experimental results indicate that the 404NAB engine model had the lowest pressure recovery (Pex/Pcell) across the diffuser of 1.6 at a Pt/Pcell of 6.6 (Figure 20). As such it was considered the baseline engine for comparison on the basis of pressure recovery. At the same Pt/Pcell the 404AB had a Pex/Pcell of 1.85 (Figure 21) for an improvement of 15 percent, the TF30 NAB had a Pex/Pcell of 2.0 (Figure 22) for a 25 percent improvement, and the TF30AB had

Pex/Pcell of 2.65 (Figure 23) for a 65 percent increase in pressure recovery. These results were not unexpected as this test system models an actual test cell at NAPC, which was designed for the TF30 and larger engines.

B. PRESSURE DISTRIBUTIONS

The ratios of diffuser pressure distribution to cell pressure (Pd/Pcell) versus the pressure tap locations normalized with respect to the inlet diameter of the ejector-diffuser (L/D) are as depicted in Figures 24 through 44. An L/D of 1.5 marks the discontinuity where the diffuser wall transitions from cylindrical to conical.

1. 404AB Engine Model

Examination of Figures 24, 25, 26, and 27 for the F404AB indicates a rising trend of Pd/Pcell as Pt is increased. Each figure depicts one Pt and three Pex settings or three test points. Figure 27 shows the flow area distribution superimposed on the pressure distribution ratios. The nearly constant ratios of Pd/Pcell above an L/D of approximately 2.5 are indicative of an unnecessary length of diffuser for this engine, as the diffusion process has been completed by an L/D of 2.5. Test point 17 (Figure 28) for 5% secondary flow behaves as expected with Pd/Pcell lower throughout almost the entire length of the diffuser, compared to test point 12 with no secondary flow. As discussed previously in the procedures section, all test

points with secondary mass flow injected were taken immediately following the maximum Pt, minimum Pex test point. Six secondary test points were sampled and the point having the closest to 5% secondary flow was plotted against the maximum Pt, minimum Pex test point.

2. TF30AB Engine Model

Pressure distributions for the TF30AB model (Figures 29, 30, and 31) again show the expected rising trend of Pd/Pcell for increasing Pt. Figures 30 and 31 show the flow area distribution superimposed on the pressure ratio distributions. As seen by the rising pressure recovery ratios, this engine effectively utilizes the entire length of the diffuser. Test point 5 (one half maximum Pt) indicates an anomalous pressure distribution which is accentuated at test point 6, with test points 7 and 8 (maximum Pt) returning to a normal pressure distribution followed by a return to an unusual pressure distribution curve at test point 9. These discontinuities are believed to be caused by severe oblique shock patterns. Figure 32 shows that 5% secondary flow has only a small effect on the pressure recovery. Limited repeatability is shown (Figure 33) in that test points 9, 10, and 12 show pressure recoveries within 0.2%. Test points 9 and 12 were with the centerbody at the same position (plus/minus 0.1 in.) and the two curves plot almost one atop the other. Test point 10 was conducted with the centerbody driven in one inch

further. The pressure distribution is lower for the first two-thirds of the length of the diffuser but ultimate pressure recovery is essentially the same. This tends to corroborate the earlier finding that Pcell approached its minimum value asymptotically as the centerbody is driven in.

3. TF30NAB Engine Model

Pressure distributions for the TF30NAB with no secondary mass injected (Figures 34, 35, 36, and 37) show a return to the patterns of the 404AB and are otherwise unremarkable. Limited repeatability of the test points for this engine model is illustrated in Figure 38 where the curves for test points 6, 7, and 8 (one-third Pt, one-half Pex) are nearly identical with only 3.3% variation in pressure recoveries. Figure 39 shows the expected slight loss of pressure recovery with injection of 5% secondary mass flow.

4. 404NAB Engine Model

Curves of pressure distribution (Figures 40, 41, 42, and 43) for the 404NAB (smallest model tested) show the diffusion process to be essentially complete by the time the flow reaches the cylindrical to conical transition on the diffuser wall. This is an indication that the variable area ejector-diffuser is much larger than optimum for the engine model. Figure 43 shows the flow area distribution superimposed on the pressure distribution ratios. The fact

that the centerbody required almost full insertion for each test point on this run (Table IV) giving a second throat area of less than 5 in**2 (Figure 11) tends to corroborate that this ejector-diffuser is too large for this engine model. Curves for test points 7, 8, and 9 (two-thirds Pt) and test points 10, 11, and 13 (maximum Pt) show pressure ratios in the conical section of the diffuser with irregular patterns. Since the exit area of this engine (.55 in**2) compared to the inlet area of the diffuser (9.46 in**2) is so much smaller it is believed that this irregular pattern may be caused by the flow shifting radially around the centerbody. Since the pressure taps are located in one radial line along the diffuser wall and the pressure scanner samples pressures at the approximate rate of one per second, a wandering flow path could account for these irregular patterns. Figure 44 shows the characteristic slight loss of pressure recovery with the injection of approximately 5% secondary mass flow.

C. COMPARISON WITH CYLINDRICAL DIFFUSER

As both this project and that of Molloy [Ref. 3] deal with models of NAPC test cells, and the same engine models and model scaling are used in both, comparison of the performance of the two diffuser designs was thought to be useful. The variable area diffuser of this project is compared only to Molloy's full size model of the straight tube diffuser and not to the 5/6 and 2/3 reductions of that

model. The TF30AB engine with a Pt/Pcell of 7.3 in the straight tube diffuser shows a Pex/Pcell of 2.8 (Figure 45). At this same Pt/Pcell the variable area ejector-diffuser indicates a Pex/Pcell of 2.8 also, for no gain in performance. Comparison of the TF30NAB at a Pt/Pcell of 9.6 indicates a Pex/Pcell of 2.5 for the straight tube diffuser (Figure 46) whereas the variable area diffuser had a Pex/Pcell of 2.45, which is slightly less efficient. It is noted, however, that the inlet diameter of the variable area ejector-diffuser was 3.47 inches where the diameter of the straight circular diffuser was 2.71 inches; the efficiencies of the two diffusers cannot, therefore, be strictly compared. A second comparison of the two figures for the TF30AB in the variable area and straight diffusers, respectively, indicates that a higher Pex/Pcell can be attained with the variable area diffuser which equates to attaining a higher altitude (higher Pex) in the exhaust chamber. For this reason and for the flexibility of responding to engine transients rapidly enough to prevent uncontrolled Pcell, the use of the variable area ejector diffuser is warranted.

D. HEATING OF EJECTOR-DIFFUSER

An investigation was made of an extraordinary heating effect on the ejector-diffuser and centerbody which was noted during trial runs of the system. Details of the investigation are contained in Appendix E.

V. CONCLUSIONS

The construction and tests of a variable area ejector-diffuser based on an actual NAPC design have been carried out and data collected indicates that it operates in agreement with the results of past experimental work.

The data collected, reduced, and plotted should provide a baseline for any further work that might be conducted with this apparatus in efforts to study new geometries with an eye to improvement of variable area ejector-diffuser performance.

The best performance in terms of pressure recovery (Pex/Pcell) across the diffuser was achieved by the TF30AB engine model, followed by (in order of decreasing pressure recovery) the TF30NAB, the 404AB, and the 404NAB engine models.

VI. RECOMMENDATIONS

For consideration in further studies evolving from this project the following recommendations are made:

1. The variable area ejector-diffuser with translating centerbody makes the cross sectional area a function of the axial position of the centerbody in relation to the ejector-diffuser. The effect of being able to create a second throat whose area and axial location could be varied independently has not been studied. Design and testing of such a geometry would be a worthwhile project to determine the effect the optimum combination of these two parameters would have on the efficiency of the ejector-diffuser. One possible model geometry which would make these two variables independent is shown in Figure 47.

2. Manual positioning of the centerbody is a tedious affair and the optimum position can be difficult to find. A timed sequence of voltage increments could be output to the centerbody drive motor under program control in conjunction with a dual trace strip chart indicating the centerbody position (function of voltage) and the cell pressure. This would make determination of the optimum centerbody position a much simpler proposition.

3. A stronger electric motor should be installed on the centerbody drive as the drive was unable to retract the

centerbody at maximum engine total pressure during testing of the TF30AB engine model. Retracting the centerbody at these test points required reducing total pressure, retracting the centerbody, and then raising total pressure back to the desired level. Lowering and raising total pressure in this manner results in many unloading-loading cycles on the compressor and must be done slowly so as to keep the compressor within its allowable RPM window.

4. Completion of the project to interface the Digital microcomputer to the HP-IB bus at TPL should be carried out. This would greatly alleviate the manhours required for data transfer to the IBM 3033. The ability to expedite this data transfer process would be beneficial to any projects carried out at TPL.

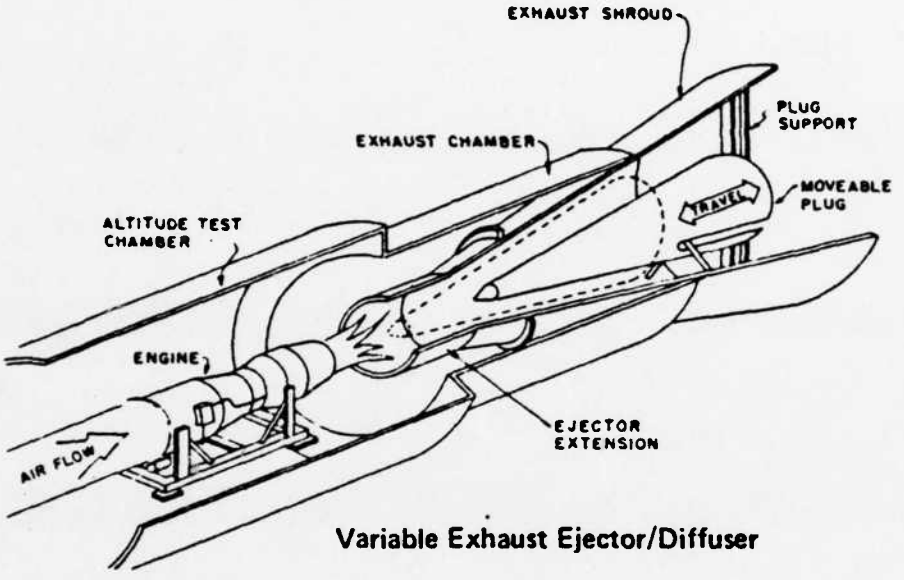

Figure 1. Variable Area Ejector-Diffuser

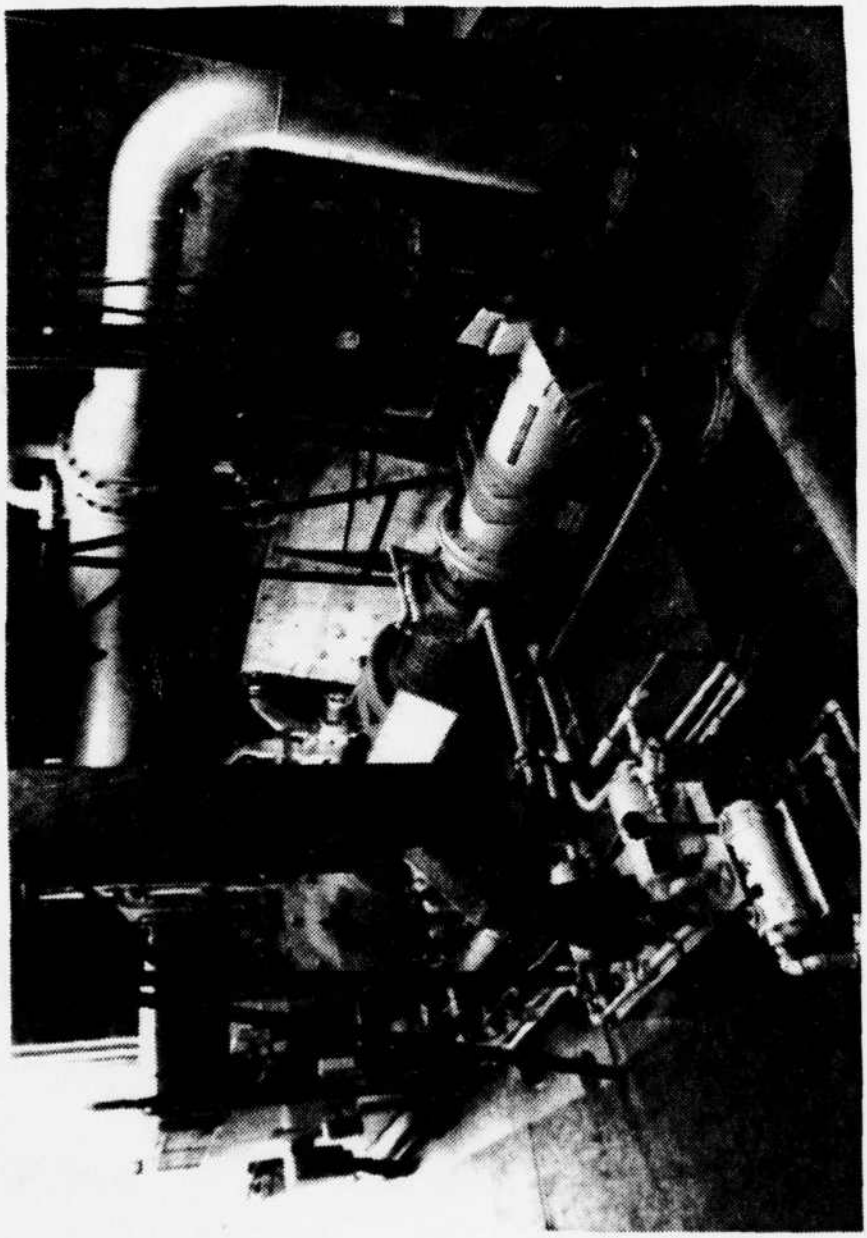

Figure 2. Allis-Chalmers Compressor

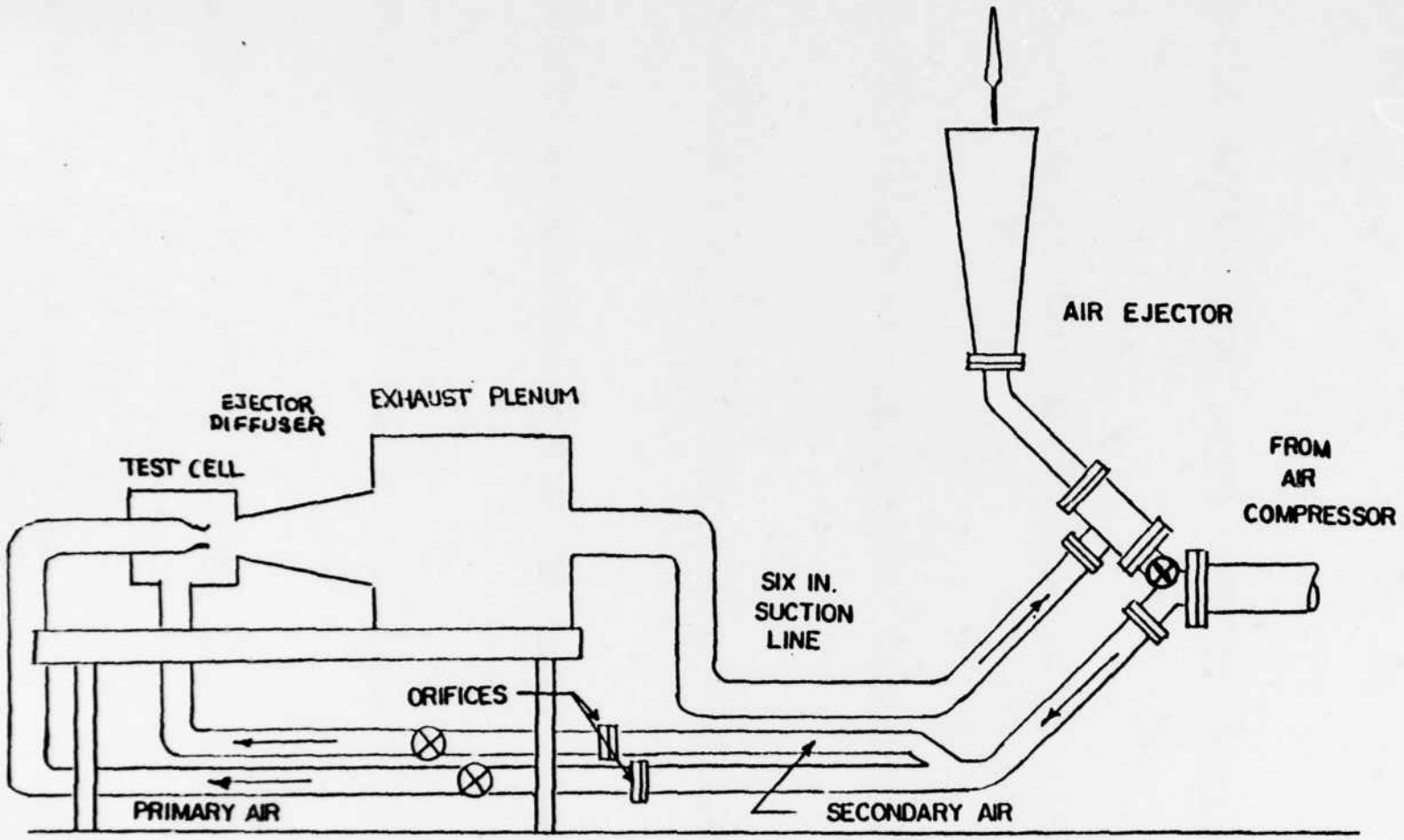

Figure 3. Test System Arrangement

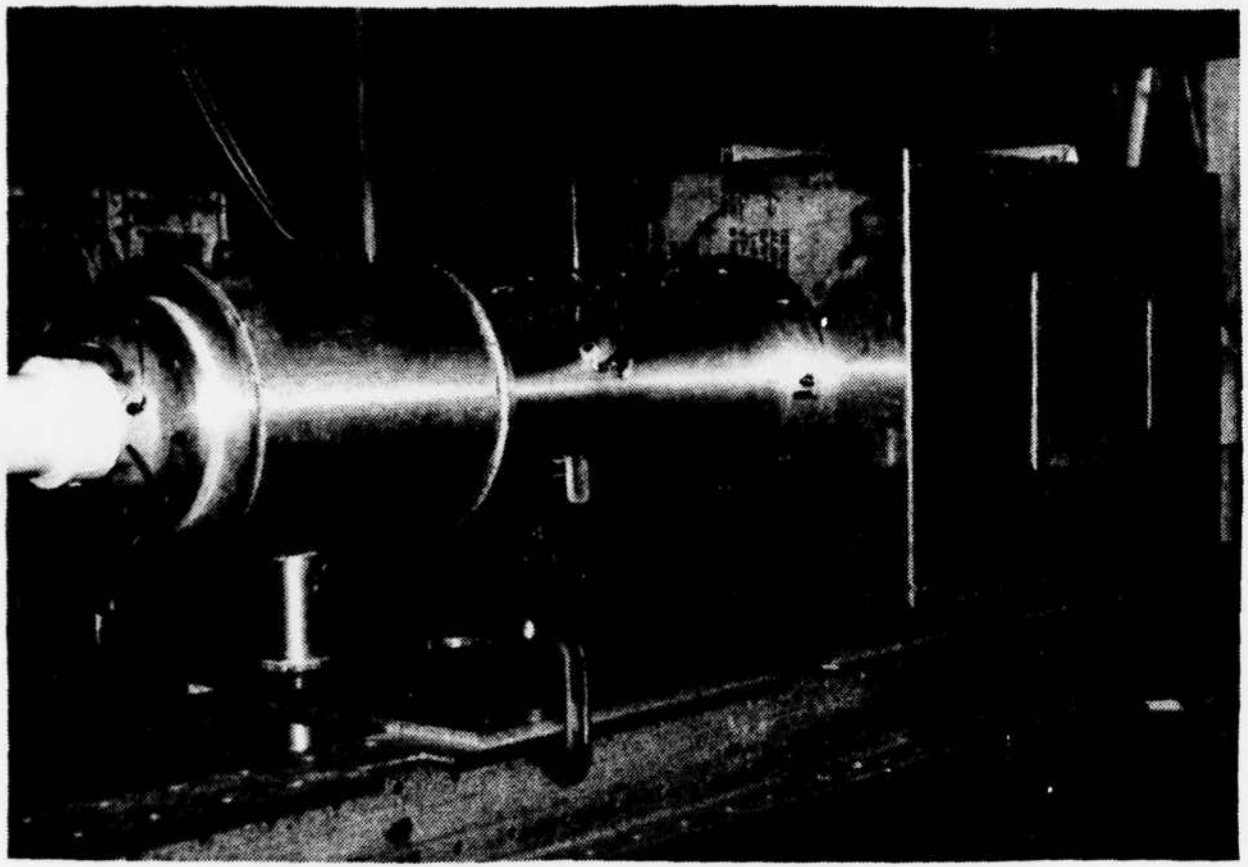

Figure 4. Test System Modules

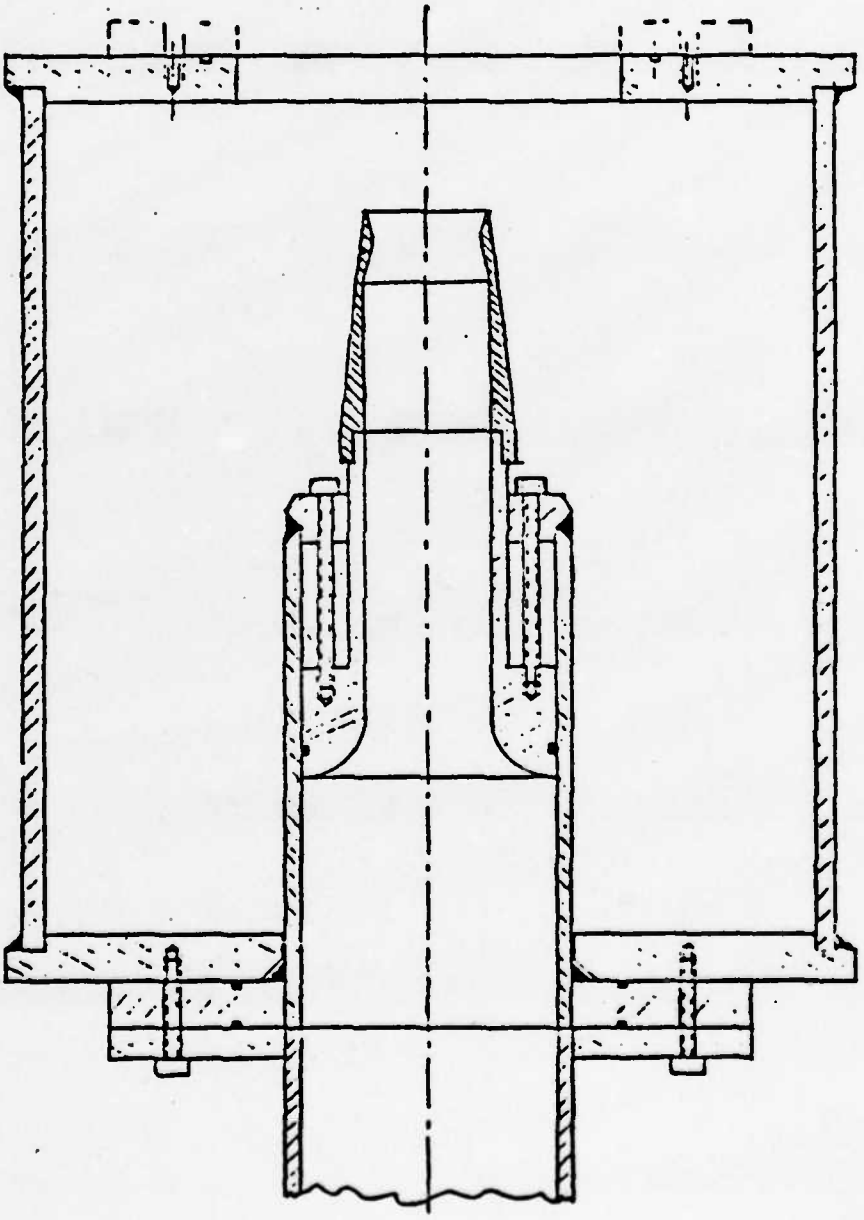

Figure 5. Engine Test Cell Assembly

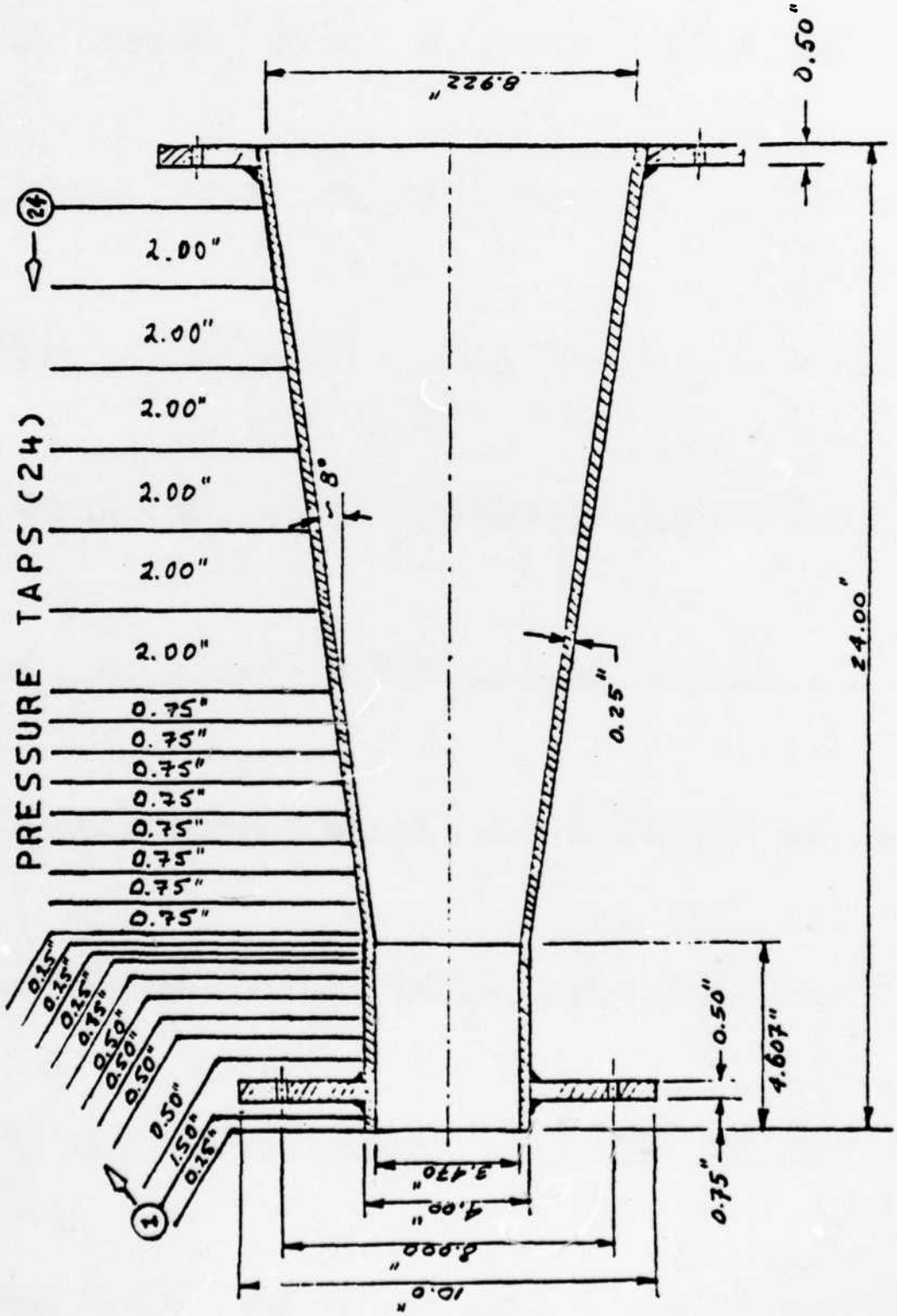

Figure 6. Ejector-Diffuser

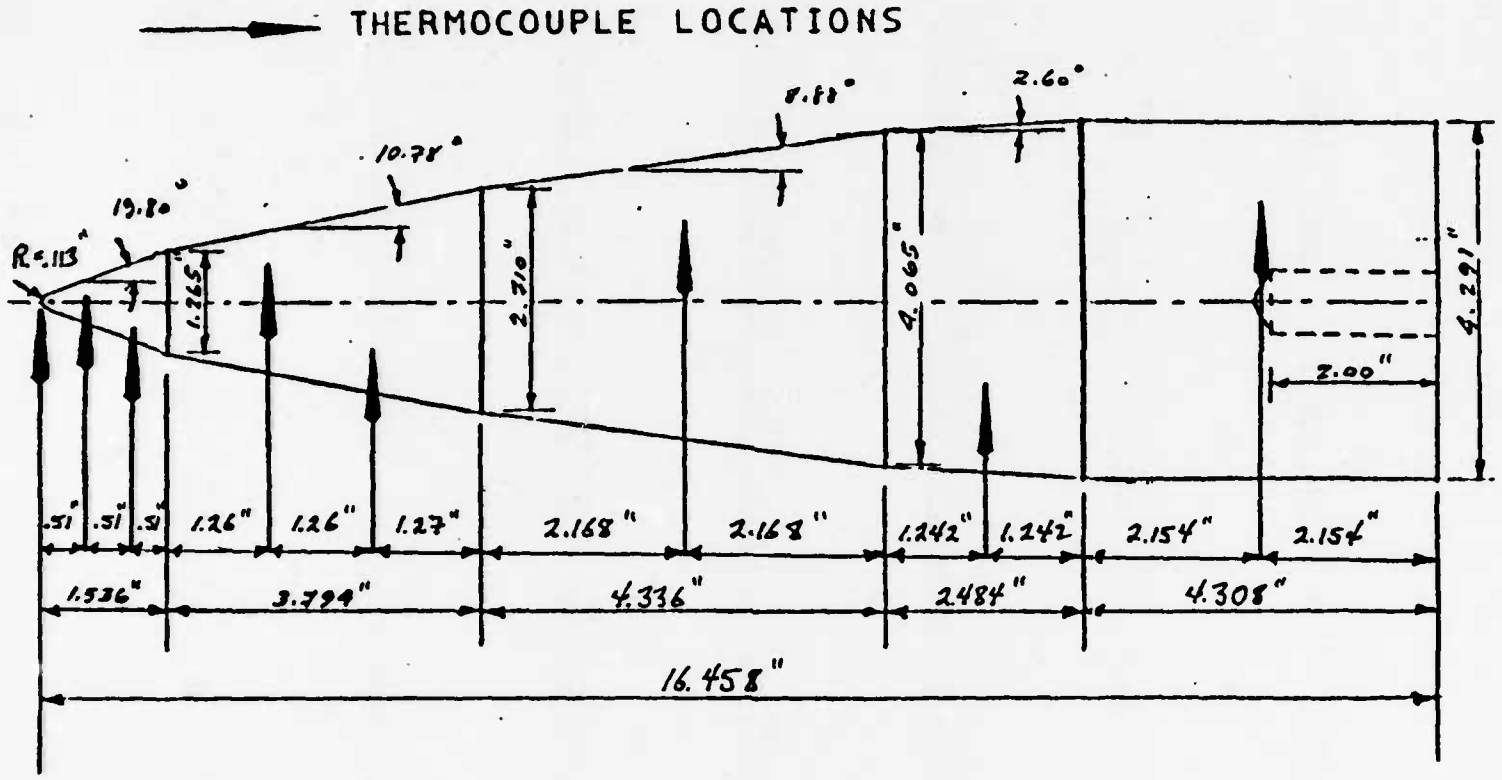

Figure 7. Translating Centerbody

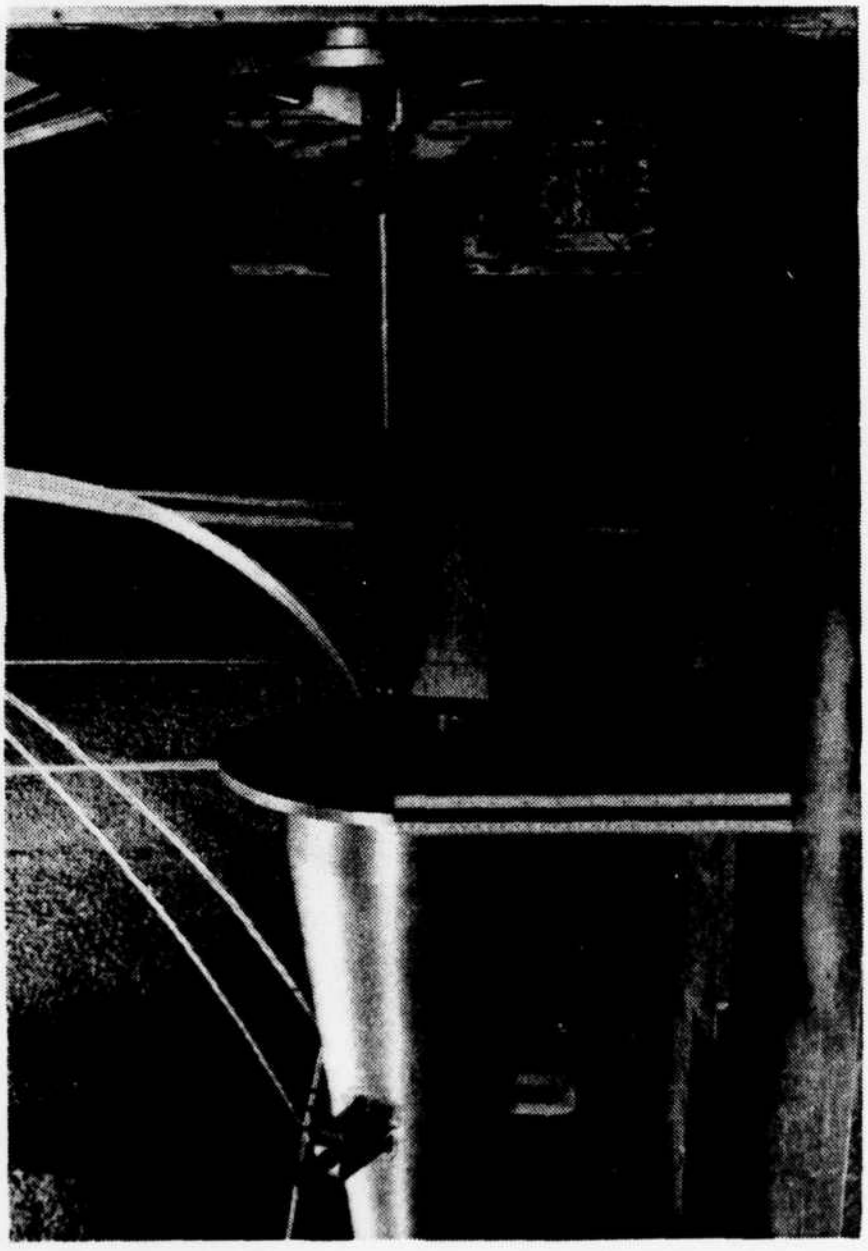

Figure 8. Ejector-Diffuser with Centerbody

Figure 9. Centerbody Support Spider

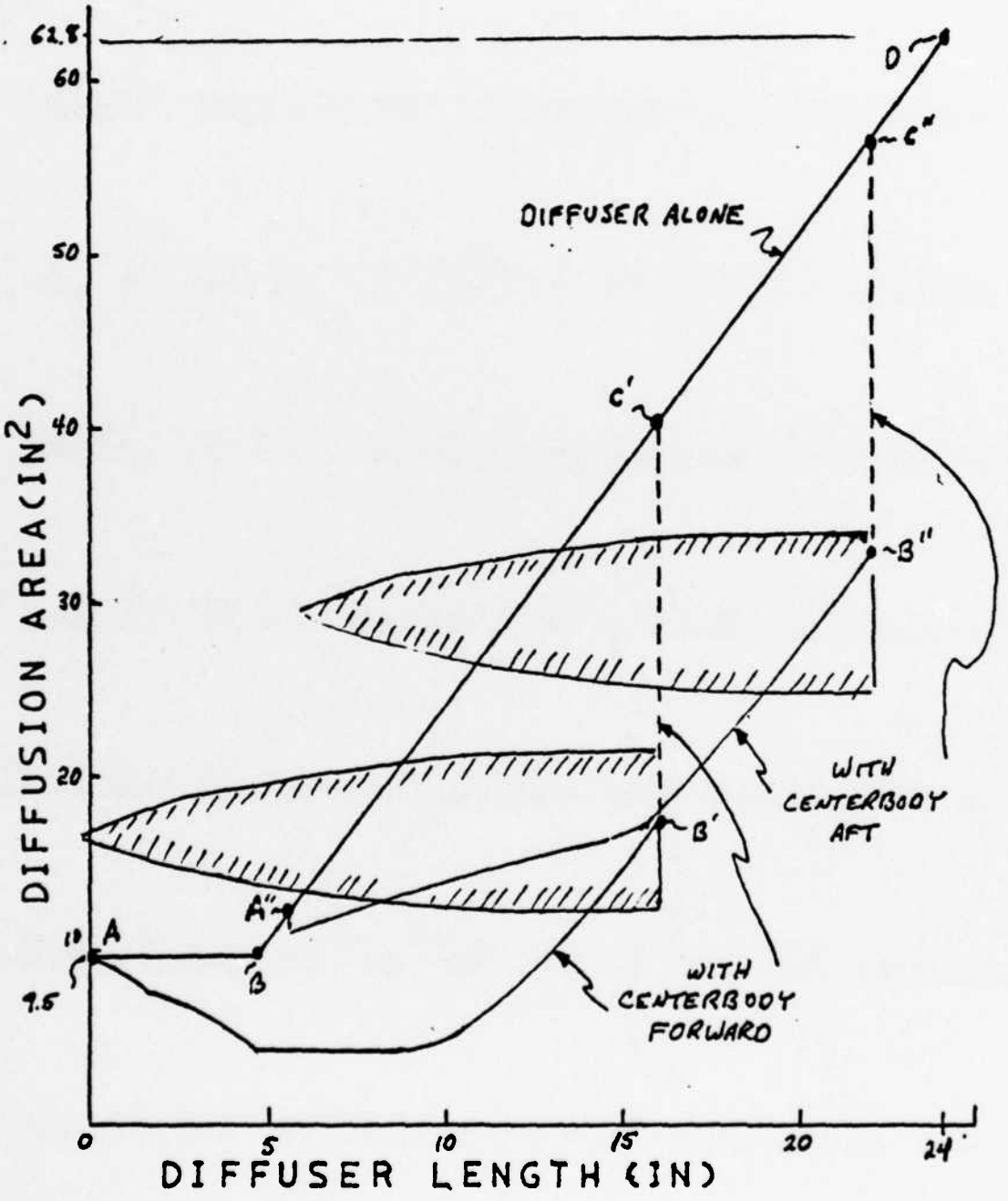

Figure 10. Limiting Cases of Diffuser Area Distributions

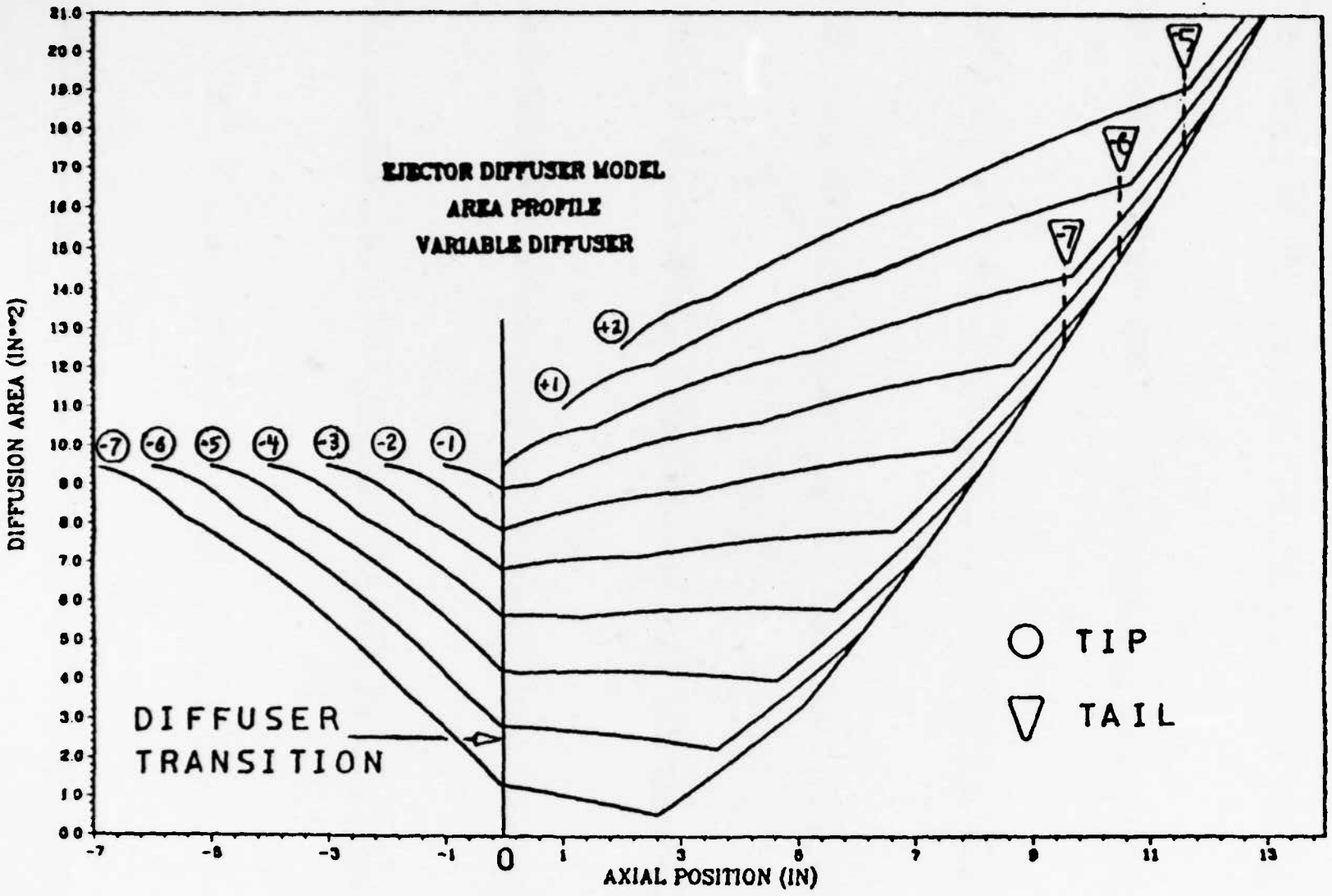

Figure 11. Ejector-Diffuser Area Distributions

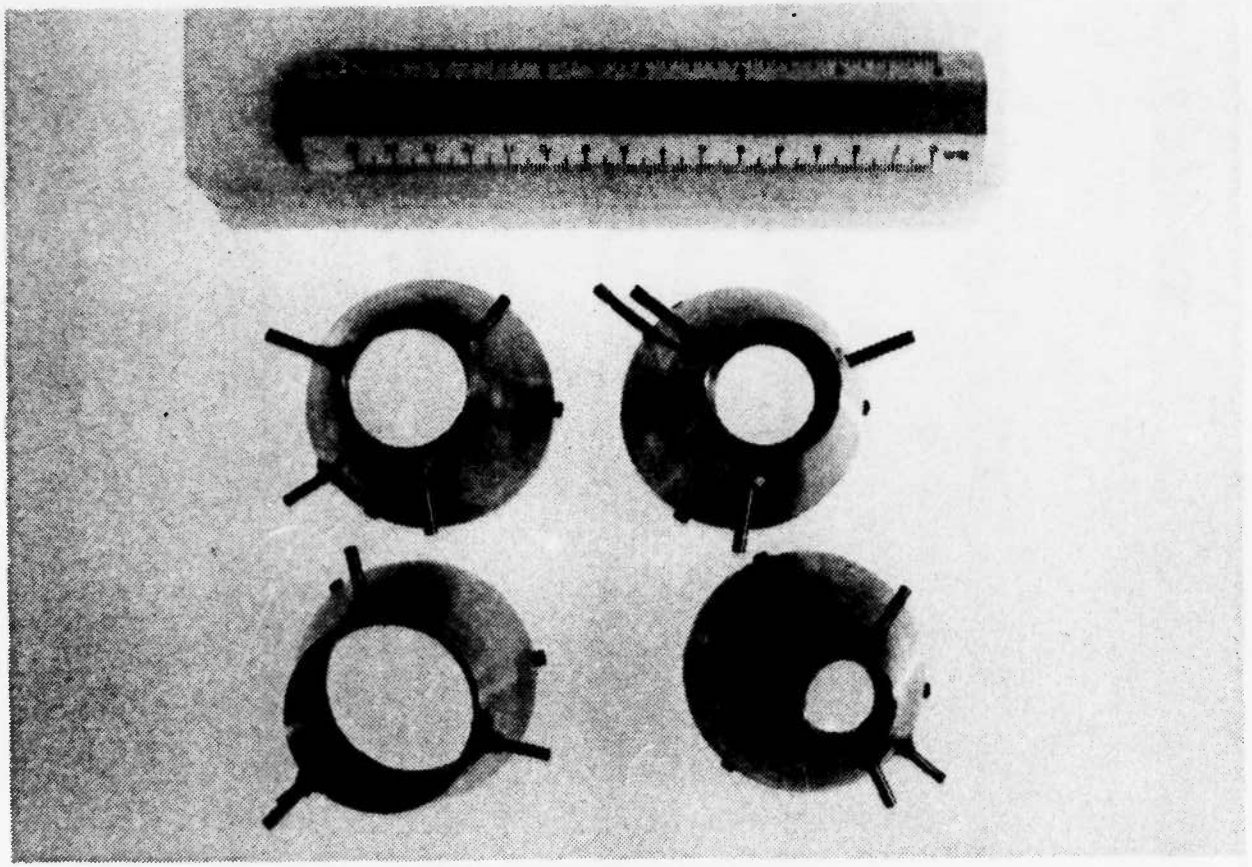

Figure 12. Engine Models

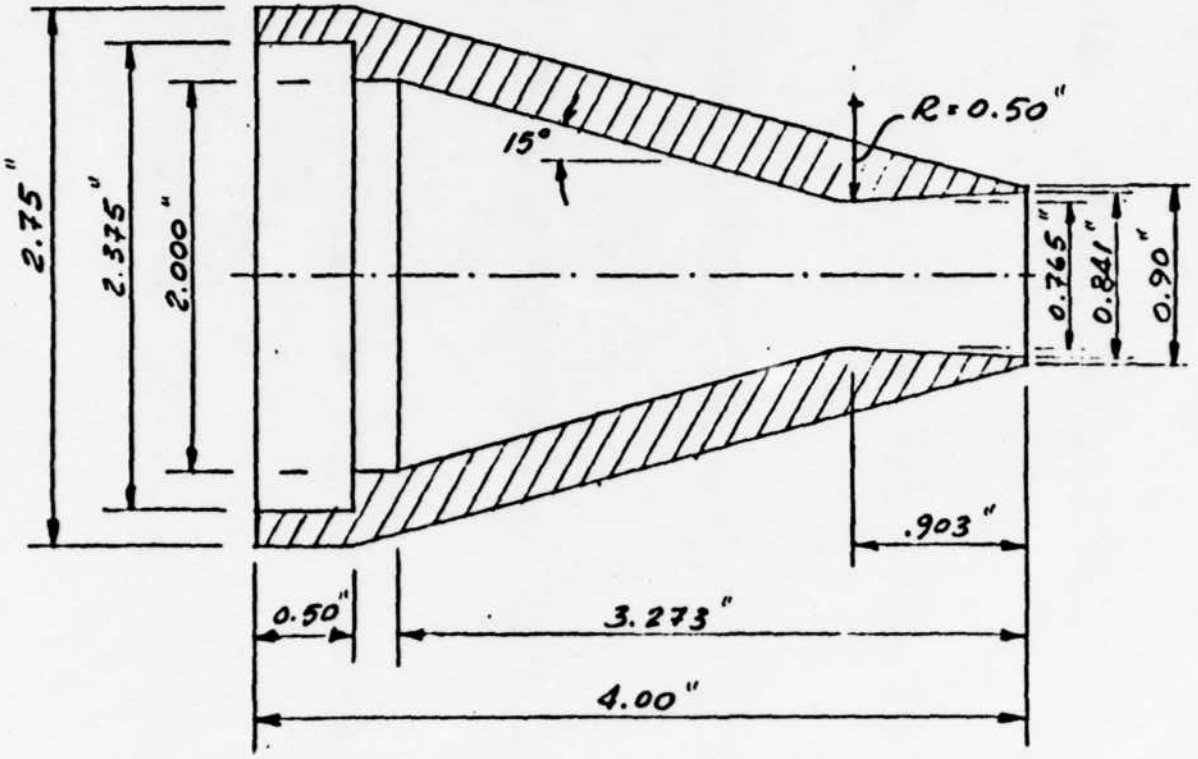

Figure 13. 404NAB Engine Model

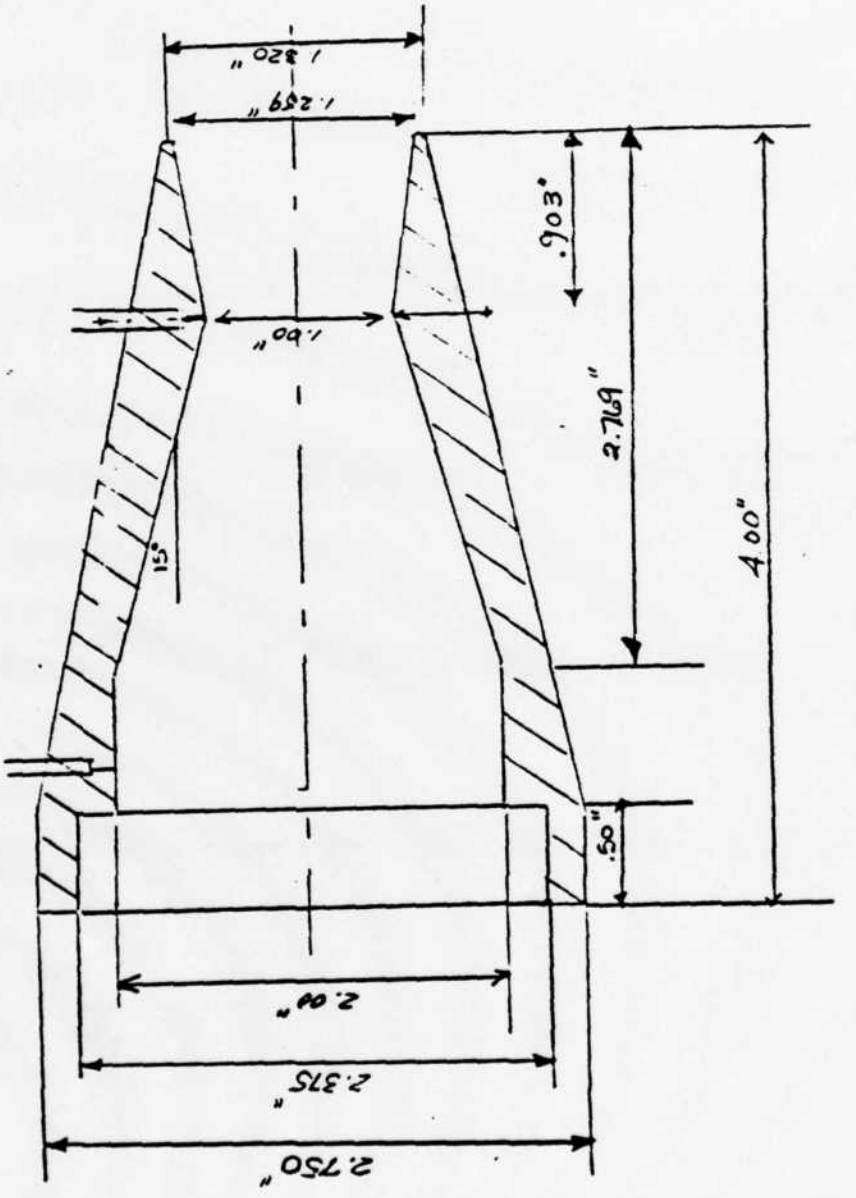

Figure 14. 404AB Engine Model

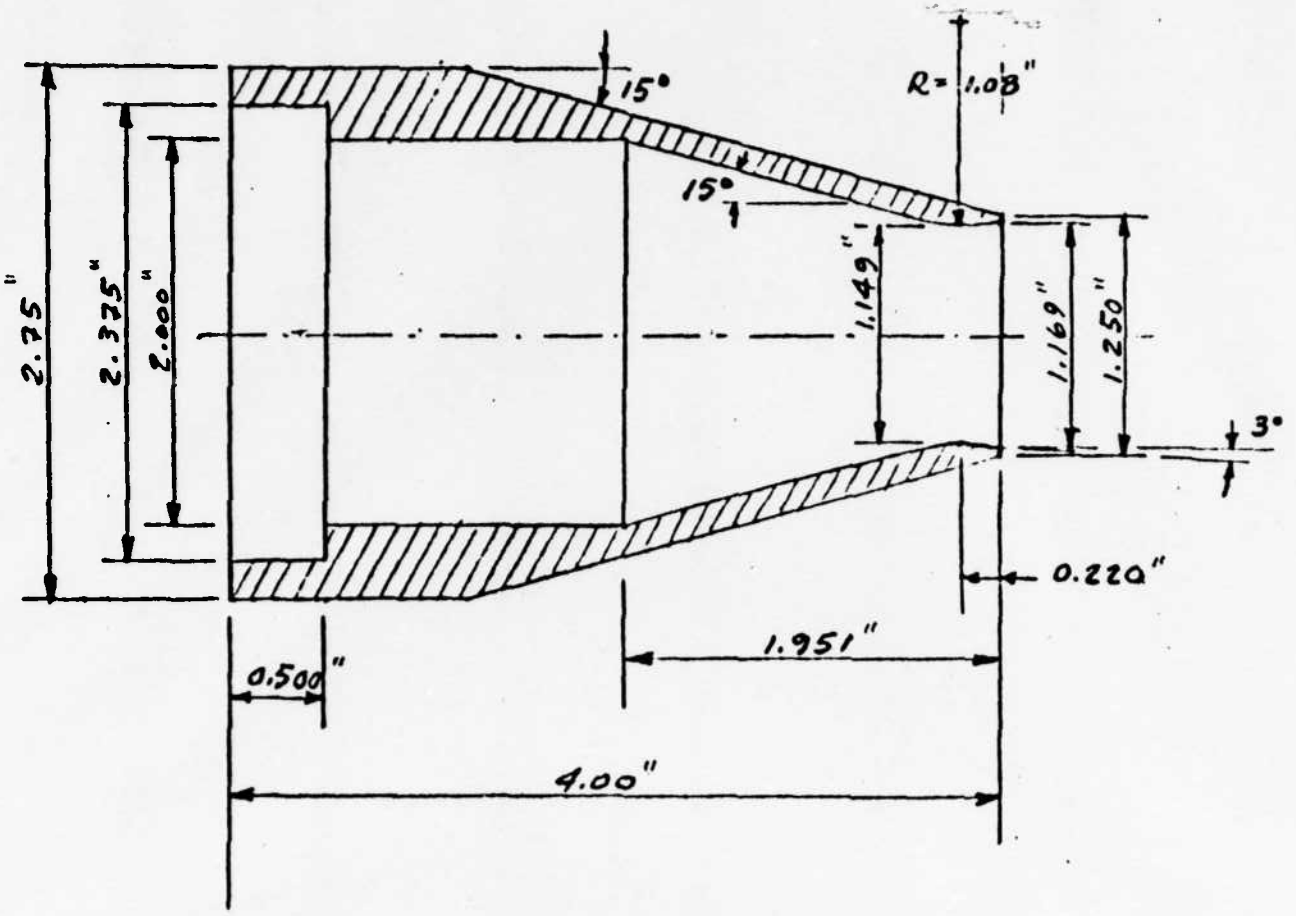

Figure 15. TF30NAB Engine Model

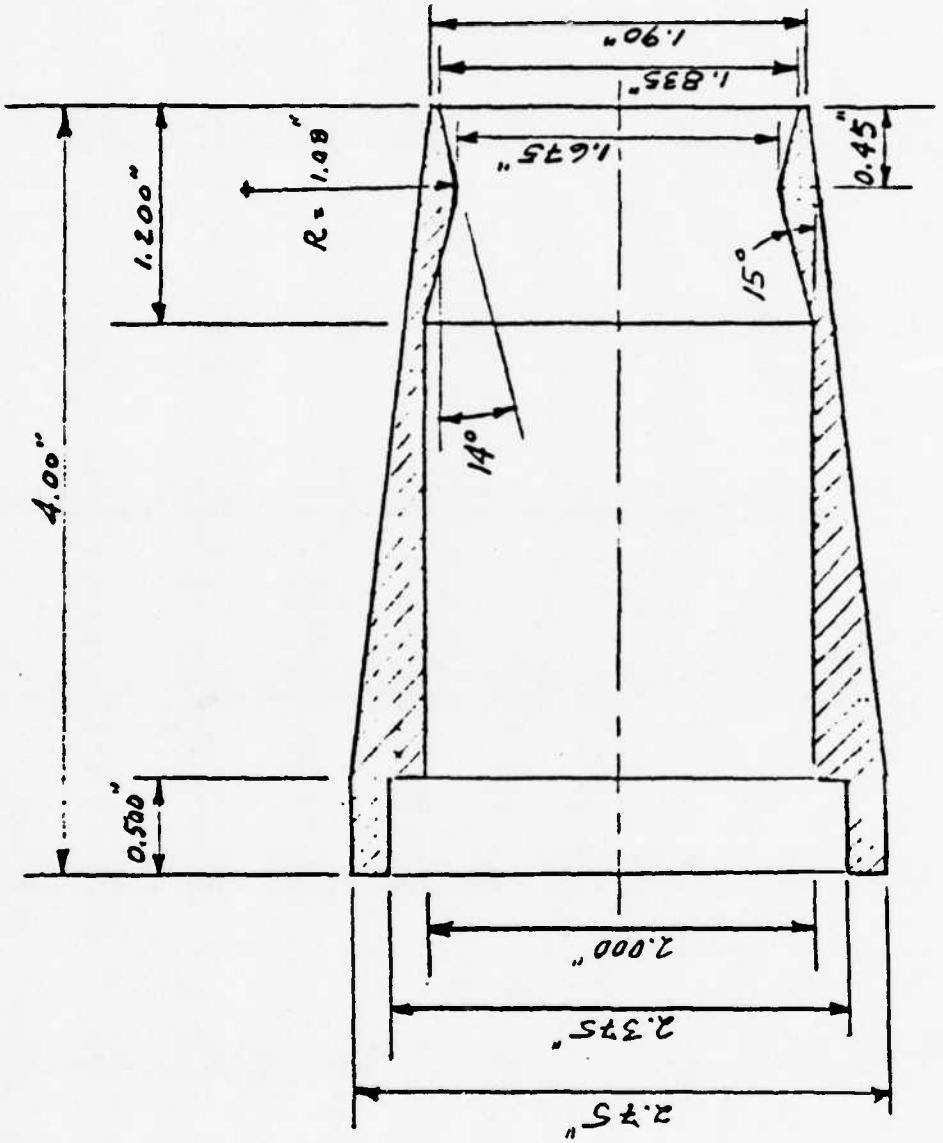

Figure 16. TF30AB Engine Model

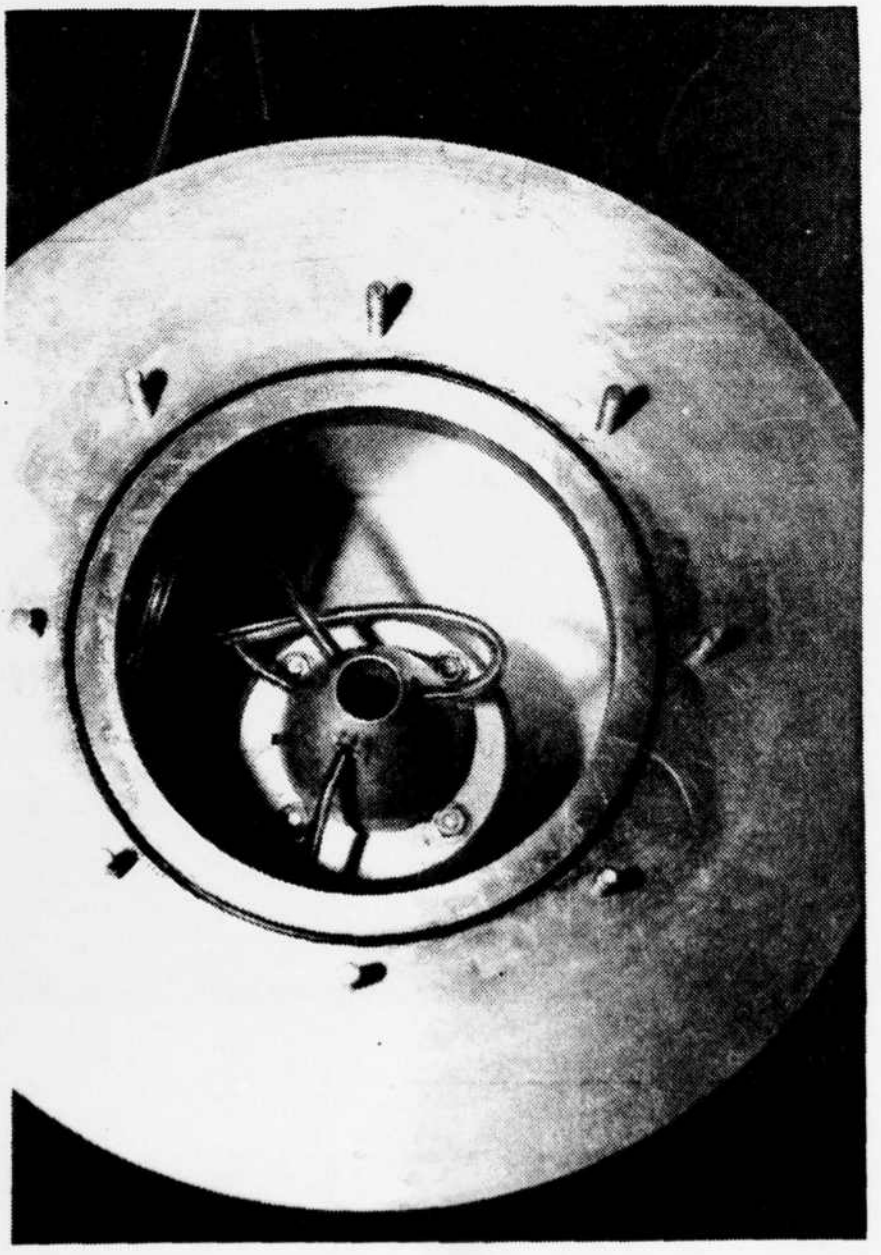

Figure 17. Engine Mounted in Test Cell

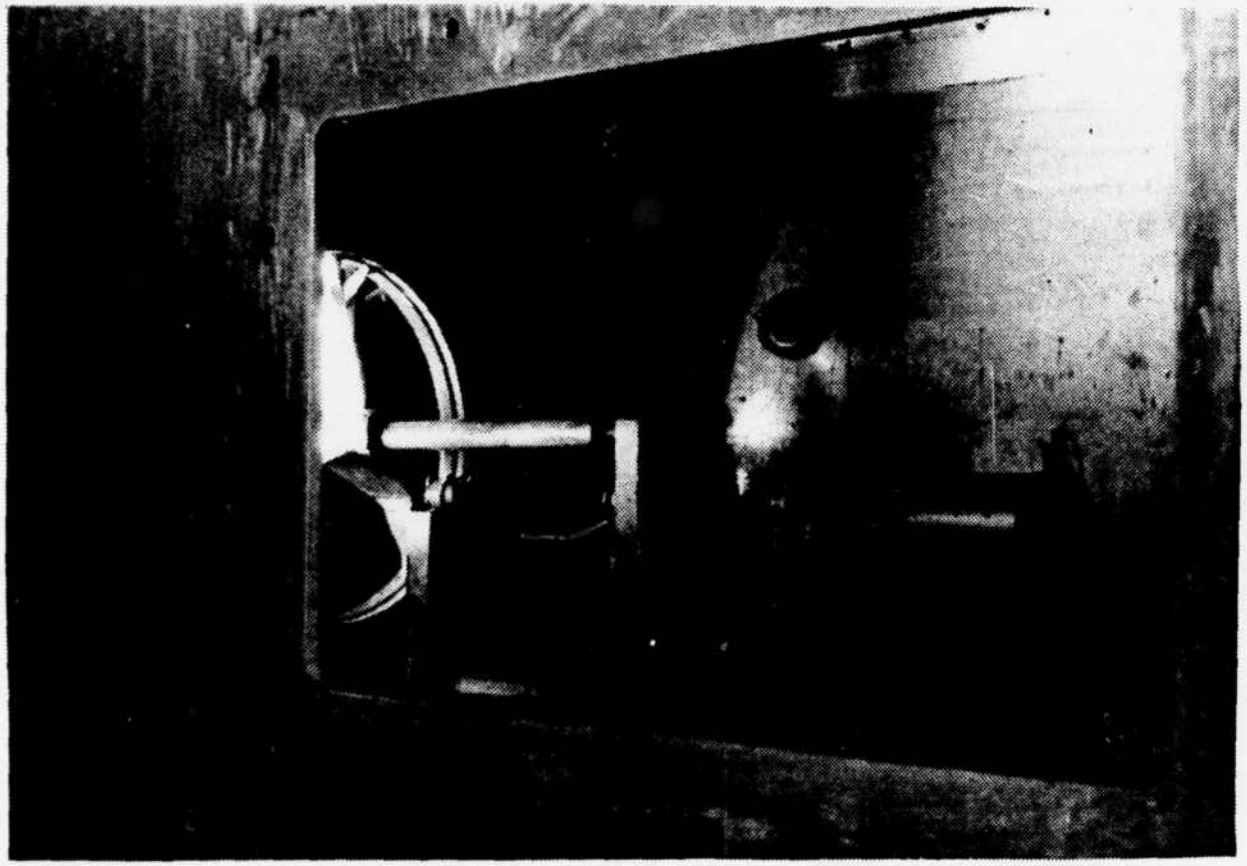

Figure 18. Centerbody Drive Mechanism

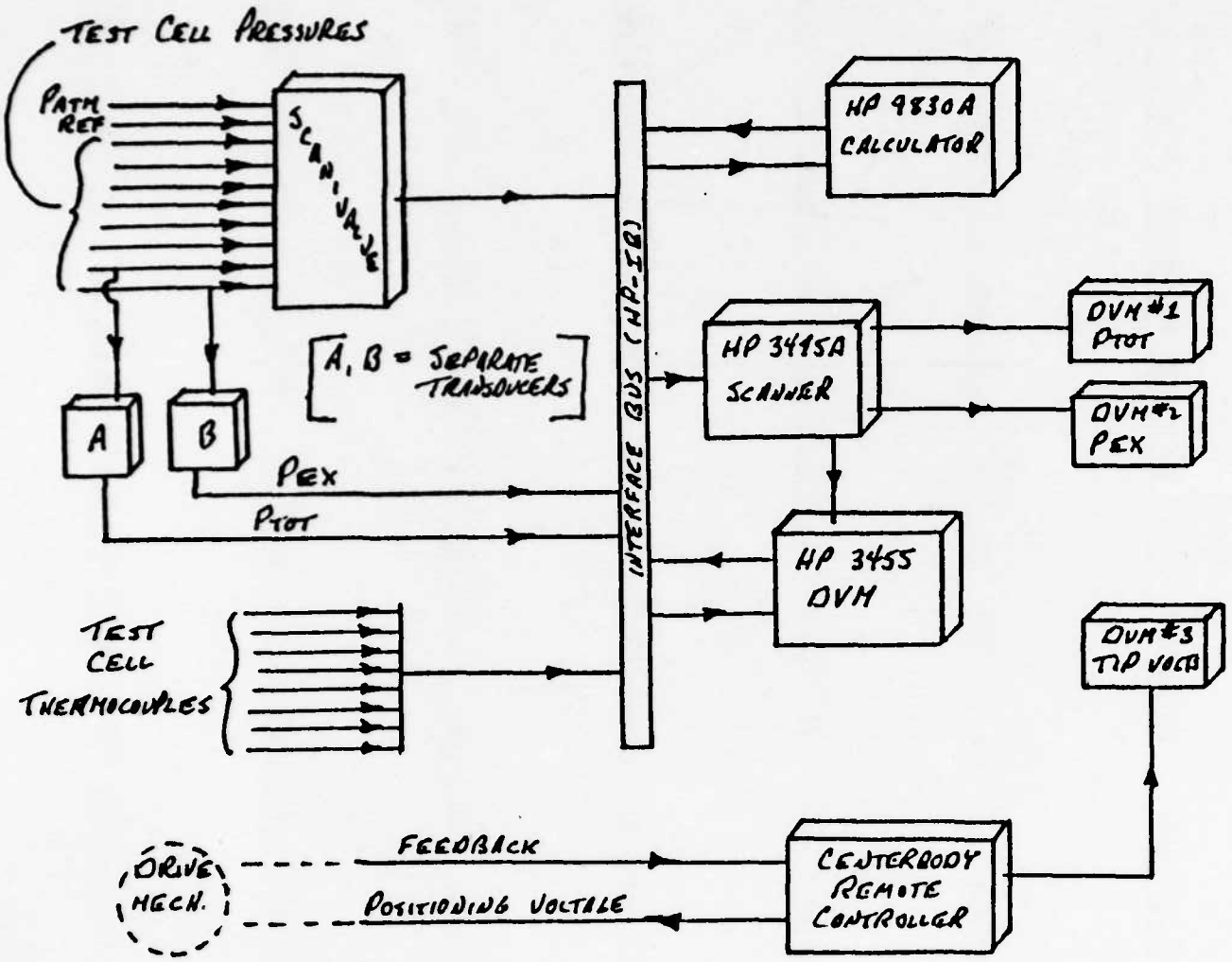

Figure 19. HP-IB Bus

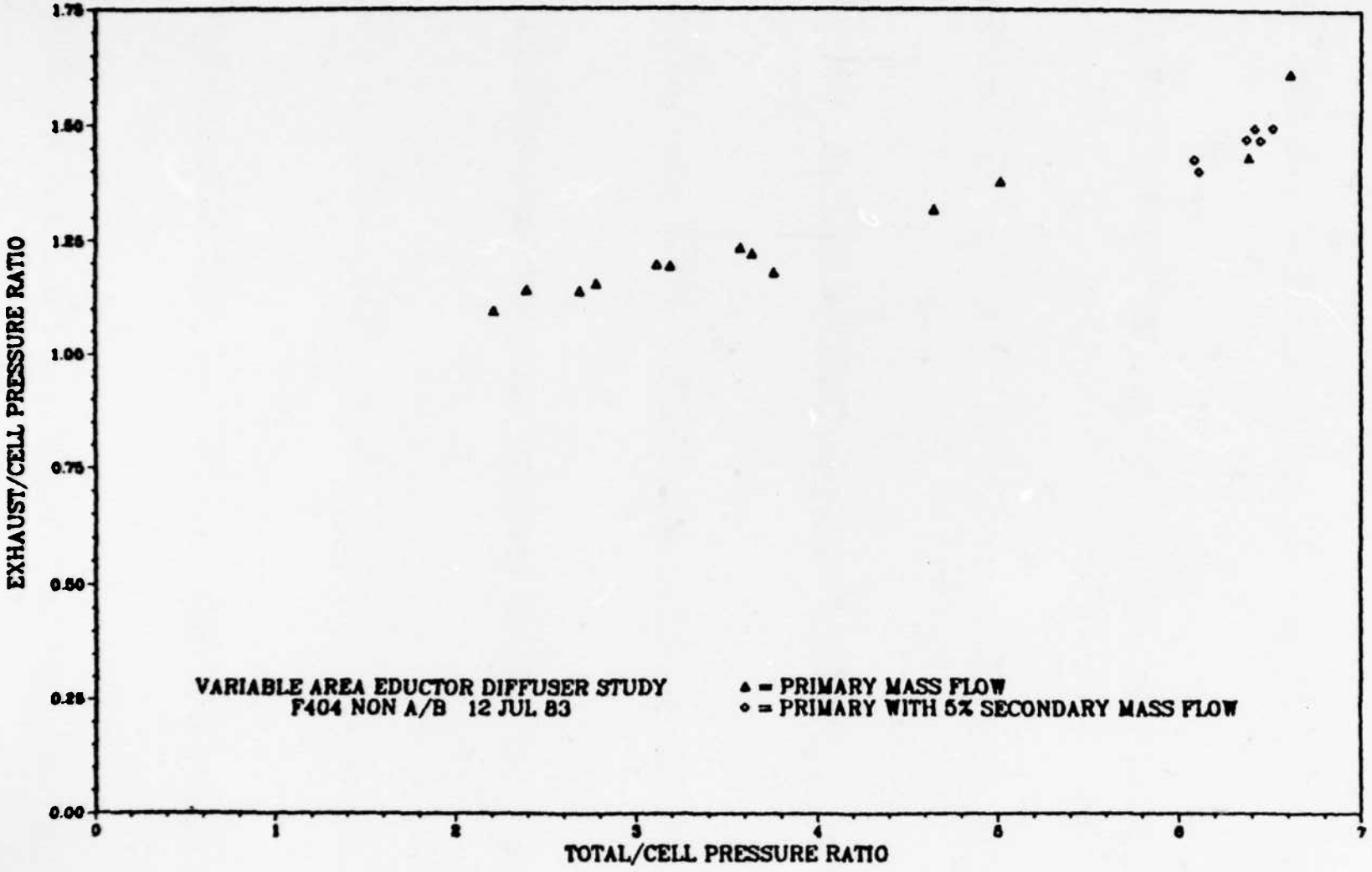

Figure 20. 404NAB Diffuser Pressure Recovery

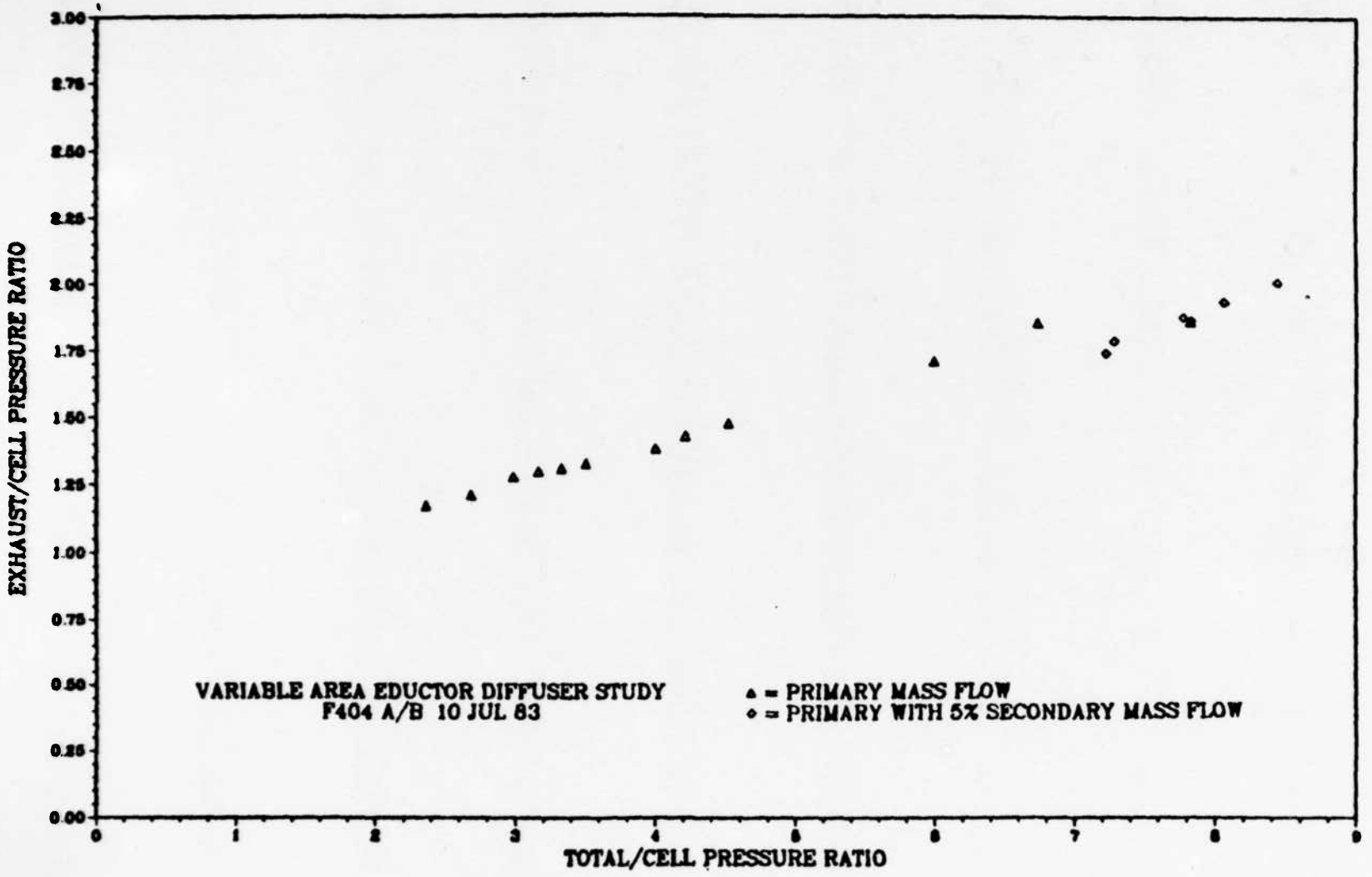

Figure 21. 404AB Diffuser Pressure Recovery

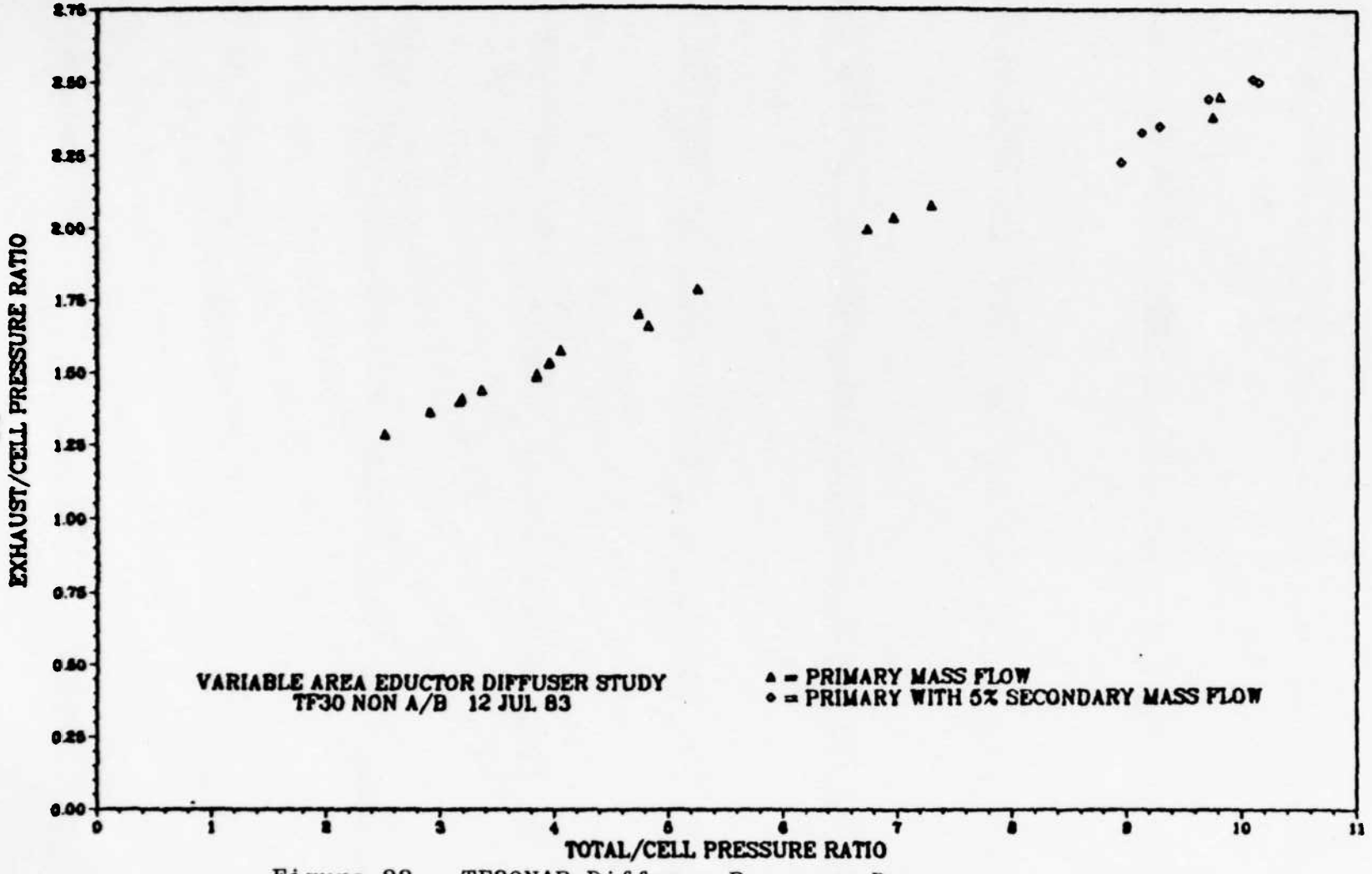

Figure 22. TF30NAB Diffuser Pressure Recovery

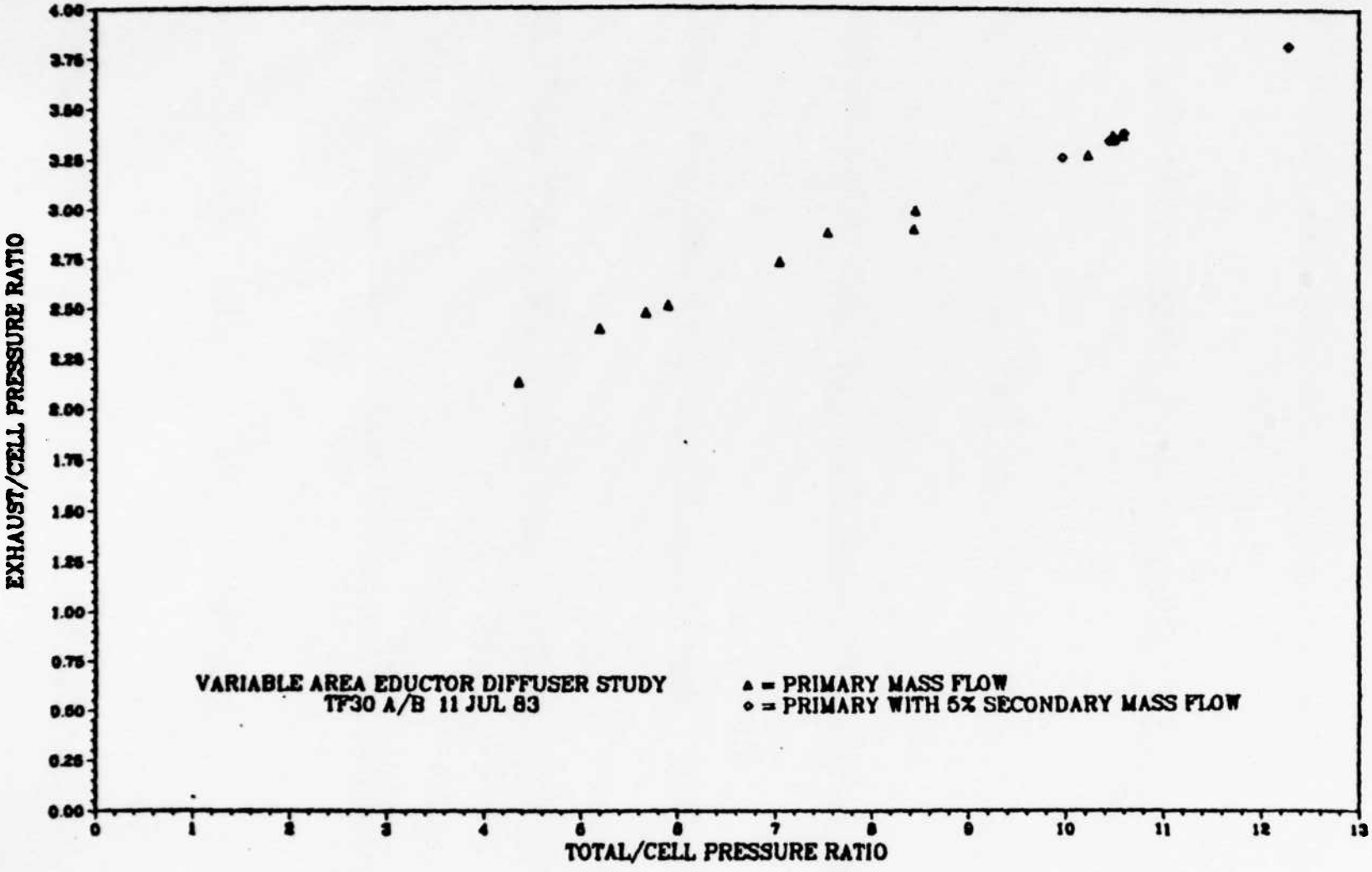

Figure 23. TF30AB Diffuser Pressure Recovery

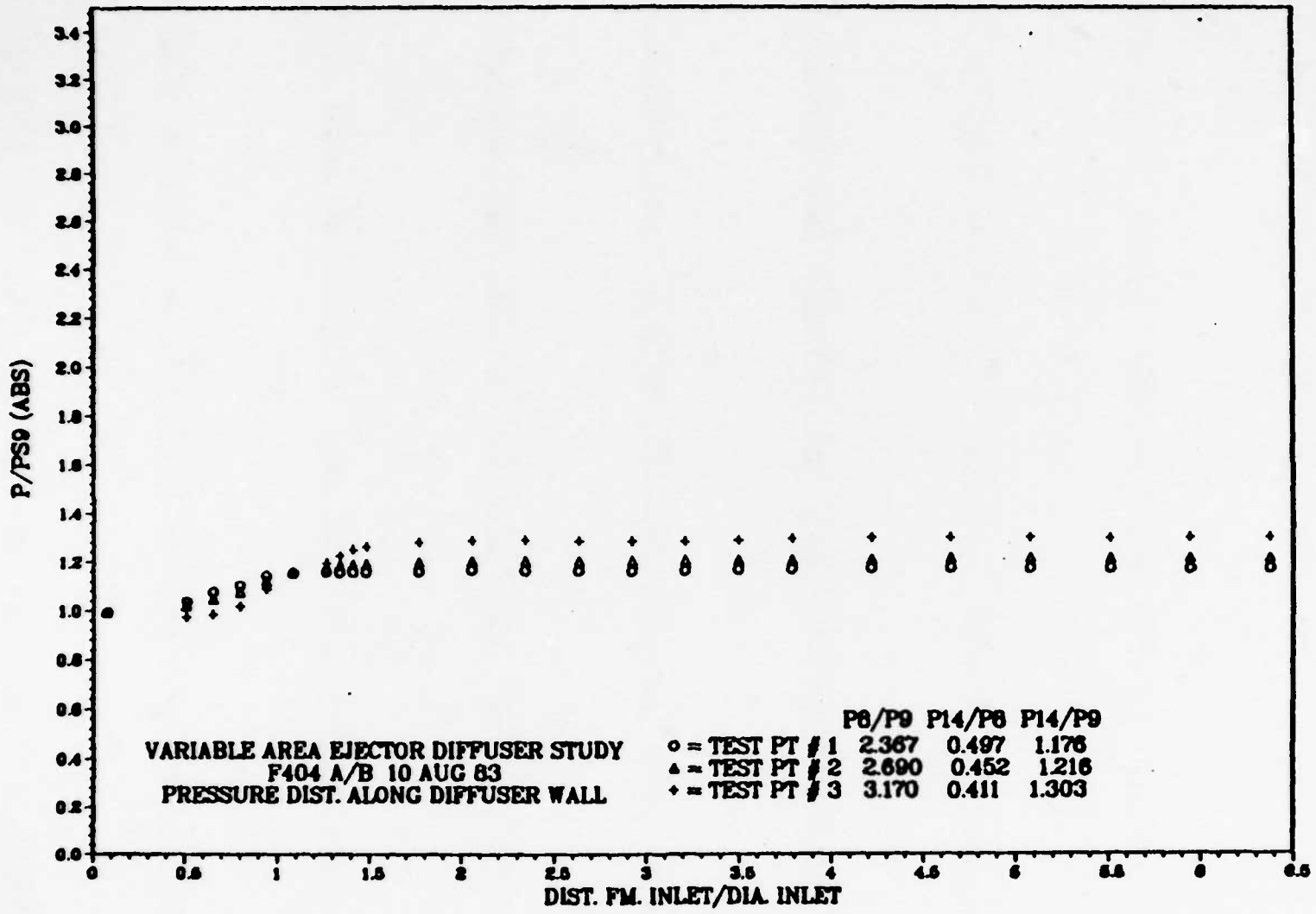

Figure 24. 404AB, Pressure Distributions, Minimum Ptotal

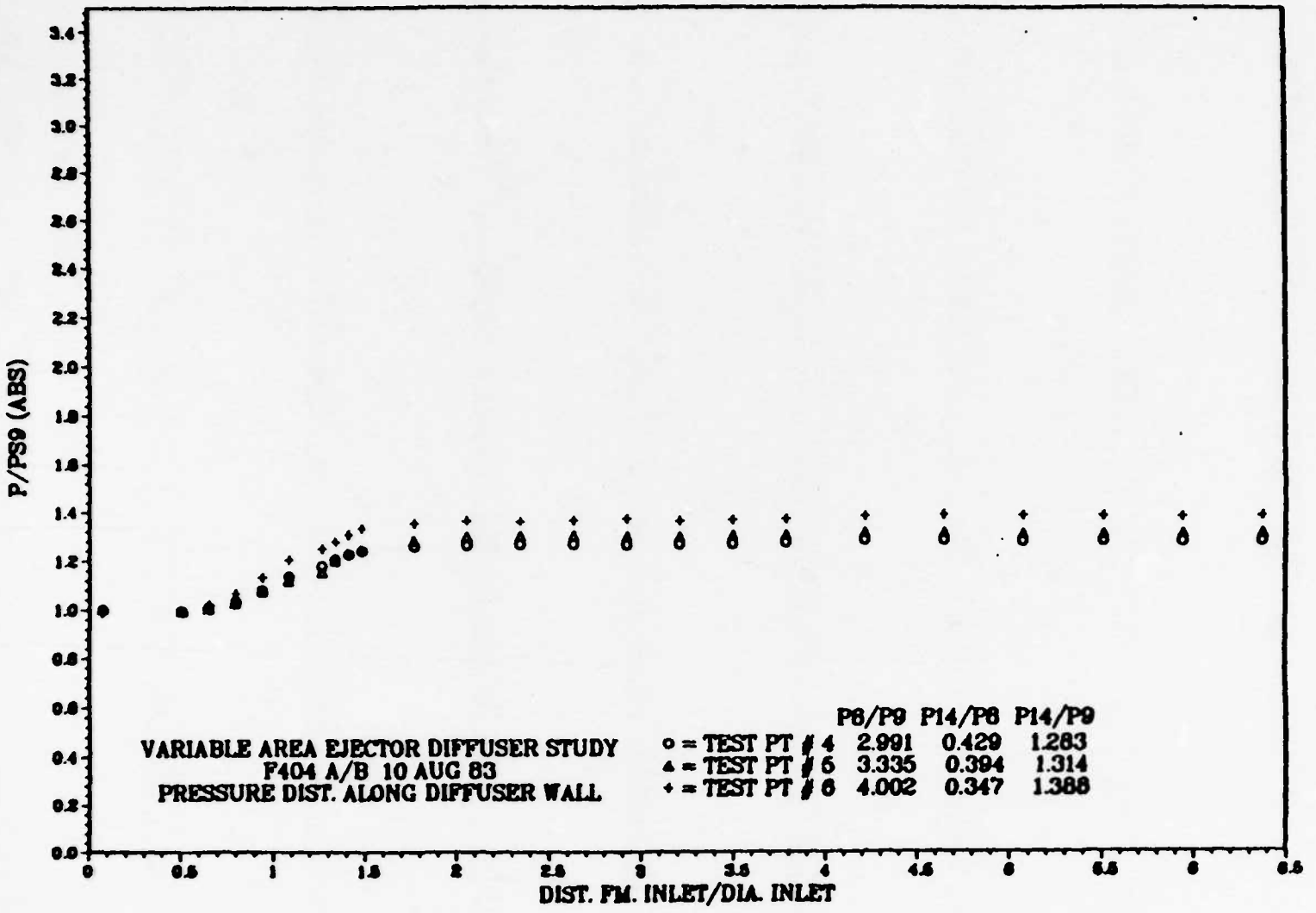

Figure 25. 404AB, Pressure Distributions, One Third Ptotal

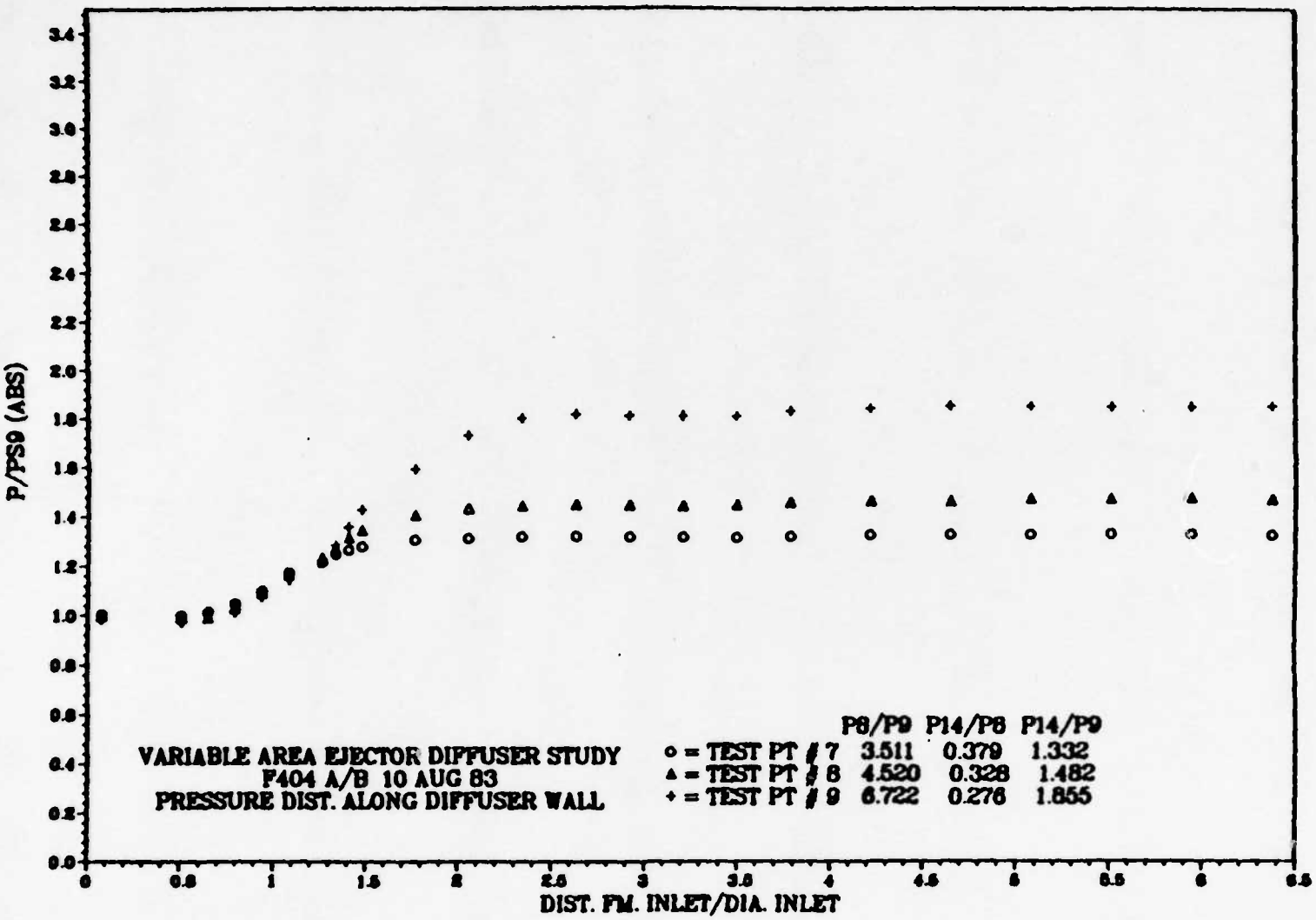

Figure 26. 404AB, Pressure Distributions, Two Thirds Ptotal

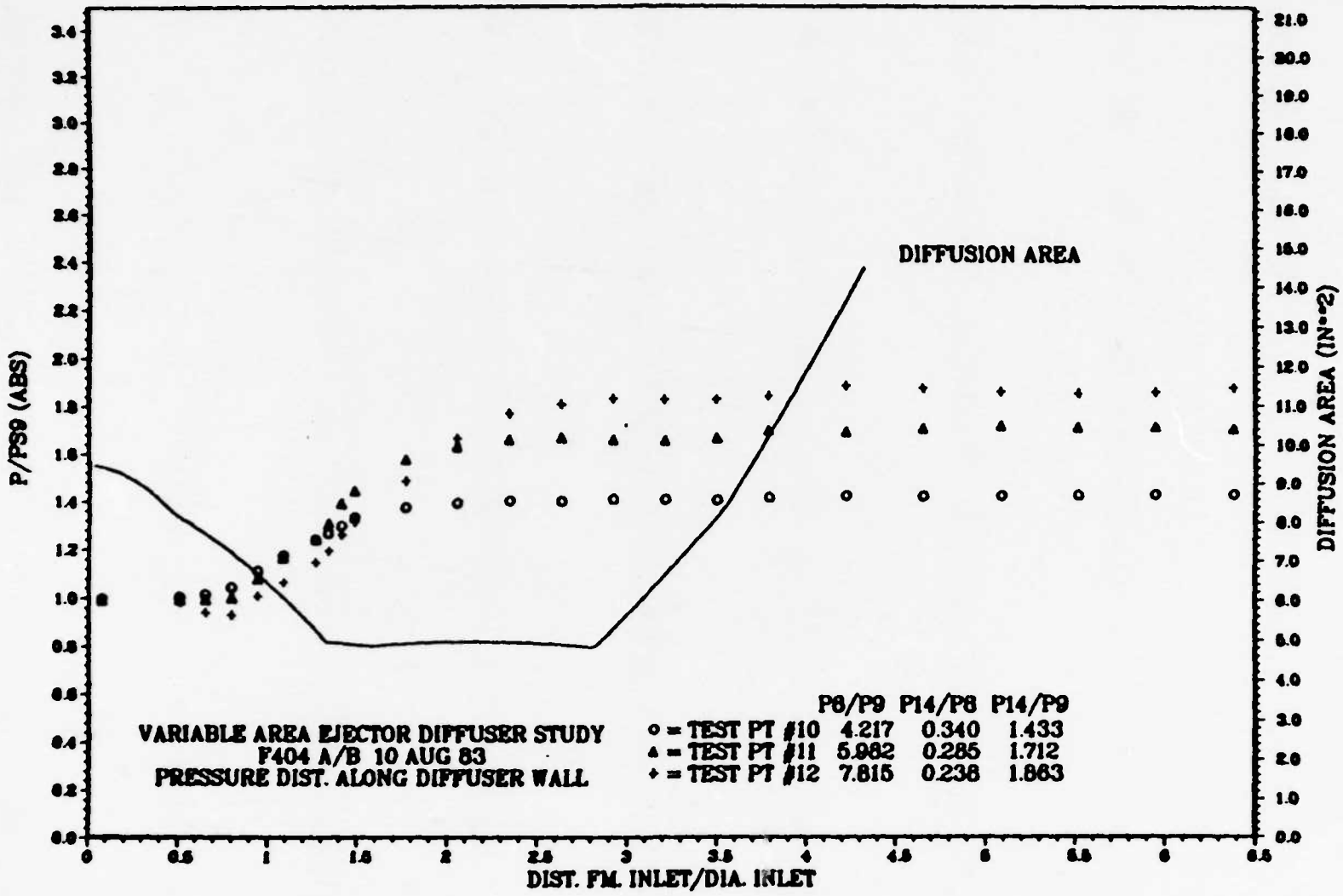

Figure 27. 404AB, Pressure Distributions, Maximum Ptotal

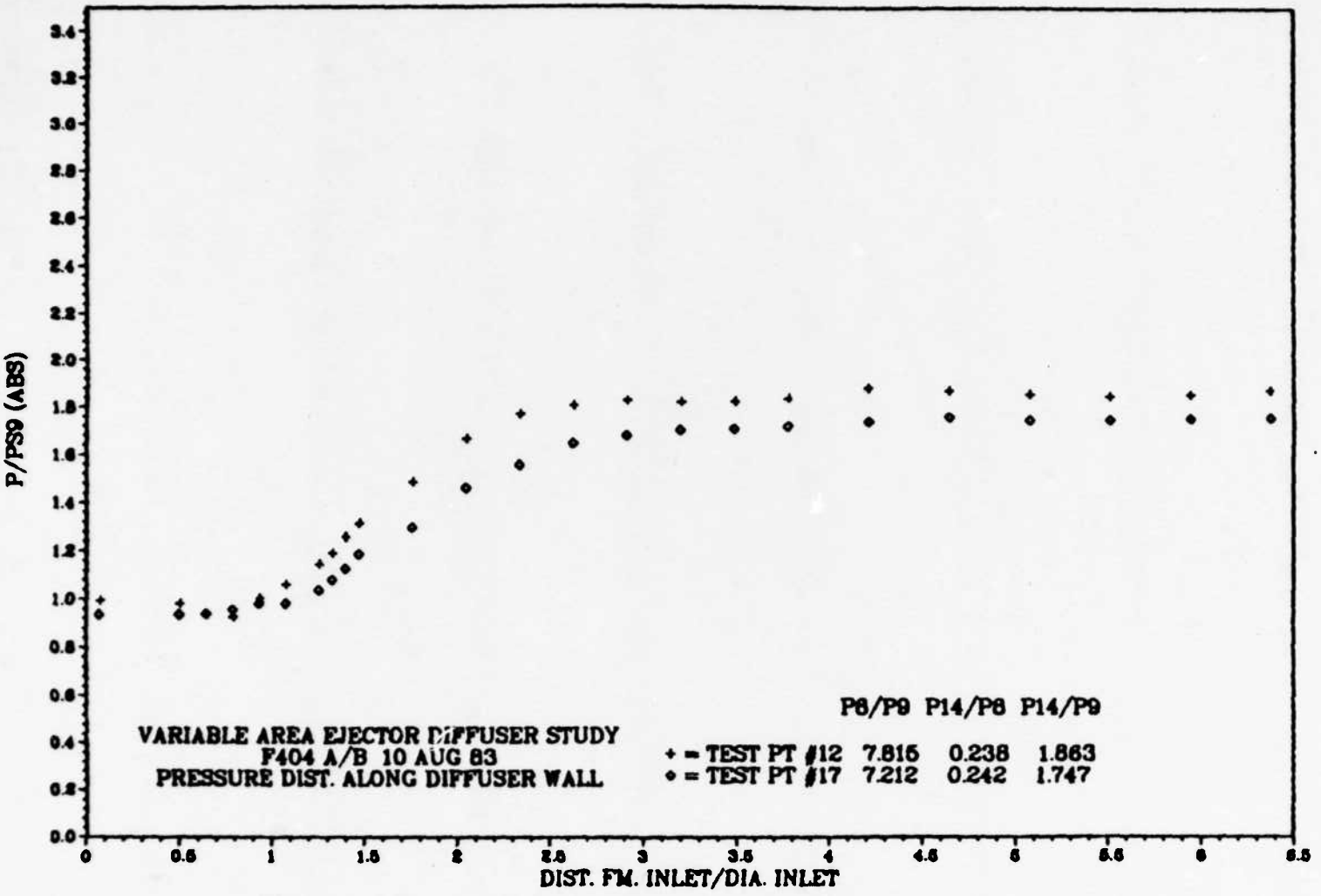

Figure 28. 404AB, Pressure Distributions, Effect of 5% Secondary Mass (#17)

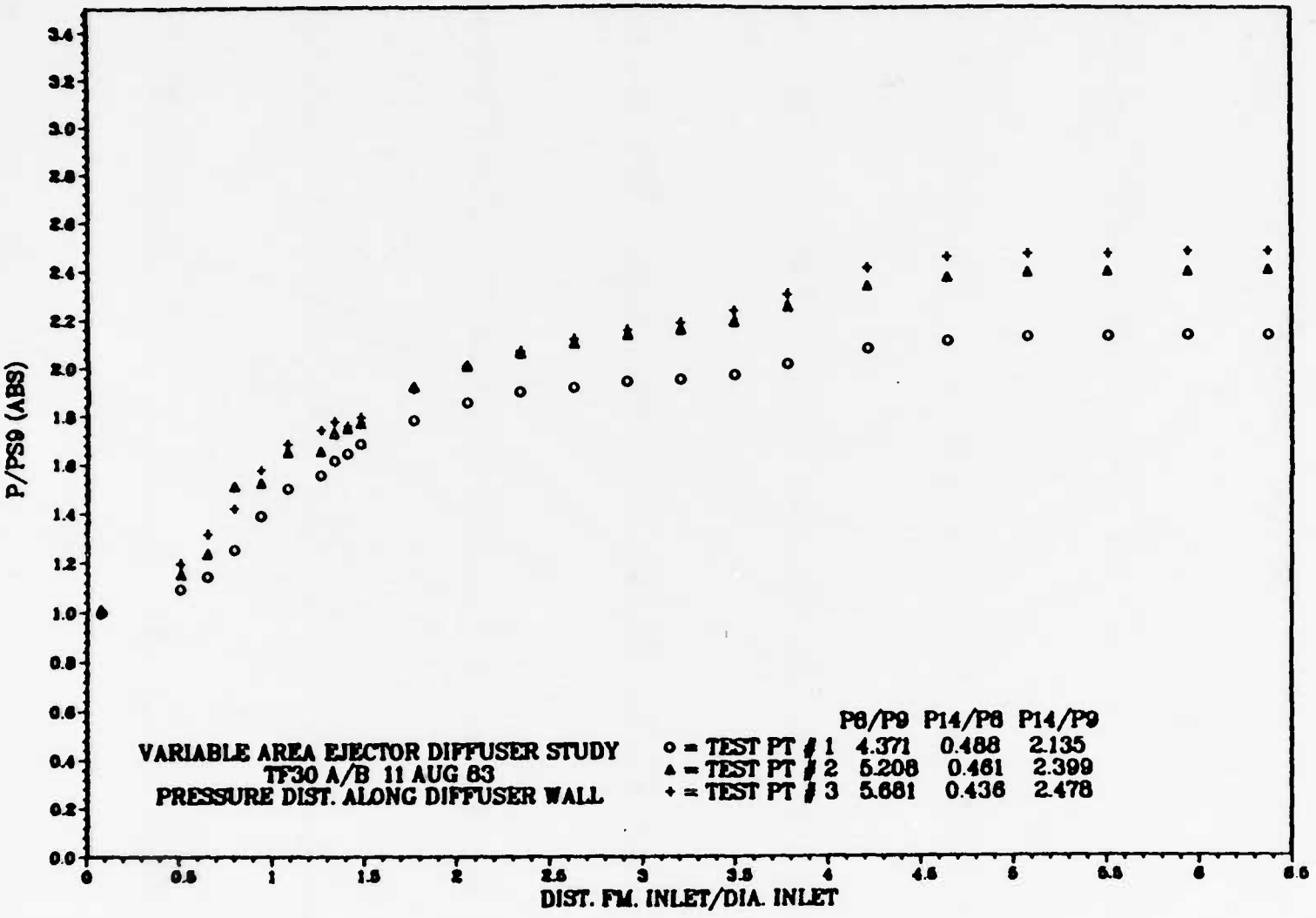

Figure 29. TF30AB, Pressure Distributions, Minimum Ptotal

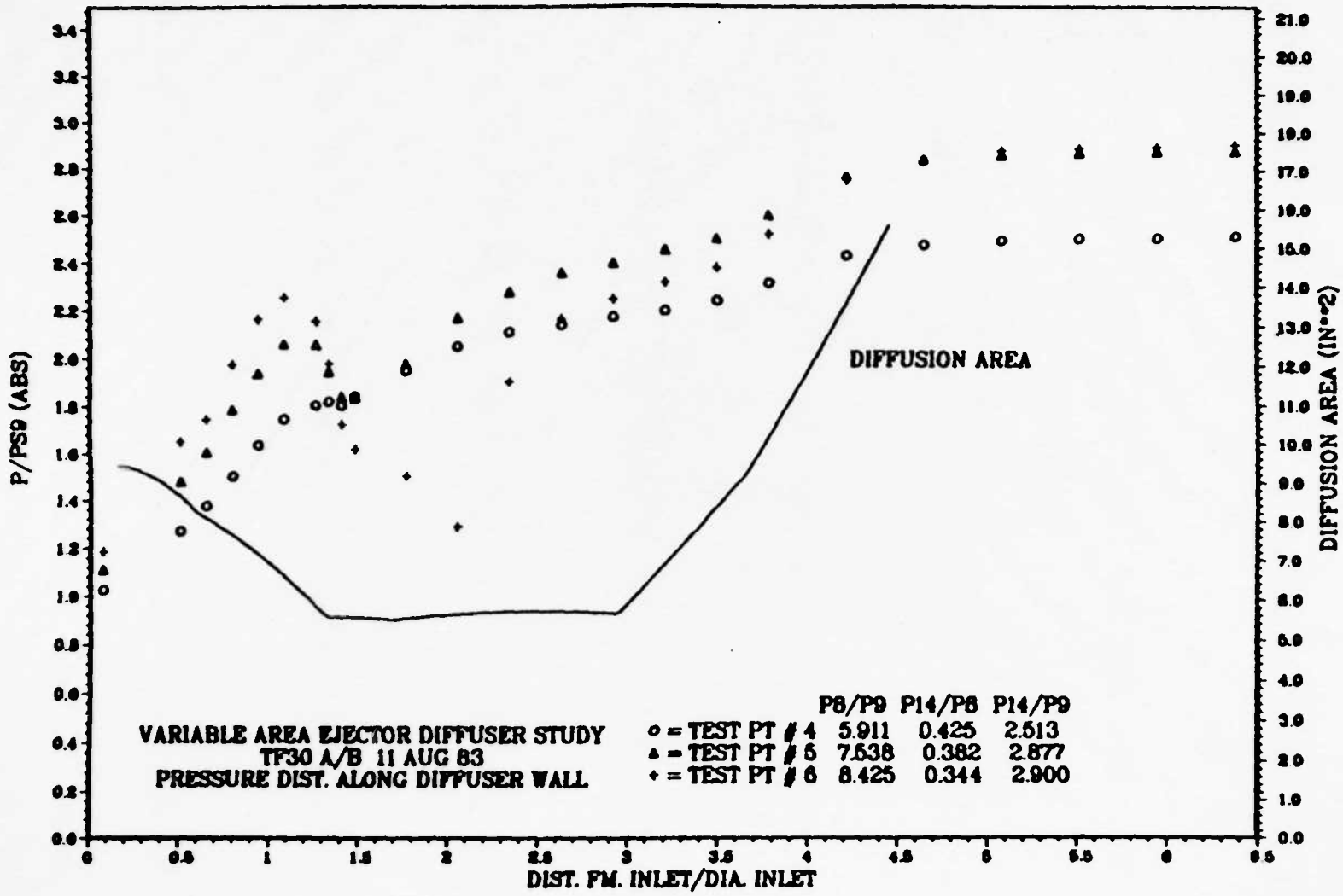

Figure 30. TF30AB, Pressure Distributions, One Half Ptotal

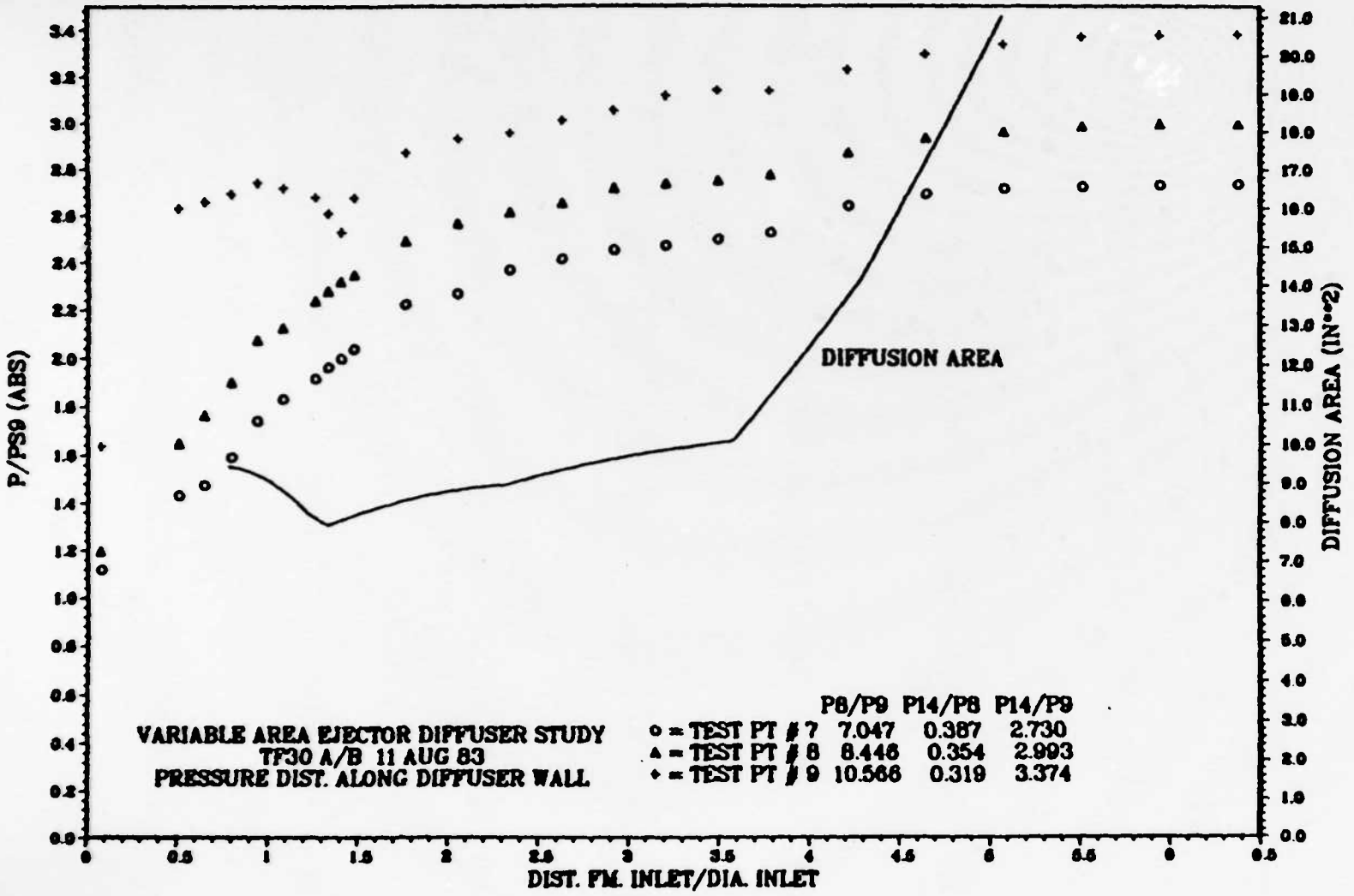

Figure 31. TF30AB, Pressure Distributions, Maximum Ptotal

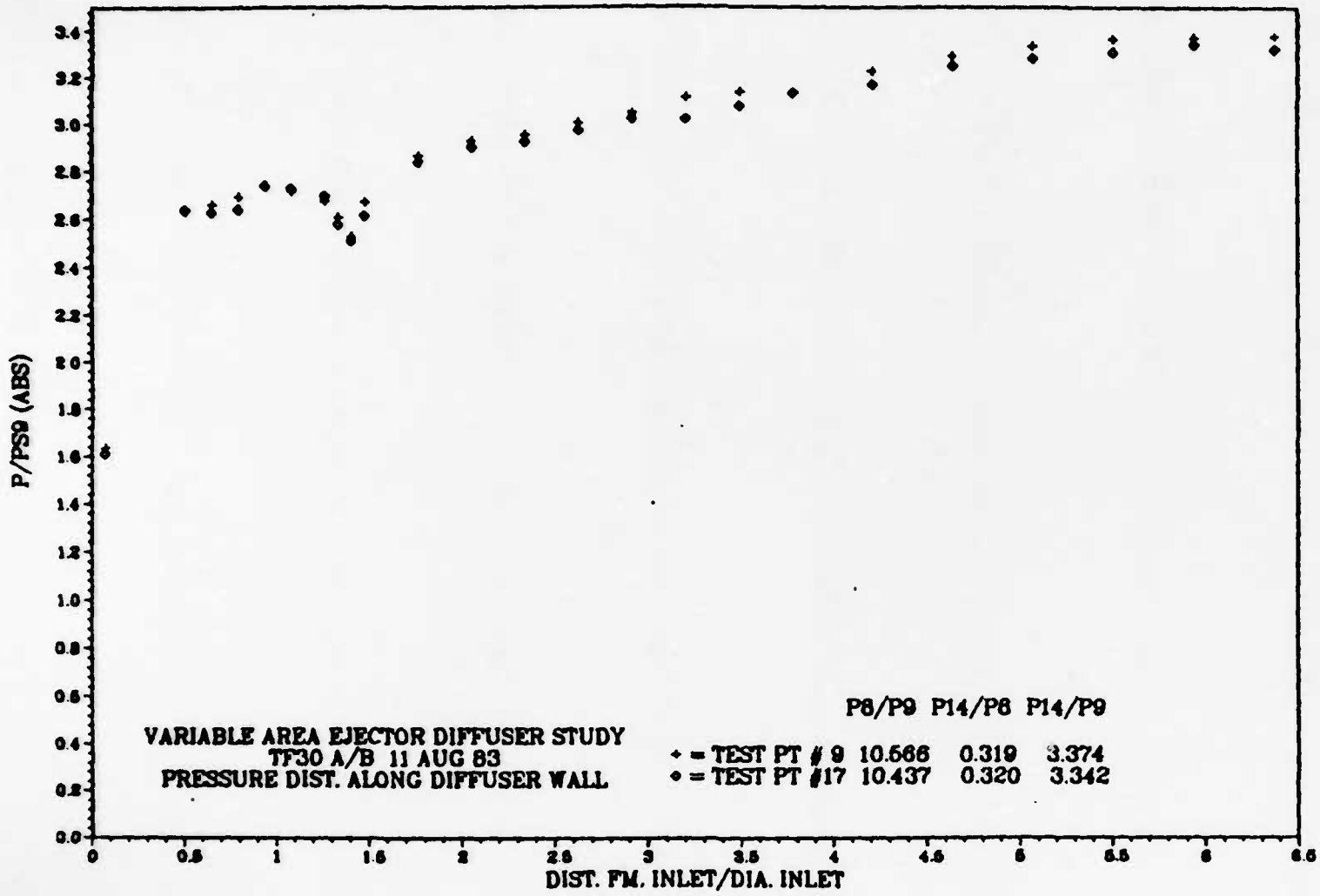

Figure 32. TF30AB, Pressure Distributions, Effect of 5% Secondary Mass (#17)

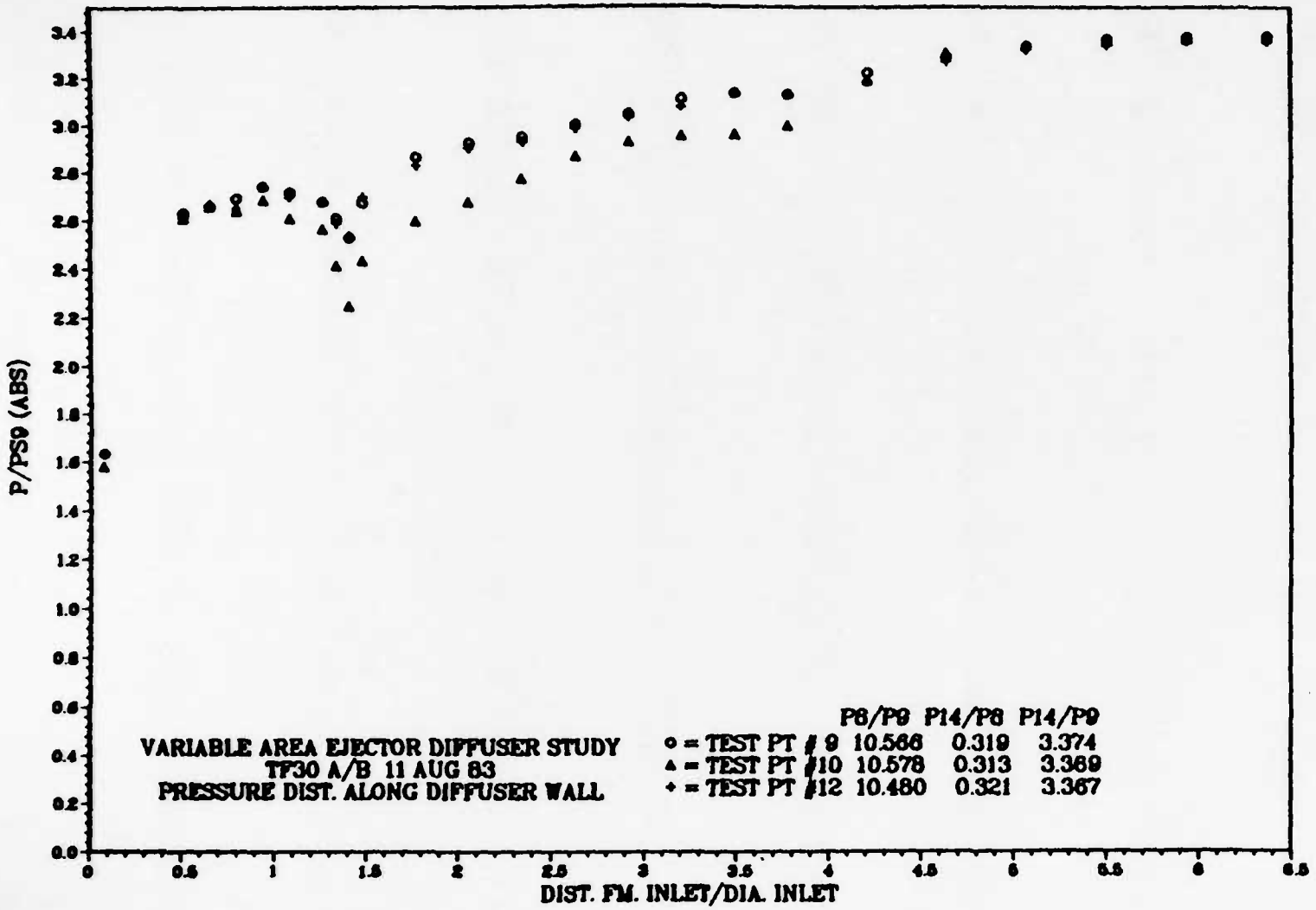

Figure 33. TF30AB, Pressure Distributions, Maximum Ptotal; Repeatability

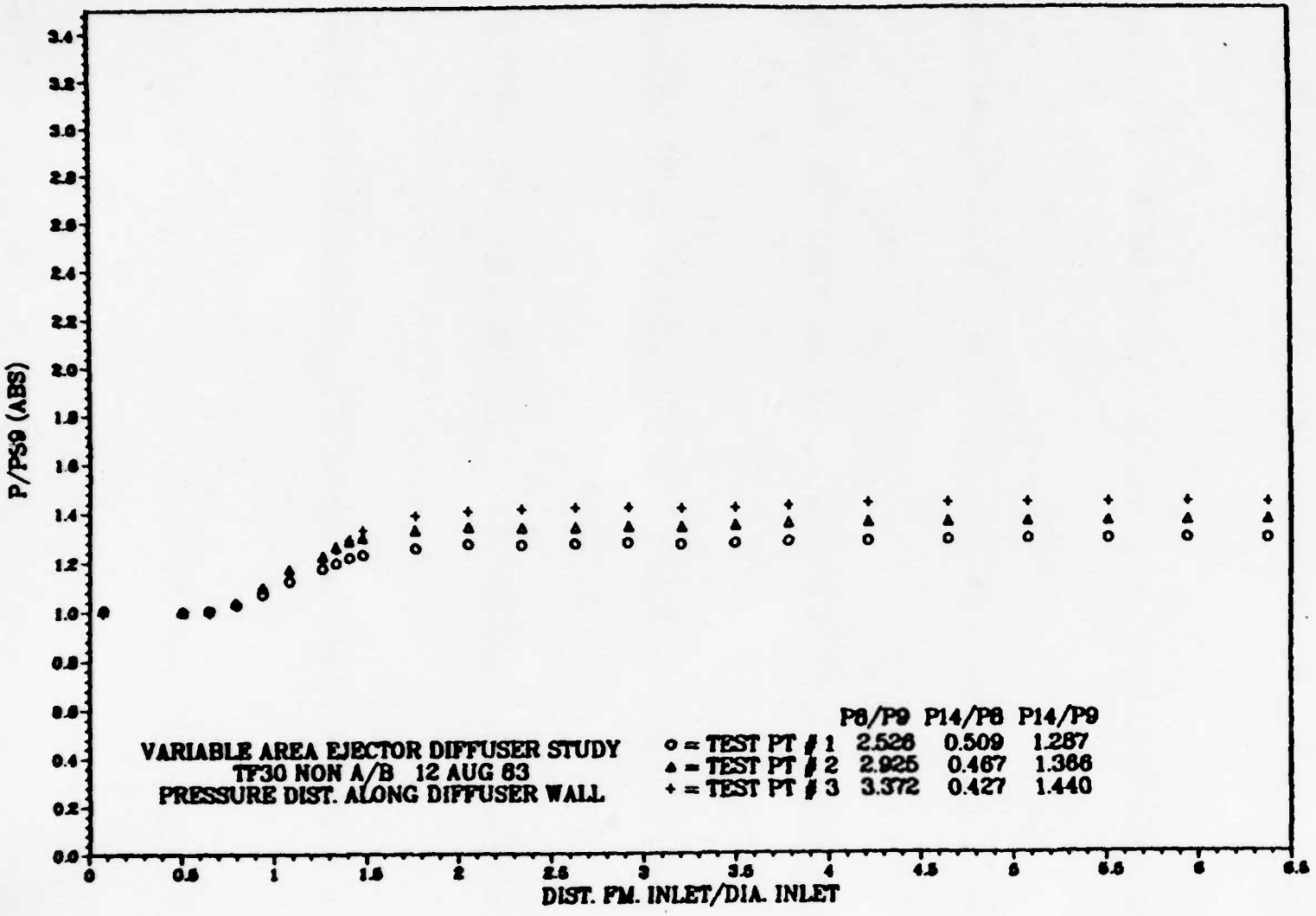

Figure 34. TF30NAB, Pressure Distributions, Minimum Ptotal

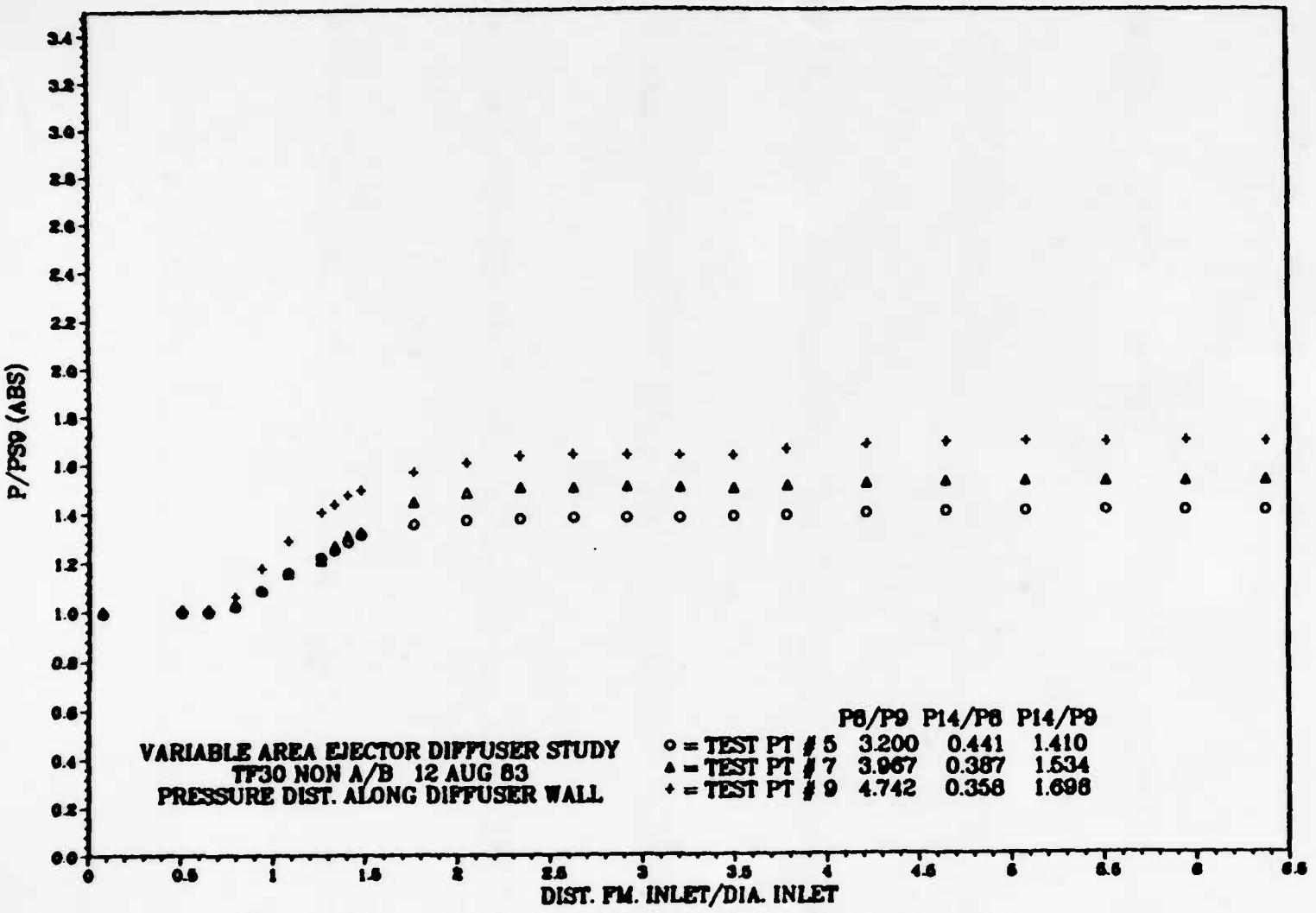

Figure 35. TF30NAB, Pressure Distributions, One Third Ptotal

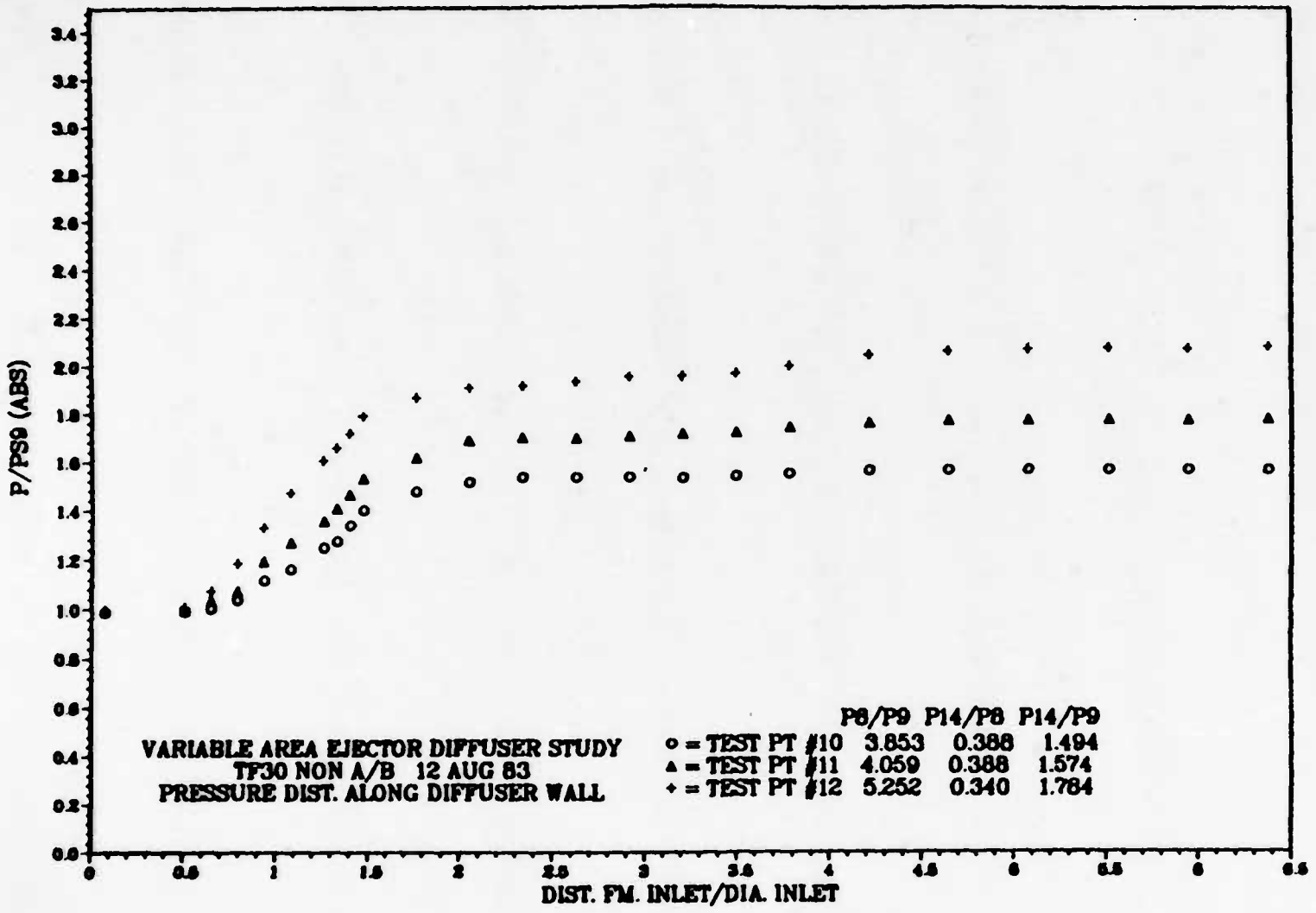

Figure 36. TF30NAB, Pressure Distributions, Two Thirds Ptotal

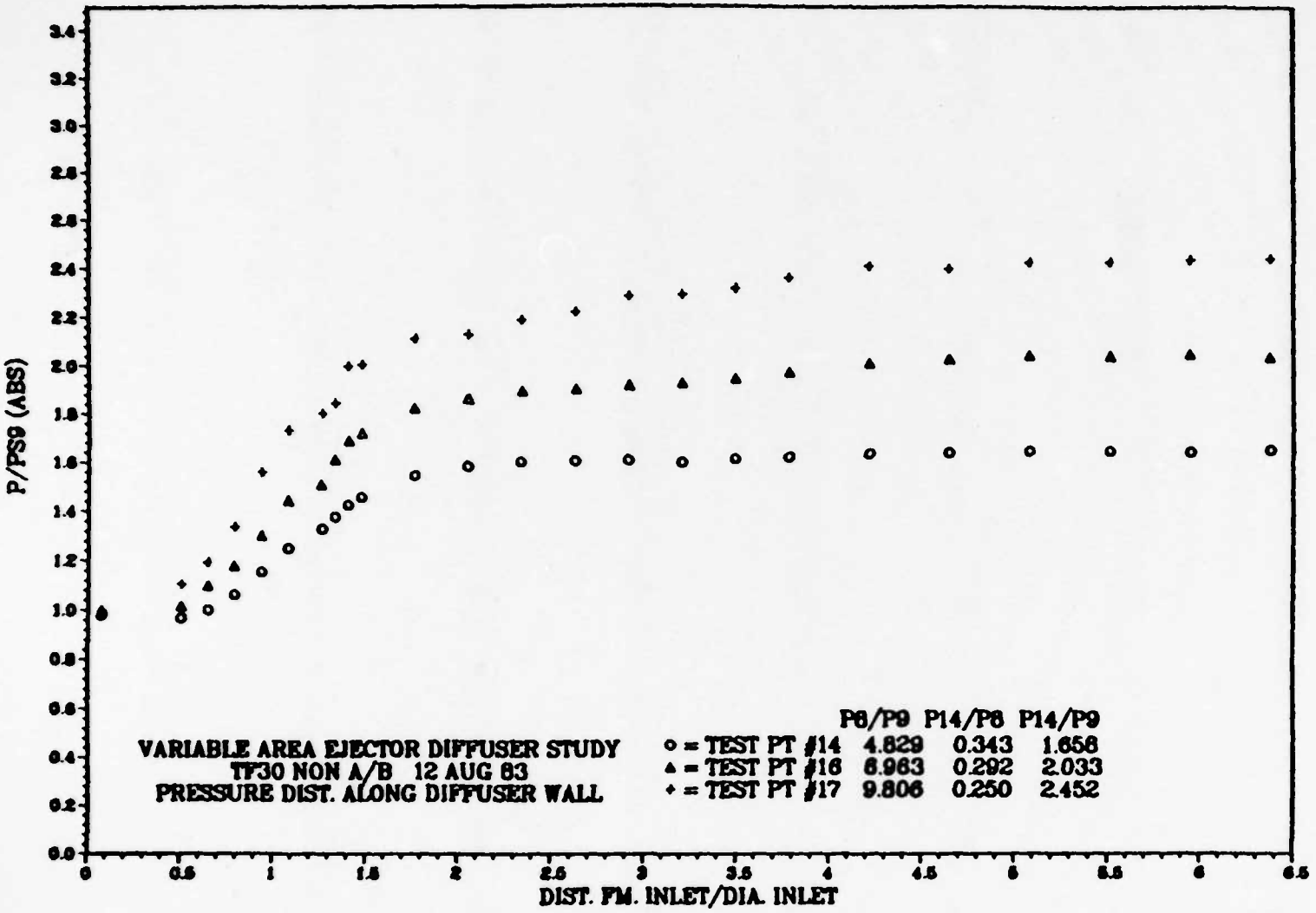

Figure 37. TF30NAB, Pressure Distributions, Maximum Ptotal

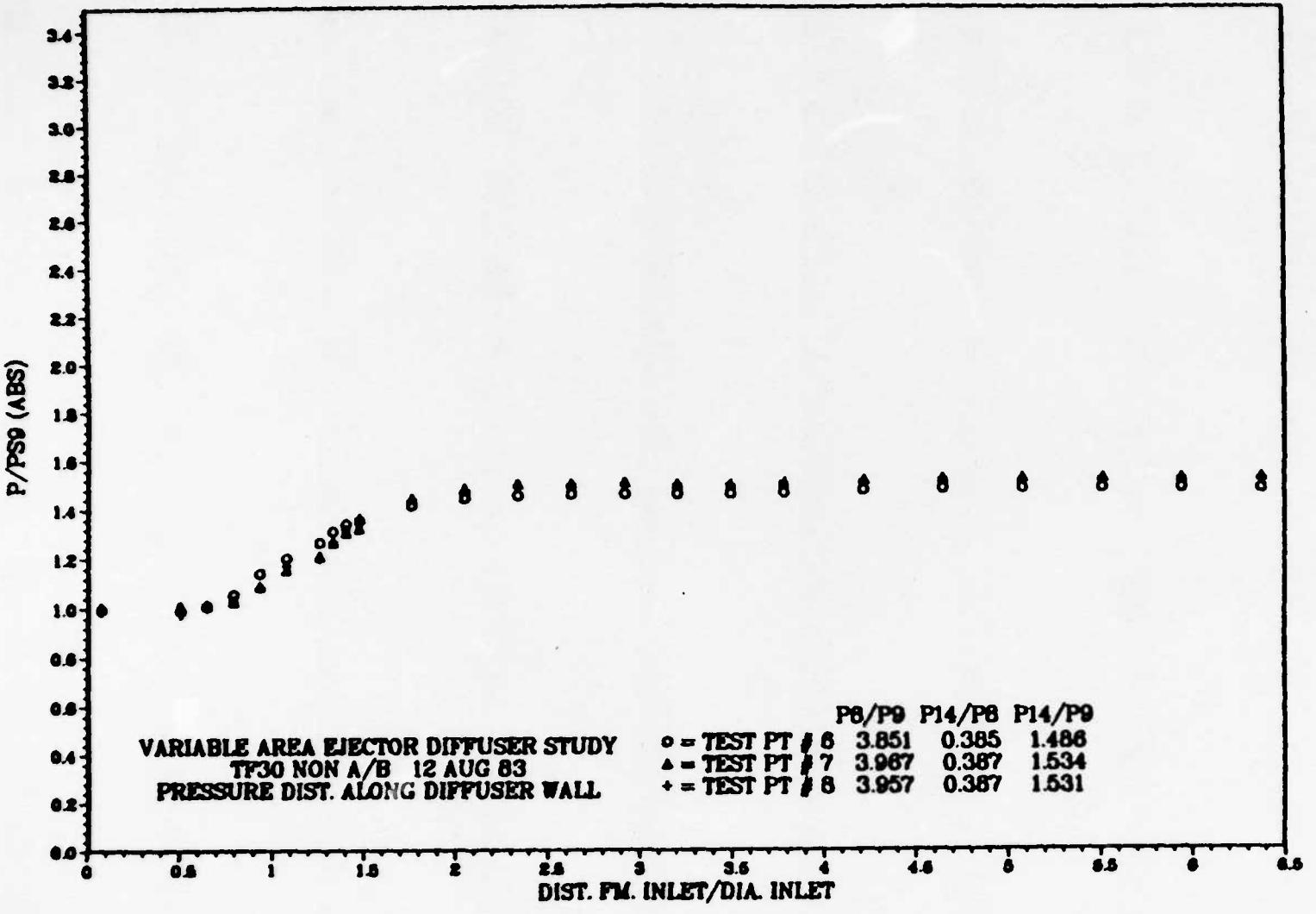

Figure 38. TF30NAB, Pressure Distributions, Maximum Ptotal; Repeatability

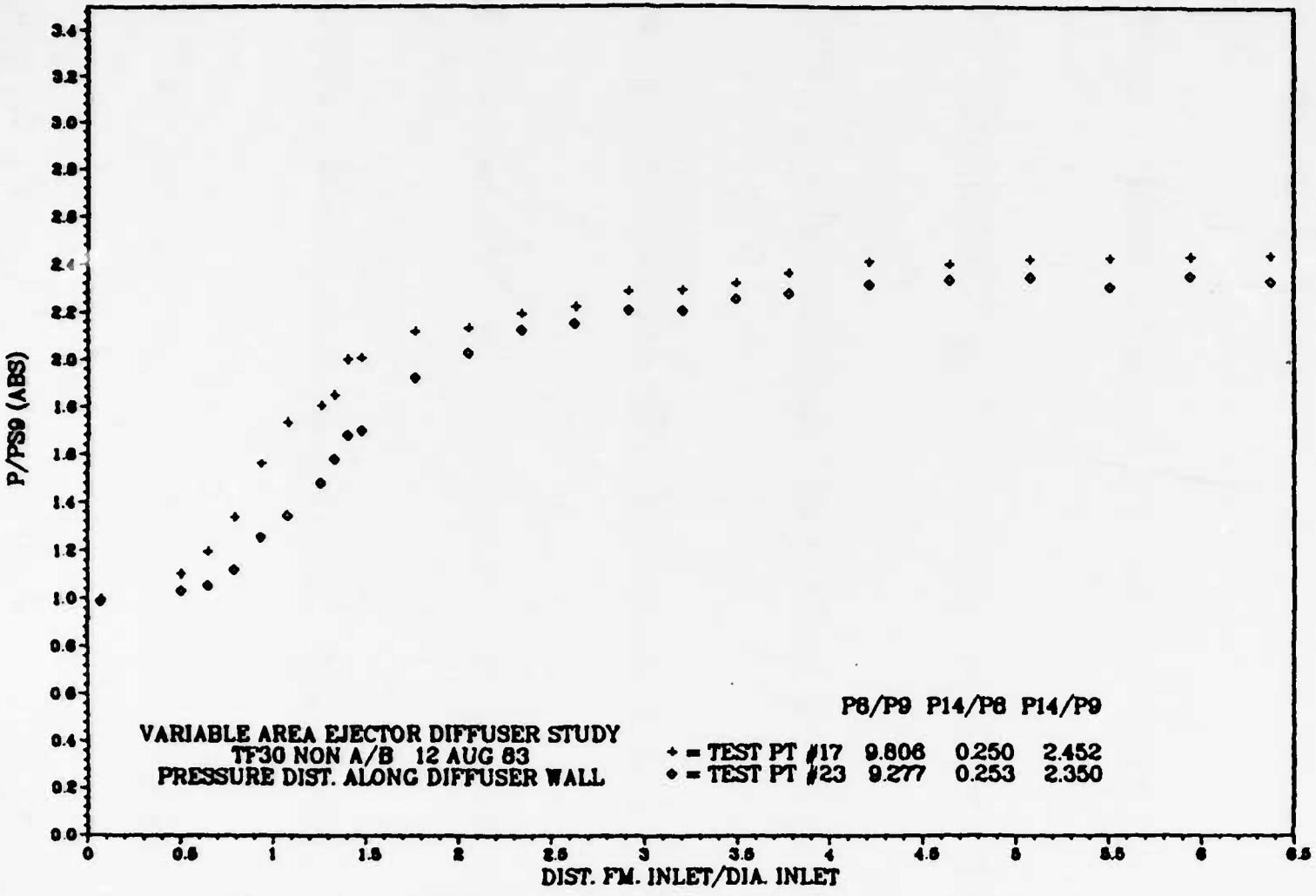

Figure 39. TF30NAB, Pressure Distributions, Effect of 5% Secondary Mass (#23)

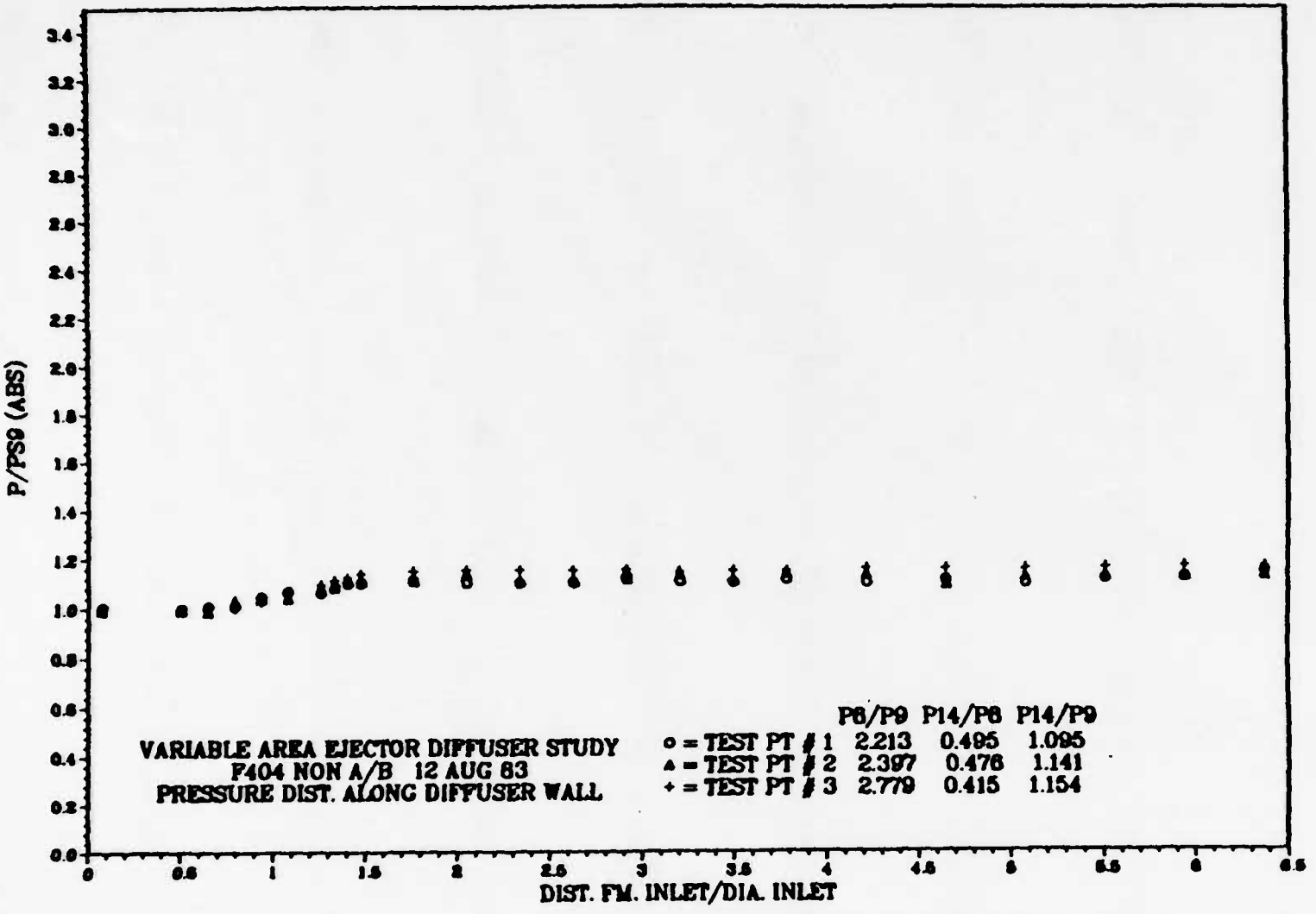

Figure 40. 404NAB, Pressure Distributions, Minimum Ptotal

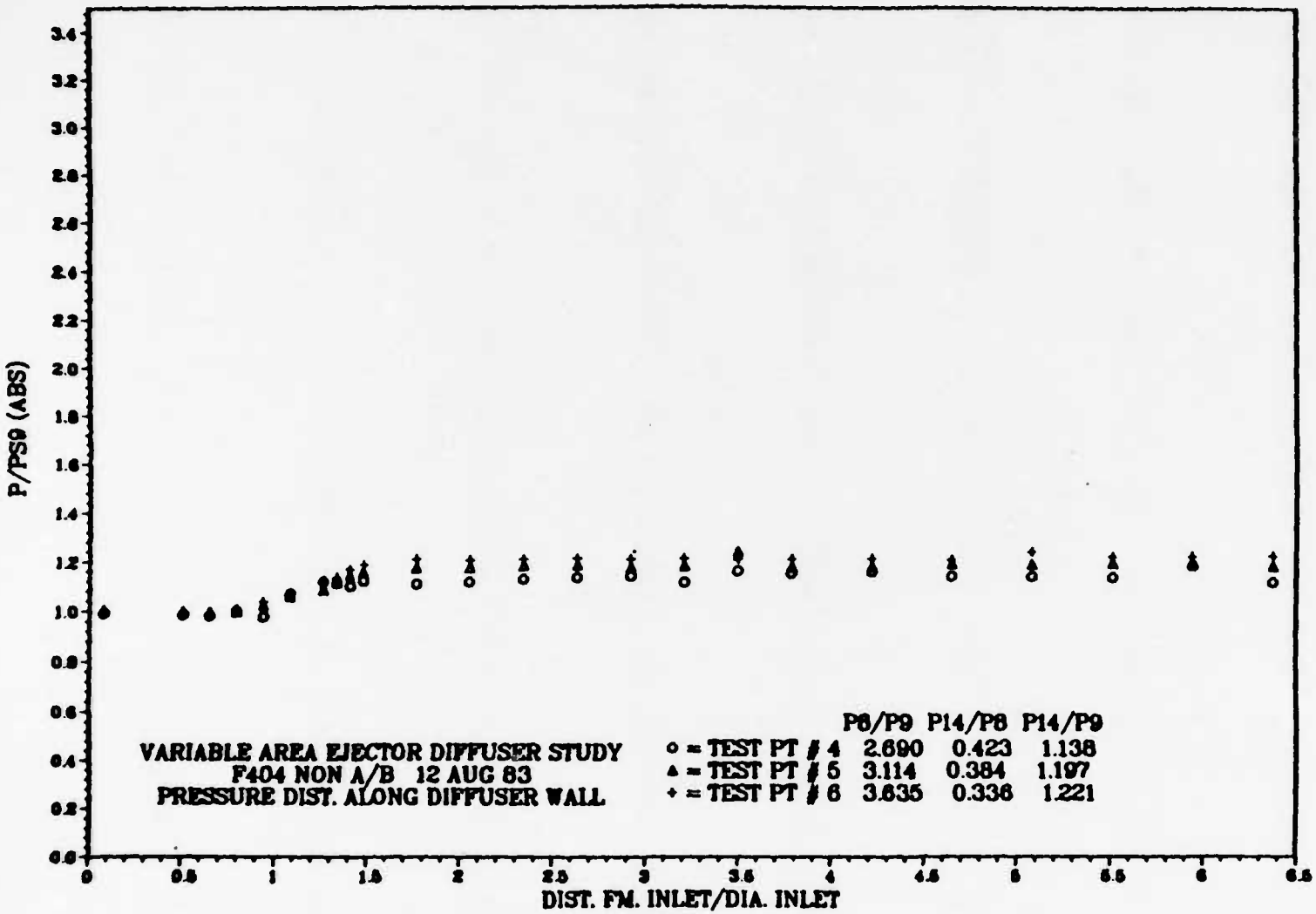

Figure 41. 404NAB, Pressure Distributions, One Third Ptotal

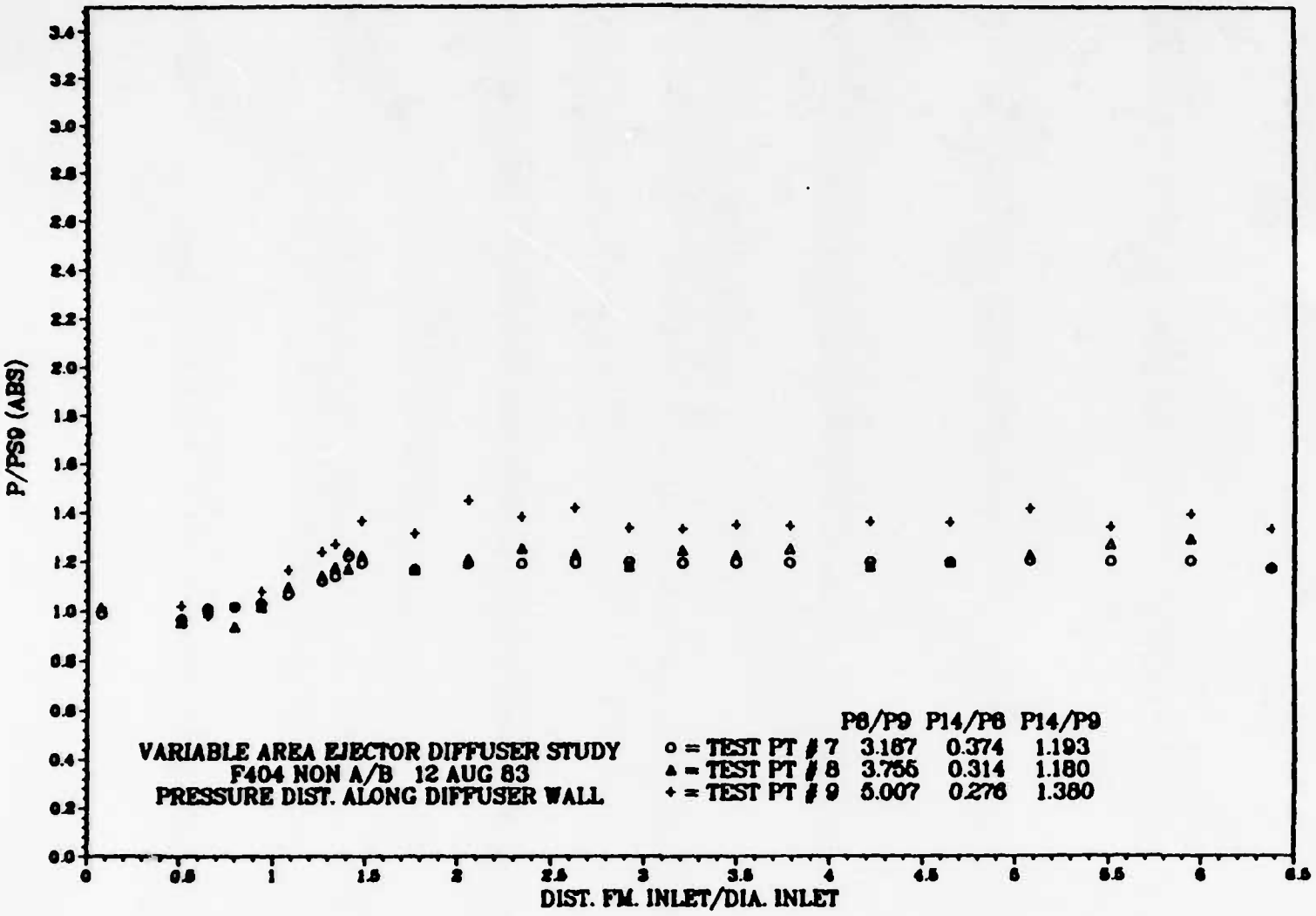

Figure 42. 404NAB, Pressure Distributions, Two Thirds Ptotal

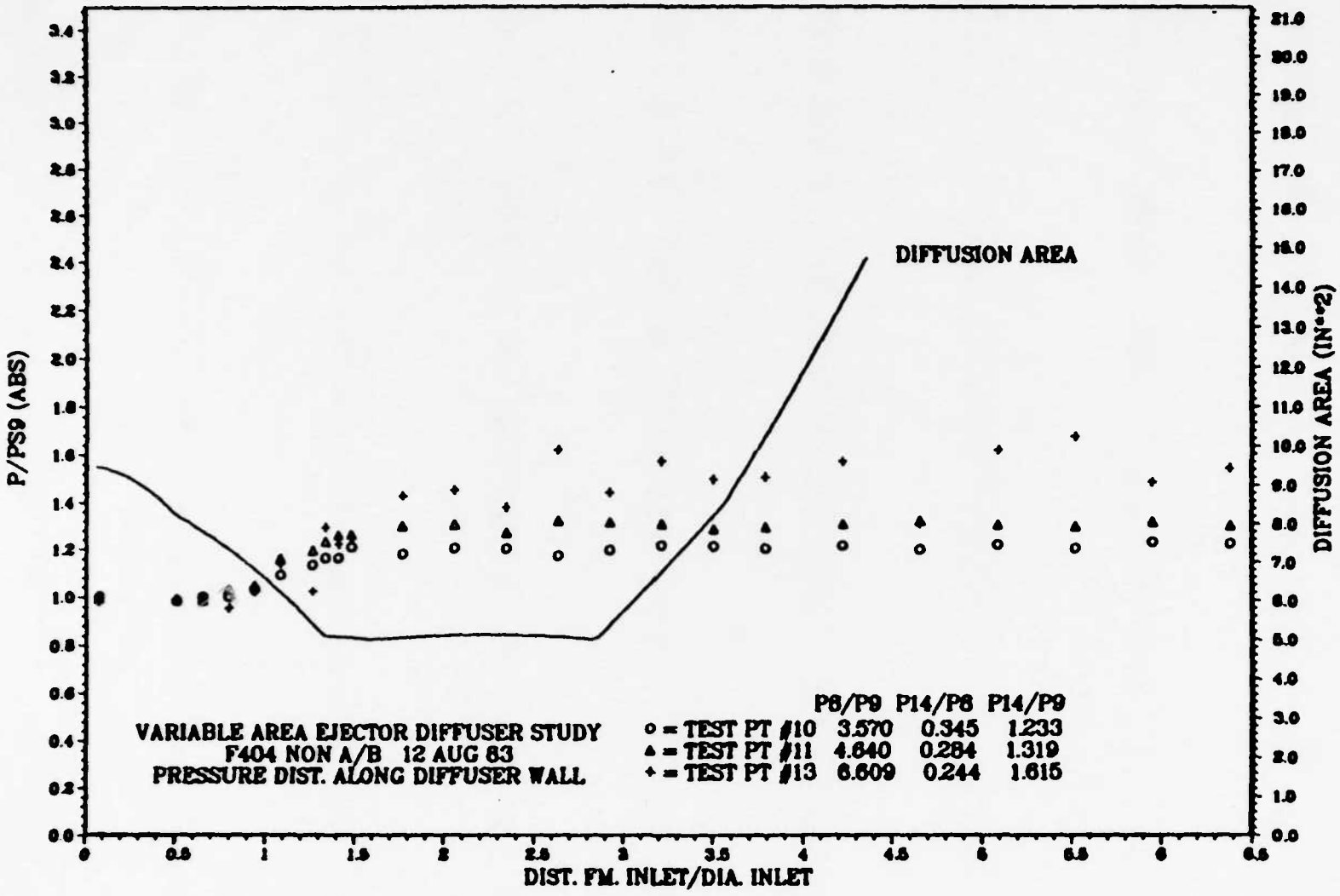

Figure 43. 404NAB, Pressure Distributions, Maximum Ptotal

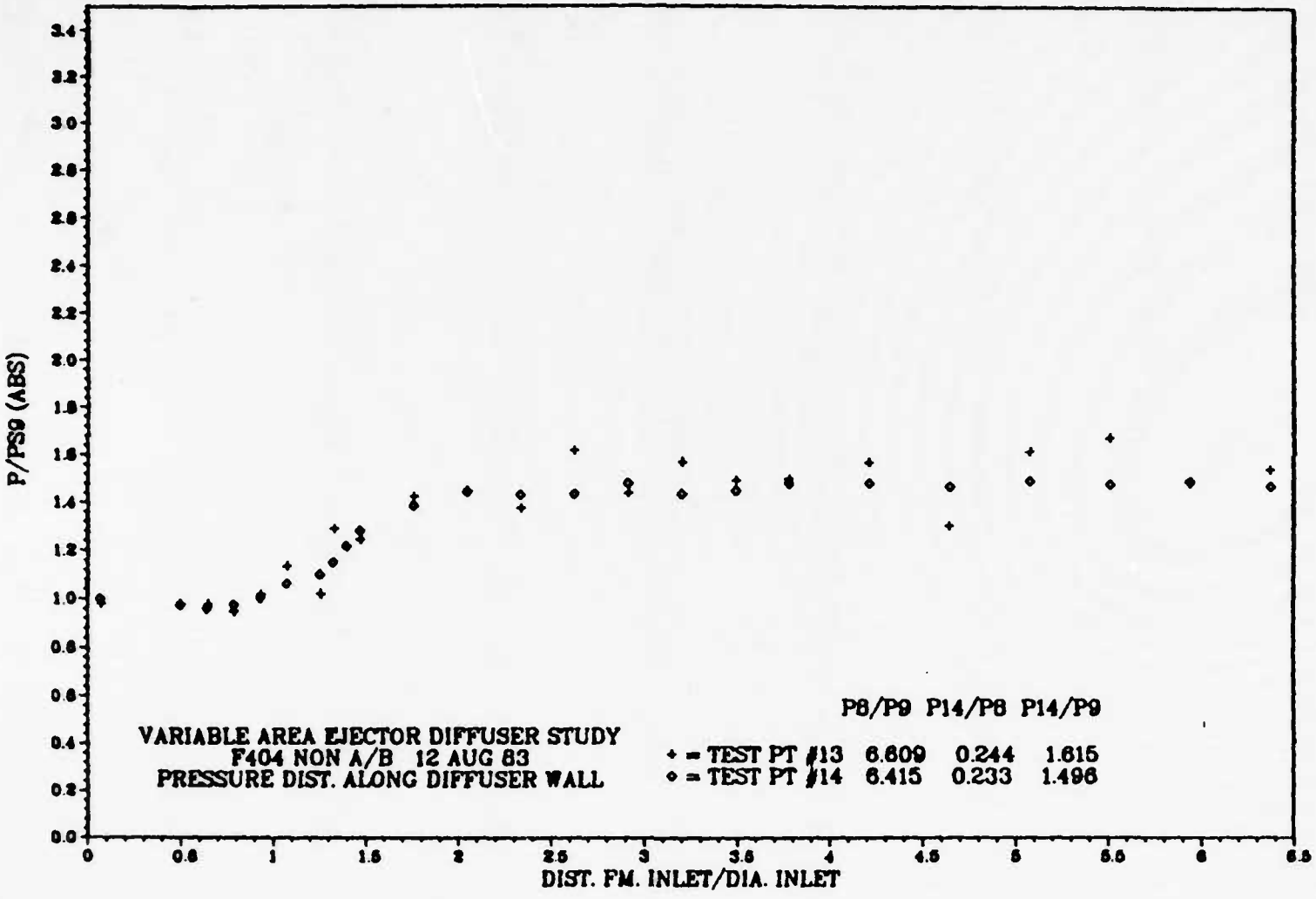

Figure 44. 404NAB, Pressure Distributions, Effect of 5% Secondary Mass (#14)

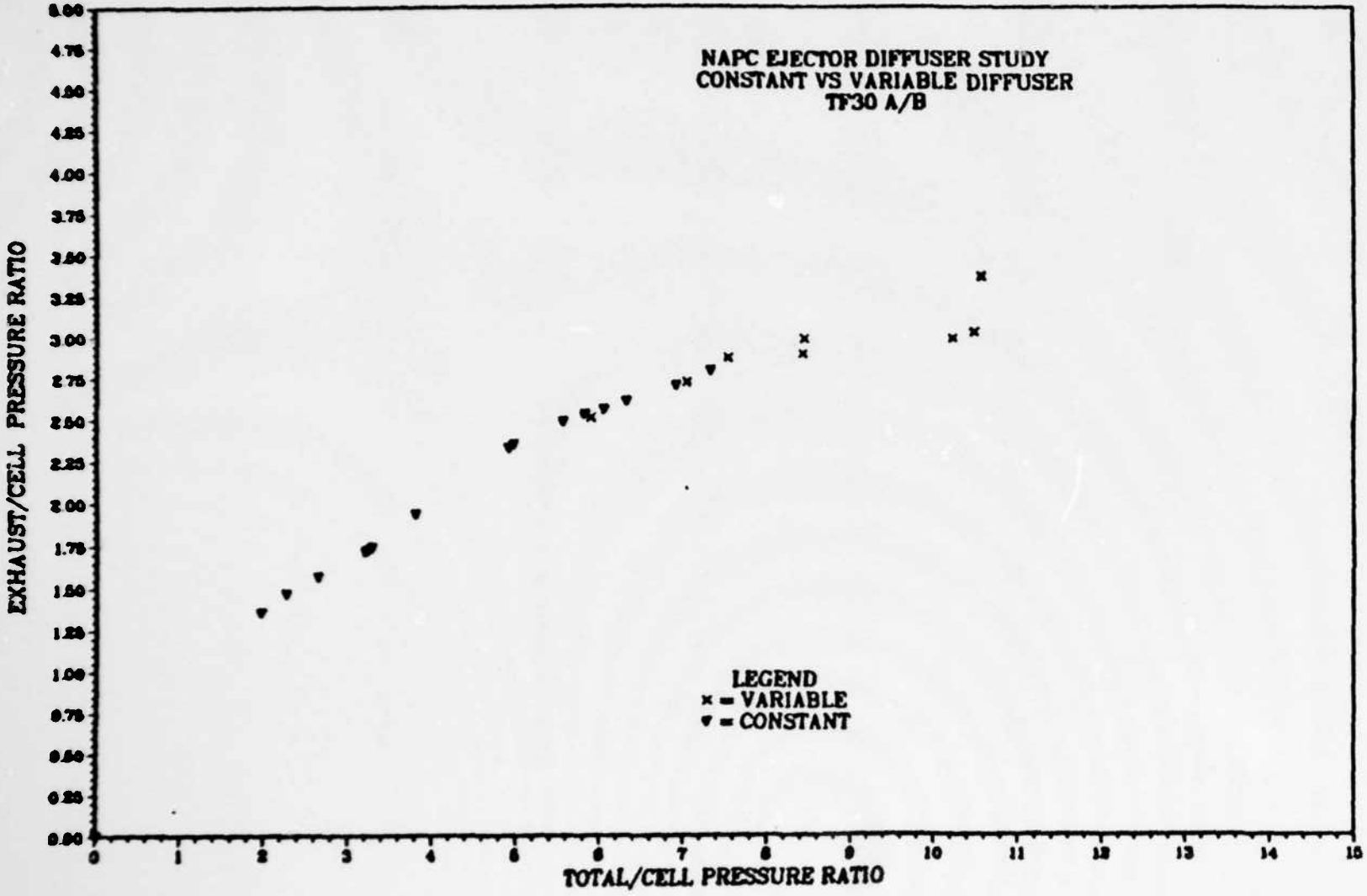

Figure 45. TF30AB, Comparison of Constant vs. Variable Area Diffusers

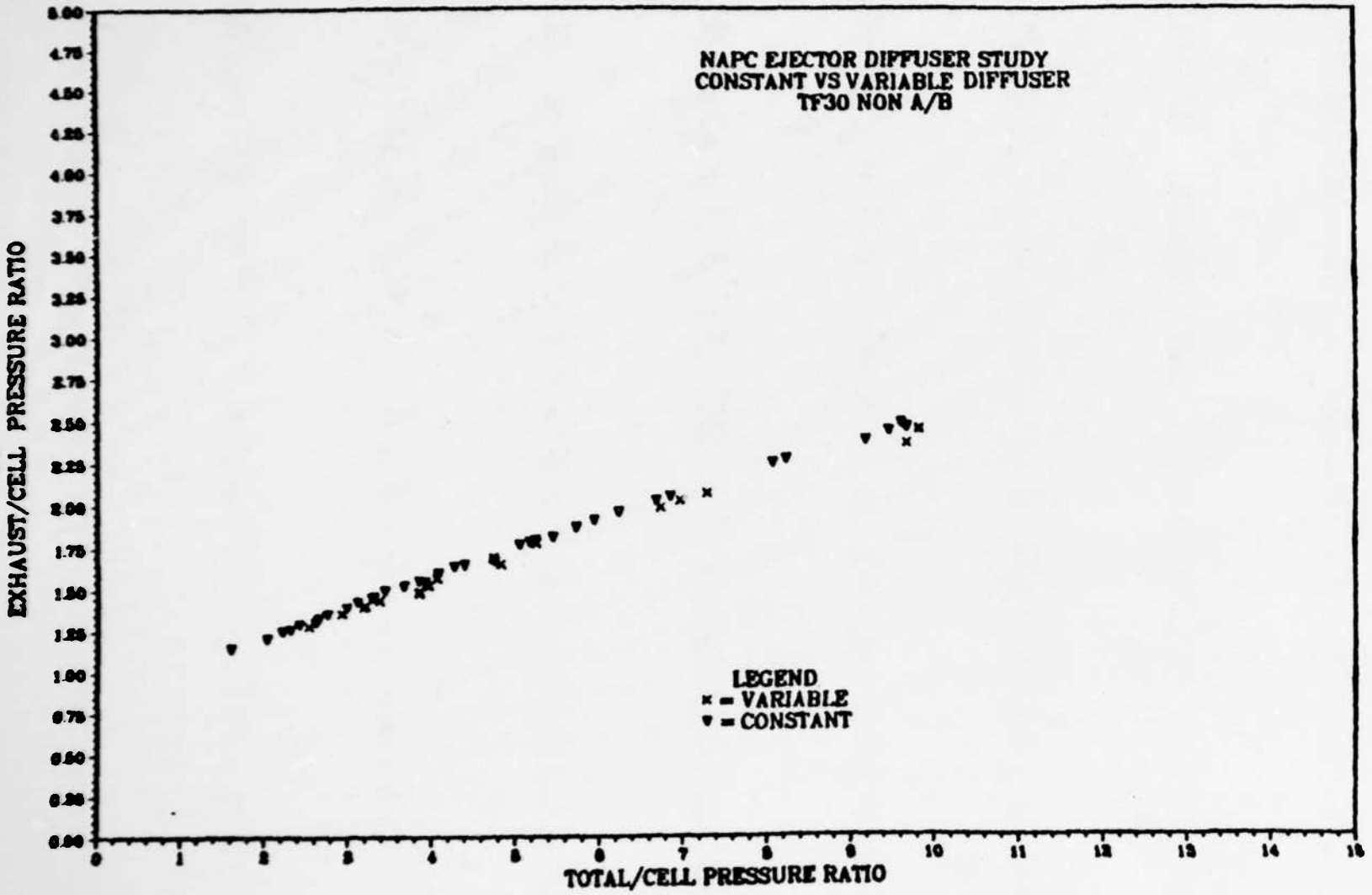

Figure 46. TF30NAB, Comparison of Constant vs. Variable Area Diffusers

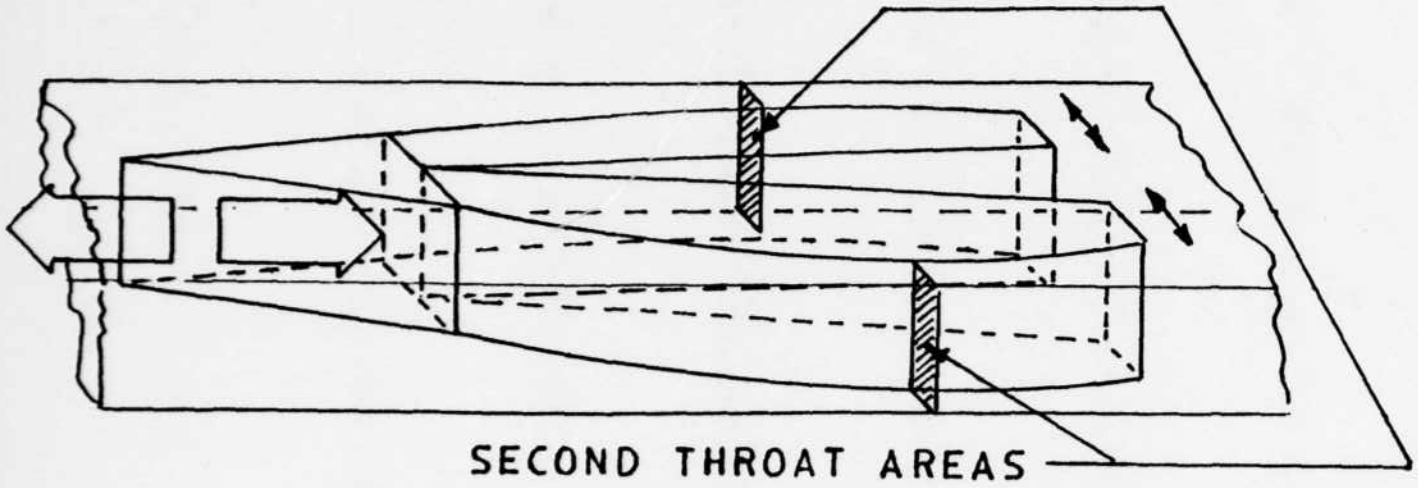

Figure 47. Proposed New Geometry

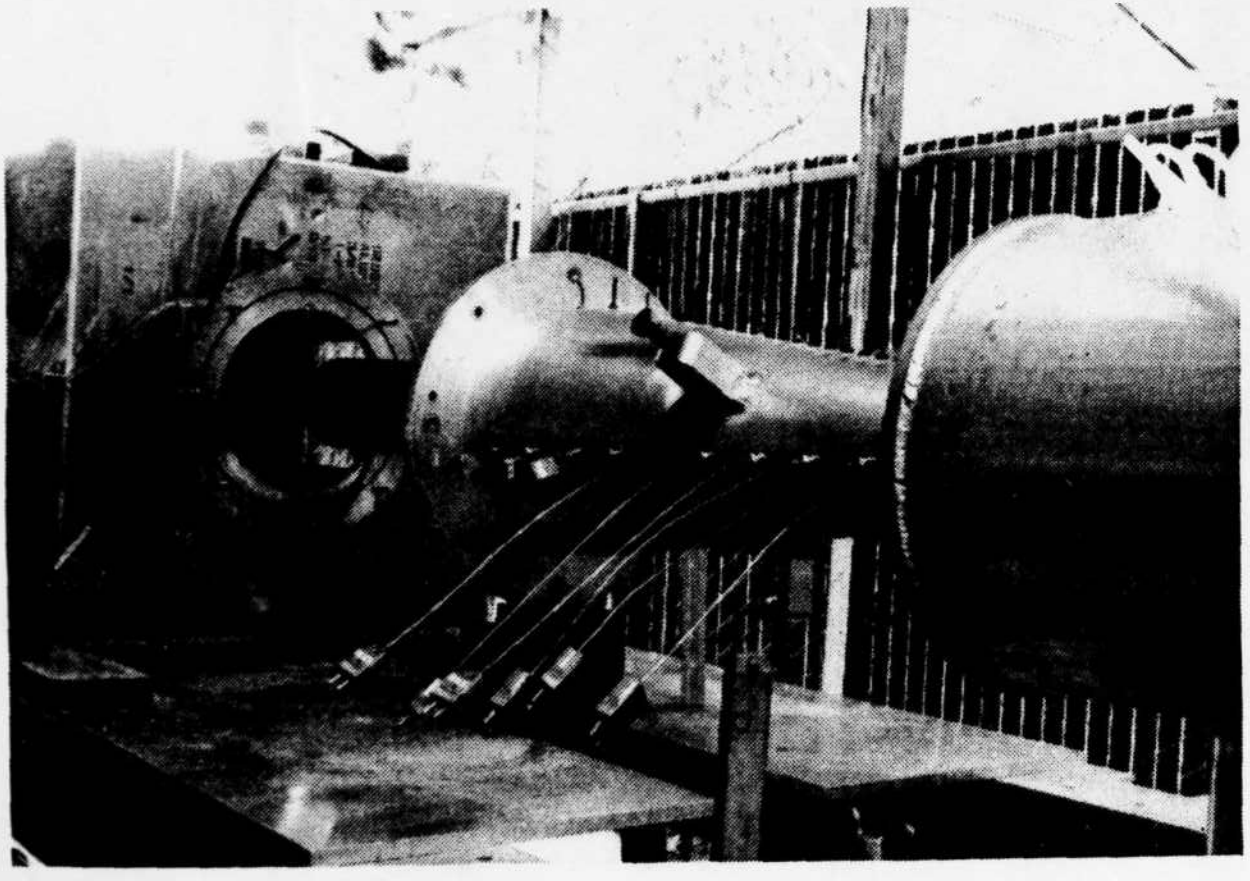

Figure 48. Ejector-Diffuser Thermocouple Installation

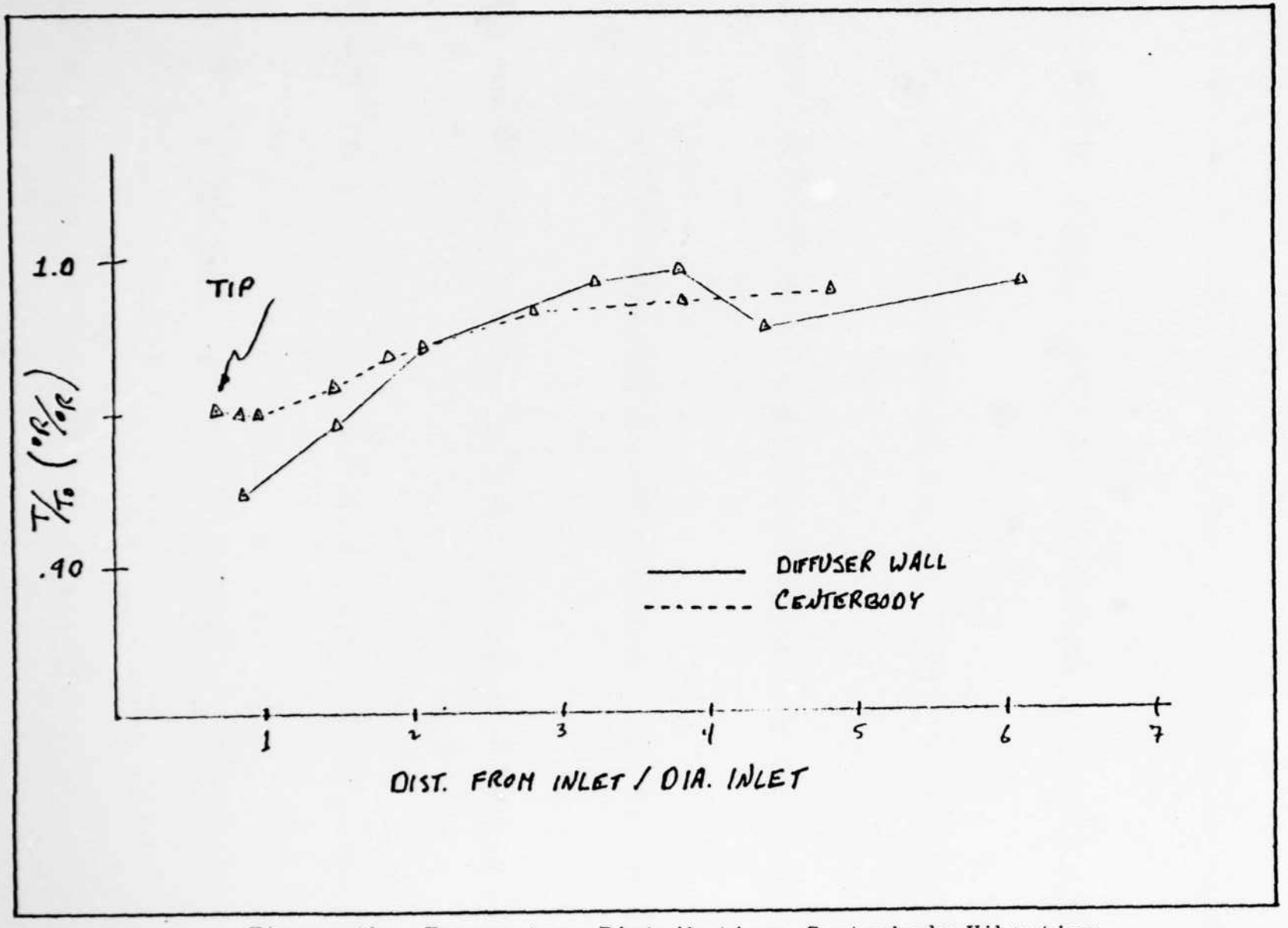

Figure 49. Temperature Distribution; Centerbody Vibrating

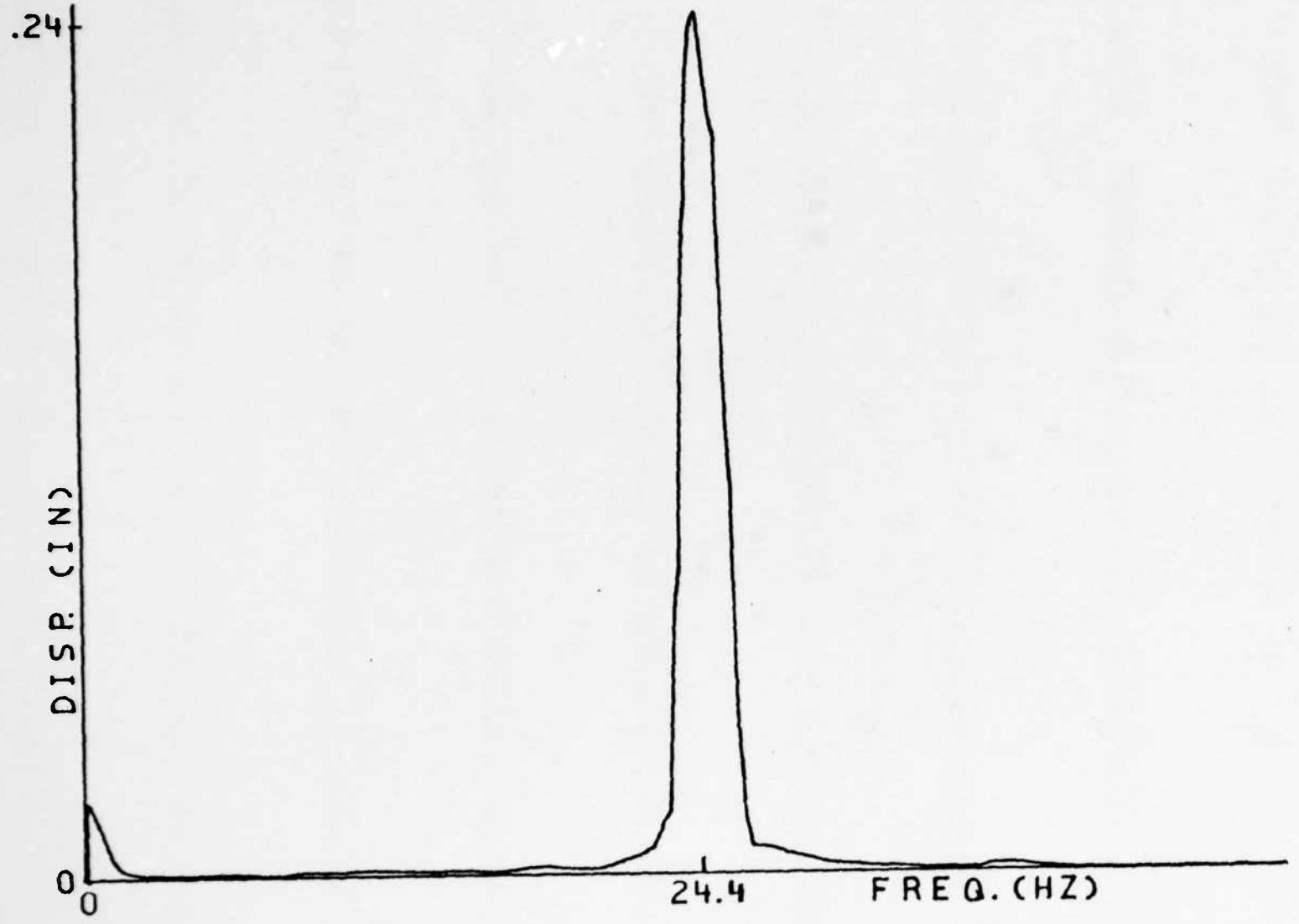

Figure 50. Centerbody Vibration; Horizontal Plane

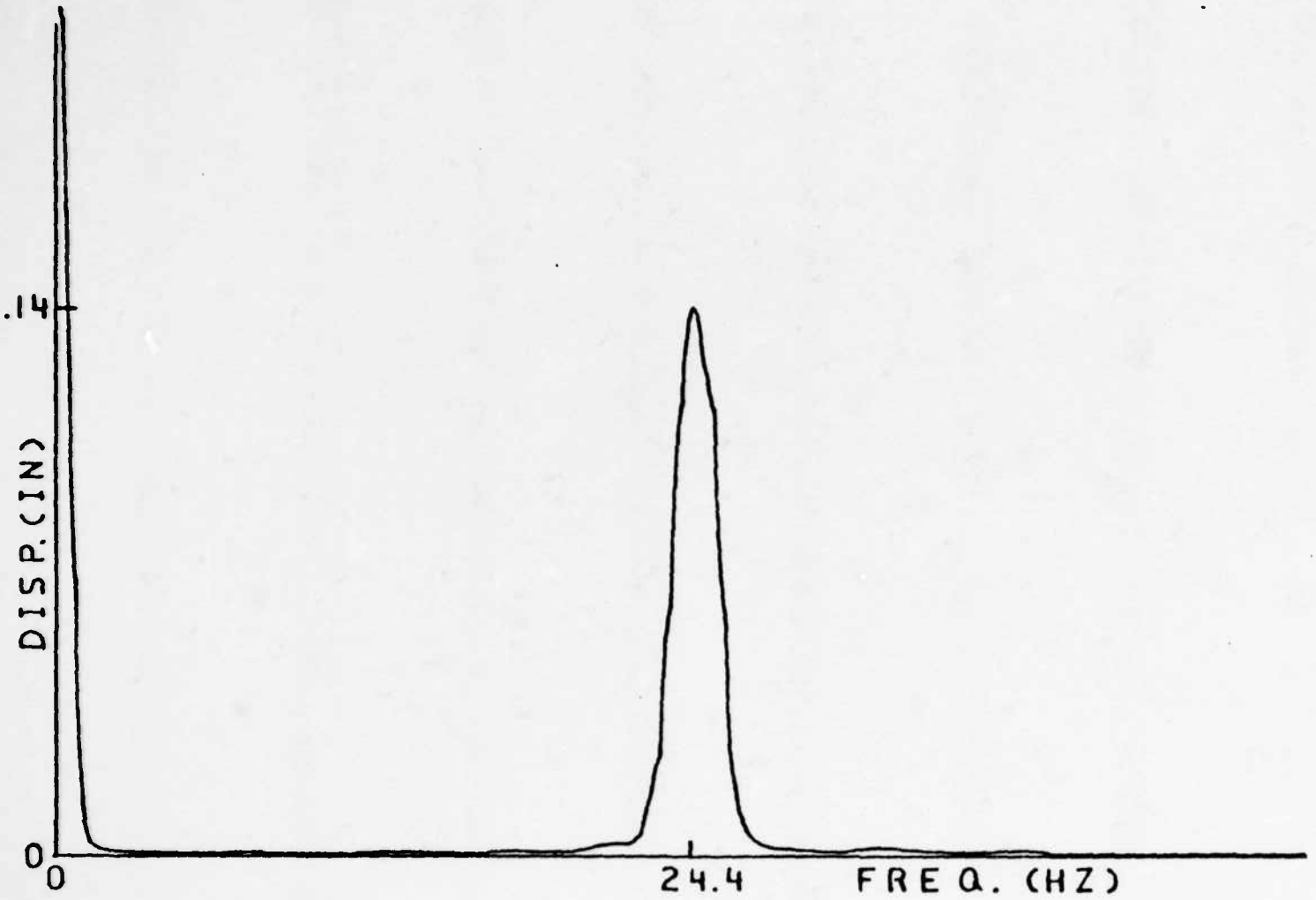

Figure 51. Centerbody Vibration; Vertical Plane

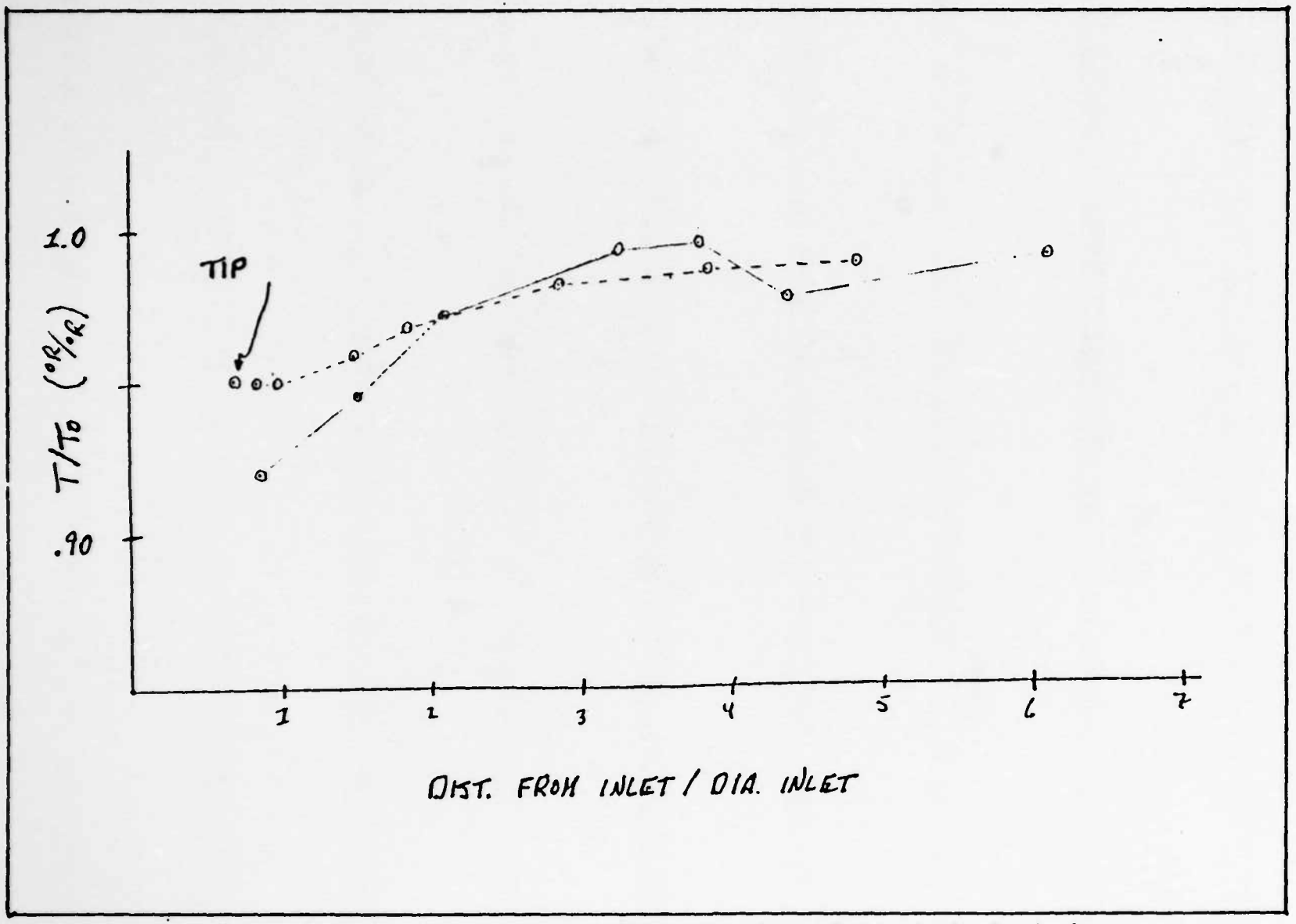

Figure 52. Temperature Distribution; Centerbody Locked

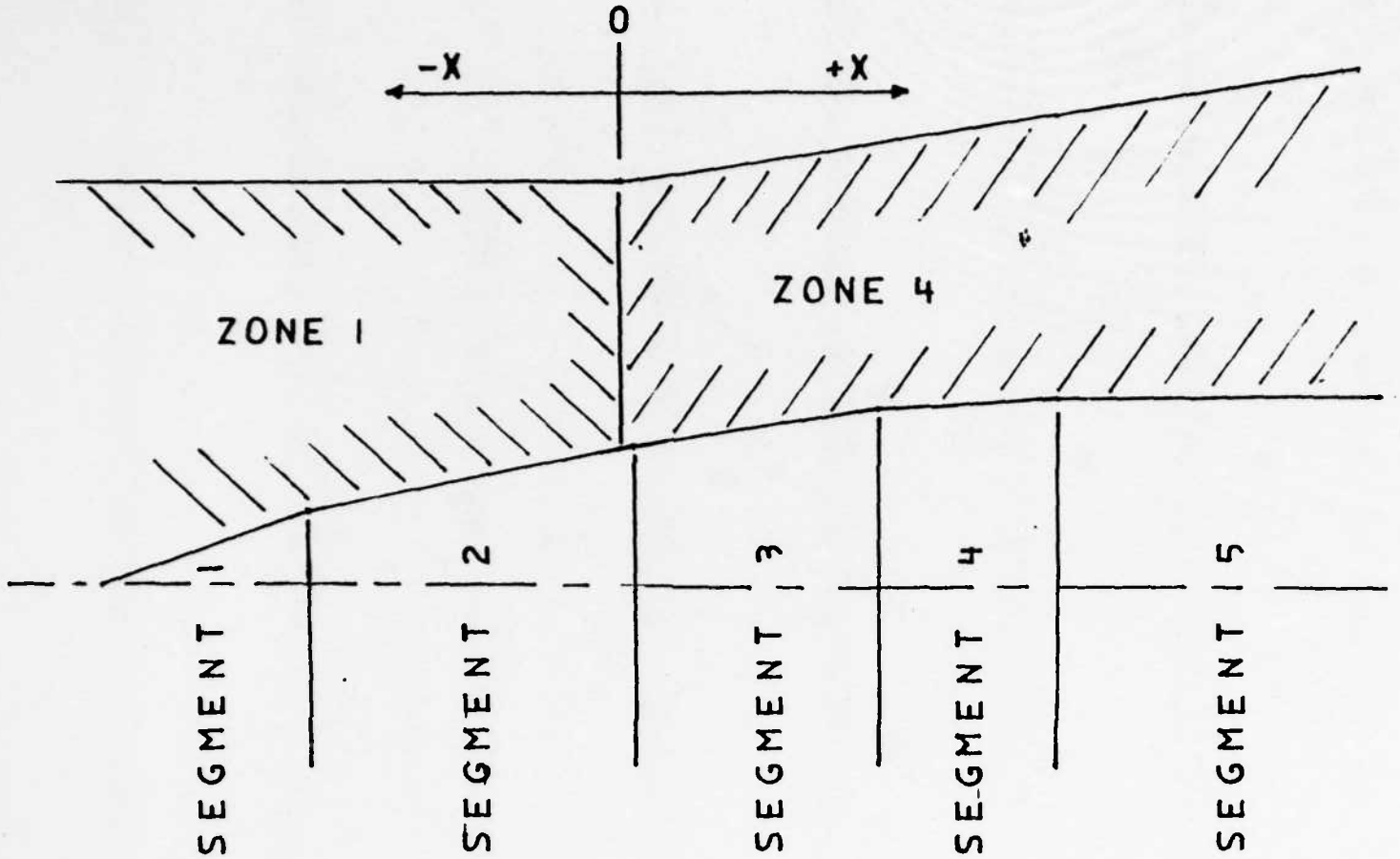

Figure 53. Diffuser/Centerbody Zones and Segments

TABLE I

Data Acquisition Program

```
10 REM      FILE NAME: "VIBTEM"
20 REM
30 REM      DESCRIPTION:
40 REM      THIS PROGRAM PERFORMS SEQUENTIAL SCANNING
50 REM      OF SCANIVALVE '5' BETWEEN PORT ADDRESSES 1-42 IN STEPS OF ONE.
60 REM      IT ALSO PERFORMS TEMPERATURE MEASUREMENTS ON SRC '2' BETWEEN
70 REM      CHANNELS 1-19
80 REM
90 REM      VARIABLES FOR S/V SECTION.
100 REM        V  = DESIRED S/V
110 REM        A1 = LOW PORT
120 REM        A2 = HIGH PORT
130 REM        P  = PRESENT S/V PORT
140 REM        S  = STEP SIZE
150 REM       VARIABLES FOR TEMPERATURE SECTION.
160 REM        S$=SCANNER LISTEN CODE
170 REM        S=SCANNER #
180 REM        C1=LO CHANNEL
190 REM        C2=HI CHANNEL
200 REM        C=TRANSMITTED CHANNEL
210 REM        V=DVM READING
220 REM        R=RPM CHANNEL
230 PRINT
240 PRINT
250 PRINT
260 PRINT
270 PRINT
280 PRINT
290 DIM X[50],Y[20],Q[10],M[30],Z[50]
300 MAT X=ZER
310 MAT Y=ZER
320 MAT Q=ZER
330 MAT M=ZER
340 MAT Z=ZER
350 DISP "ENTER MONTH,DAY,YEAR OF RUN";
360 INPUT X[44],X[45],X[46]
```

```
370 WRITE (15,380)X[44],X[45],X[46]
380 FORMAT "DATE OF RUN:",F2.0,2X,F3.0,2X,F4.0
390 PRINT
400 PRINT
410 DISP "ENTER RUN #";
420 INPUT X[47]
430 X[49]=1
440 DISP "BAROMETER READING=?";
450 INPUT X[48]
460 PRINT "BAROMETER READING INCHES OF HG="X[48]
470 PRINT
480 PRINT
490 FORMAT B
500 FORMAT 2B
510 FORMAT 4B
520 FORMAT F3.0
530 GOTO 600
540 FOR I=1 TO 42
550 X[I]=0
560 NEXT I
570 FOR I=1 TO 19
580 Y[I]=0
590 NEXT I
600 WRITE (15,610)X[47],X[49]
610 FORMAT /,"RUN #",F3.0,4X,"PT #",F3.0
620 GOSUB 1320
625 PRINT "PRESSURES ? 1=YES 0=NO";
626 INPUT K1
627 IF K1=0 THEN 900
630 PRINT
640 PRINT
650 REM*****START OF PROGRAM SEGMENT TO RECORD PRESSURES**********************
660 WRITE (13,510)256,20,768,512;
670 CMD "?D#","F1R7M3A1H1T3"
680 V=5
690 A1=1
```

```
700 A2=42
710 S=1
720 CMD "?D'"
730 WRITE (13,490)V;
740 WRITE (15,750)V
750 FORMAT "SCANIVALVE #",F3.0,/,/," PORT",8X,"IN H20 "
760 FOR A=A1 TO A2
770 GOSUB 1040
780 CMD "?D!"
790 WRITE (13,520)V+9
800 CMD "?D#","T3"
810 CMD "?C$"
820 ENTER (13,*)V0
830 X[A]=V0*100000
840 V0=V0*100000
850 WRITE (15,860)P,X[A]
860 FORMAT 1X,F3.0,4X,F8.2
870 CMD "?D!","C"
880 NEXT A
890 GOTO 900
900 DISP "ENTER TIP VOLTAGE ";
910 INPUT V9
920 P9=(V9-4.5839)/(-0.8248)-4.886
930 WRITE (15,940)P9
940 FORMAT 1X,"TIP POSITION ",F7.3,1X,"INCHES"
950 PRINT "---------------------------------"
960 DISP "ENTER 1 TO REPEAT";
980 INPUT R
990 X[49]=X[49]+1
1000 IF R=1 THEN 540
1010 STOP
1020 END
1030 REM  SUBROUTINE "POSIT"
1040 GOSUB 1220
1050 D=A-P
1060 CMD "?D!"
```

```
1070 IF D<0 THEN 1100
1080 IF D>0 THEN 1150
1090 RETURN
1100 REM    HOME S/V
1110 WRITE (13,520)V+4
1120 WRITE (13,*)"C"
1130 WAIT 4000
1140 GOTO 1040
1150 REM     ADVANCE S/V
1160 FOR I=1 TO D STEP S
1170 WRITE (13,520)V-1
1180 WRITE (13,*)"C"
1190 WAIT 200
1200 NEXT I
1210 GOTO 1040
1220 REM     READ S/V ADDRESS
1230 CMD "?G$"
1240 P0=RBYTE13
1250 L=BIAND(P0,15)
1260 T=ROT(P0,4)
1270 M=BIAND(T,7)
1280 P=10*M+L
1290 WRITE (13,500)256,95;
1300 RETURN
1310 REM*****SUBROUTINE TO RECORD TEMPS*****************************************
1320 DIM S$[3]
1330 FORMAT F3.0
1340 FORMAT 3B
1350 FORMAT 4B
1360 REM
1370 OUTPUT (13,1350)256,20,768,512;
1380 CMD "?D#","F1R7M3A1H1T3"
1390 S=2
1400 C1=60
1410 C2=78
1420 S$="?D("
```

```
1430 WRITE (15,1440)S
1440 FORMAT 5X,"SCANNER #",F2.0,/,/,2X,"CHAN",6X,"TEMP DEG. R"
1450 FOR C=C1 TO C2
1460 CMD S$
1470 OUTPUT (13,1330)C
1480 CMD "?D#"
1490 OUTPUT (13,1340)256,8,512;
1500 CMD "?C$"
1510 ENTER (13,*)V
1520 B=C-59
1530 Y[B]=V
1540 NEXT C
1550 Y1=Y[1]
1560 FOR I=1 TO 19
1570 Y[I]=Y1+Y[I]
1580 Y[1]=Y[1]/2
1590 Y[I]=FNT(Y[I]*1000)+460-0.42
1600 IF I<14 THEN 1610
1610 Y[I]=Y[I]+1.26
1620 IF I<8 THEN 1630
1630 Y[I]=Y[I]+0.42
1640 WRITE (15,1650)I,Y[I]
1650 FORMAT 2X,F3.0,3X,F14.6
1660 NEXT I
1670 WRITE (15,1680)
1680 FORMAT /,/
1690 CMD S$,"C"
1700 RETURN
1710 STOP
1720 DEF FNT(V)
1730 S1=32.0787+46.34*V-1.0515*V↑2
1740 S2=25.661297*V-0.61954869*V↑2+0.022181644*V↑3-0.00035009*V↑4
1750 S3=32.0787+9*S2/5
1760 RETURN S3
1770 STOP
```

AD-A134 843 VARIABLE AREA EJECTOR-DIFFUSER MODEL TESTS(U) NAVAL POSTGRADUATE SCHOOL MONTEREY CA T H WALSH SEP 83 2/2

UNCLASSIFIED F/G 21/5 NL

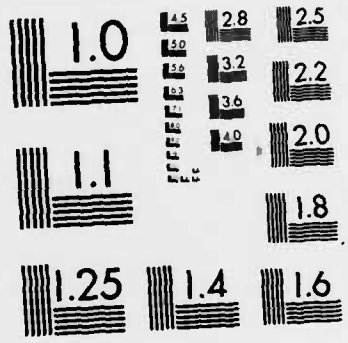

MICROCOPY RESOLUTION TEST CHART
NATIONAL BUREAU OF STANDARDS-1963-A

TABLE II

Test System Matrix

1 Minimum Ptotal Minimum Pexhaust	2 Minimum Ptotal One Half Pexhaust	3 Minimum Ptotal Atmospheric Pexhaust
6 One Third Ptotal Minimum Pexhaust	5 One Third Ptotal One Half Pexhaust	4 One Third Ptotal Atmospheric Pexhaust
7 Two Thirds Ptotal Minimum Pexhaust	8 Two Thirds Ptotal One Half Pexhaust	9 Two Thirds Ptotal Atmospheric Pexhaust
12 Maximum Ptotal Minimum Pexhaust	11 Maximum Ptotal One Half Pexhaust	10 Maximum Ptotal Atmospheric Pexhaust
13 Maximum Ptotal Minimum Pexhaust Secondary Mass Added		

TABLE III

Raw Data

DATE OF RUN 8/10/83
ENGINE TESTED J404 W/AFTER BURNER
REFERENCE DATA FILE MODEL
RUN 1A

	TEST PT. NUMBER									
	1	2	3	4	5	6	7	8	9	10
P ATM	29.92	29.92	29.92	29.92	29.92	29.92	29.92	29.92	29.92	29.92
P 01S	-64.70	-103.90	-152.60	-92.20	-125.33	-175.40	-102.10	-173.00	-248.20	-123.60
P 02S	-64.70	-104.00	-150.40	-92.10	-125.33	-175.90	-102.00	-173.00	-248.80	-124.90
P 03S	-65.40	-104.20	-153.60	-92.00	-127.00	-174.90	-102.50	-173.10	-249.20	-123.10
P 04S	-66.70	-103.90	-155.90	-91.90	-127.10	-174.90	-103.30	-171.70	-246.30	-125.80
P 01P	411.50	416.60	417.10	543.70	539.60	538.00	670.60	670.30	666.30	798.90
P 02P	411.20	416.80	415.40	543.20	538.63	536.53	669.40	671.30	665.70	797.50
P 03P	410.80	415.50	416.20	543.30	537.10	538.00	668.90	669.60	667.50	798.60
P 04P	410.80	415.50	416.20	543.30	537.13	538.30	668.90	669.63	667.50	798.60
P TOT	407.20	412.80	412.70	539.20	533.90	533.40	664.30	665.40	662.40	792.10
P TST	436.60	412.60	411.90	536.50	531.70	531.50	663.70	663.70	660.10	791.30
P CEL	-64.70	-104.00	-150.30	-92.50	-126.90	-174.10	-103.90	-171.90	-250.30	-124.80
P THS	395.40	401.40	400.80	526.50	518.90	519.80	649.10	649.30	648.30	775.90
P THT	-50.30	-47.90	-48.70	5.90	3.33	3.43	59.70	60.00	59.30	115.10
P THT	-71.20	-68.60	-69.50	-18.90	-21.33	-21.20	31.20	31.80	31.00	83.10
P D01	-66.80	-105.60	-152.60	-92.50	-125.73	-177.00	-102.70	-172.90	-253.20	-125.70
P D02	-52.10	-97.90	-157.20	-94.10	-128.20	-176.80	-103.70	-174.00	-254.50	-124.30
P D03	-38.40	-89.70	-154.60	-90.10	-125.80	-169.40	-99.40	-173.80	-249.40	-121.20
P D04	-29.20	-80.70	-145.70	-82.40	-119.50	-158.80	-89.00	-163.30	-248.20	-113.20
P D05	-15.70	-67.30	-127.30	-67.80	-105.80	-143.60	-73.50	-148.20	-238.50	-98.20
P D06	-11.60	-55.30	-109.30	-49.50	-93.50	-125.90	-50.60	-131.00	-227.00	-75.70
P D07	-9.20	-50.50	-99.50	-35.90	-83.20	-115.40	-37.50	-116.10	-215.10	-57.00
P D08	-10.40	-47.20	-91.90	-27.00	-69.80	-108.30	-27.50	-107.50	-204.60	-49.40
P D09	-10.20	-46.00	-85.00	-20.10	-61.70	-101.50	-22.60	-97.10	-193.00	-40.60
P D010	-9.60	-45.10	-81.50	-15.90	-57.10	-95.50	-17.60	-89.20	-182.00	-30.40
P D011	-9.50	-43.10	-77.60	-10.60	-46.53	-90.50	-9.30	-74.20	-155.40	-18.10
P D012	-7.70	-42.50	-76.50	-9.40	-43.13	-88.70	-7.20	-68.00	-133.30	-12.80
P D013	-8.20	-41.80	-75.60	-8.10	-41.33	-89.20	-5.50	-65.33	-122.40	-10.10
P D014	-7.80	-41.60	-76.10	-7.40	-40.73	-87.60	-5.50	-64.90	-119.80	-11.10
P D015	-7.70	-41.30	-76.10	-7.60	-41.70	-87.00	-6.30	-65.00	-120.60	-9.00

DATE OF RUN 8/10/83
ENGINE TESTED F404 W/AFTER BURNER (CONTINUATION)
REFERENCE DATA FILE
RUN 1A

	TEST PT. NUMBER									
	1	2	3	4	5	6	7	8	9	10
P D016	-7.50	-41.00	-76.80	-7.70	-41.90	-88.40	-6.60	-66.20	-121.00	-9.30
P D017	-6.70	-41.30	-75.90	-7.40	-41.30	-88.10	-6.40	-64.40	-120.70	-9.80
P D018	-5.80	-40.40	-74.20	-5.80	-40.60	-87.40	-4.90	-61.90	-117.30	-6.30
P D019	-4.80	-39.30	-72.40	-3.50	-38.30	-84.30	-3.30	-60.30	-115.40	-4.30
P D020	-4.40	-38.10	-72.60	-2.90	-38.10	-82.80	-2.50	-60.50	-113.60	-3.70
P D021	-4.60	-37.80	-72.10	-2.80	-38.40	-82.60	-2.50	-58.20	-113.50	-3.40
P D022	-4.70	-38.00	-72.40	-2.60	-38.80	-83.10	-2.30	-58.80	-114.10	-3.60
P D023	-4.30	-37.50	-71.90	-3.00	-37.70	-83.60	-2.70	-57.70	-114.30	-2.60
P D024	-4.30	-37.80	-71.80	-2.80	-37.50	-83.10	-2.50	-58.60	-113.70	-2.20
P EXH	-4.10	-38.00	-71.80	-2.70	-37.90	-82.60	-2.30	-57.20	-114.00	-1.50
C POS	-4.66	-3.81	-4.52	-4.18	-4.35	-4.21	-4.15	-4.54	-4.23	-4.41
T PRI	559.90	556.50	549.70	564.90	567.30	567.30	573.10	571.60	569.00	576.80
T SEC	562.30	551.00	539.70	568.30	563.30	559.90	579.20	565.80	559.40	594.10
T TOT	563.20	558.70	549.60	569.50	570.70	570.30	578.30	578.20	571.90	581.70
T C01	560.50	558.10	547.40	562.40	564.30	563.60	571.10	565.60	563.30	573.70
T C02	560.50	558.00	547.10	561.90	563.90	562.80	570.70	565.30	562.50	572.40
T C03	560.30	557.50	545.80	561.10	562.80	561.80	569.50	564.10	560.60	570.90
T C04	561.40	557.20	543.10	561.20	562.10	561.10	569.00	562.10	555.80	569.20
T C05	563.00	558.30	548.90	564.80	562.30	565.30	573.10	564.30	557.10	572.80
T C06	564.50	559.00	547.50	569.20	570.80	571.20	578.40	572.90	569.30	580.90
T C07	564.50	558.70	546.70	569.90	572.10	572.80	579.30	575.10	572.90	583.00
T C08	564.40	558.30	546.00	569.90	572.30	573.20	579.40	575.70	573.70	583.60
T D01	559.60	552.70	542.10	560.40	561.20	561.00	567.20	565.20	558.70	571.80
T D02	562.30	557.60	548.30	567.70	568.50	568.30	575.60	571.40	564.40	578.40
T D03	570.50	567.20	559.80	576.30	579.30	580.00	587.20	585.10	582.50	591.90
T D04	563.00	558.40	548.40	569.30	571.30	571.70	579.20	575.70	573.60	583.30
T D05	562.30	557.60	547.10	568.40	570.50	571.50	578.80	575.50	573.20	583.10
T D06	565.60	560.10	548.30	570.30	572.40	572.80	581.30	578.00	573.90	586.70
T D07	563.60	555.90	545.80	567.70	570.50	570.40	580.70	575.90	569.00	586.10
T D08	560.90	554.00	544.20	565.60	569.30	569.90	579.20	574.90	570.00	584.50

TABLE IV

Reduced Data

DATE OF RUN 8/10/1983
ENGINE TESTED MODEL F404 W/AFTER BURNER

TEST PT.	MDOT PRI	MDOT SEC	P STAG	T STAG	PTOT/ PCELL	PEXH/ PTOT	PEXH/ PCELL	CB TIP POSIT.
1	0.43450	0.00000	817.0	560.9	2.367	0.497	1.176	-4.66
2	0.43881	0.00000	822.6	554.0	2.690	0.452	1.216	-3.81
3	0.44146	0.00000	822.5	544.2	3.170	0.411	1.303	-4.52
4	0.50246	0.00000	949.0	565.6	2.991	0.429	1.283	-4.18
5	0.49873	0.00000	943.7	569.3	3.335	0.394	1.314	-4.05
6	0.49833	0.00000	943.2	569.9	4.002	0.347	1.388	-4.21
7	0.56461	0.00000	1074.1	579.2	3.511	0.379	1.332	-4.15
8	0.56593	0.00000	1075.2	574.9	4.520	0.328	1.482	-4.54
9	0.56564	0.00000	1072.2	570.0	6.722	0.276	1.855	-4.23
10	0.62976	0.00000	1201.9	584.5	4.217	0.340	1.433	-4.41
11	0.62817	0.00000	1202.4	584.6	5.982	0.286	1.712	-4.63
12	0.62806	0.00000	1202.7	582.5	7.815	0.238	1.863	-3.95
13	0.62847	0.09673	1203.9	534.6	8.437	0.238	2.009	-3.95
14	0.62659	0.06196	1200.1	534.9	8.054	0.240	1.936	-3.95
15	0.62587	0.06712	1201.4	535.2	7.822	0.239	1.870	-3.95
16	0.62564	0.13039	1198.9	535.4	7.765	0.242	1.880	-3.95
17	0.62523	0.04900	1197.9	537.6	7.212	0.242	1.747	-3.95
18	0.62440	0.05232	1196.1	544.3	7.271	0.246	1.791	-3.78

DATE OF RUN 8/11/1983
ENGINE TESTED MODEL TF30 W/AFTER BURNER

TEST PT.	MDOT PRI	MDOT SEC	P STAG	T STAG	PTOT/ PCELL	PEXH/ PTOT	PEXH/ PCELL	CB TIP POSIT.
1	1.39501	0.00000	831.9	531.5	4.371	0.488	2.135	-4.13
2	1.39695	0.00000	831.4	529.9	5.208	0.461	2.399	-4.21
3	1.40966	0.00000	828.4	524.4	5.681	0.436	2.478	-4.29
4	1.59896	0.00000	956.5	533.1	5.911	0.425	2.513	-4.13
5	1.60693	0.00000	964.4	535.2	7.538	0.382	2.877	-4.05
6	1.60072	0.00000	962.4	536.7	8.425	0.344	2.900	-3.86
7	1.73542	0.00000	1049.5	541.1	7.047	0.387	2.730	-3.27
8	1.74172	0.00000	1051.0	539.2	8.446	0.354	2.993	-2.59
9	1.73237	0.00000	1044.3	539.0	10.566	0.319	3.374	-1.89
10	1.73652	0.00000	1047.6	539.4	10.578	0.318	3.369	-2.88
11	1.74048	0.00000	1053.0	541.7	10.474	0.319	3.346	-1.83
12	1.74132	0.00000	1053.6	541.9	10.480	0.321	3.367	-1.86
13	1.74273	0.00000	1054.1	542.1	10.221	0.320	3.272	-1.86
14	1.74494	0.01426	1055.7	542.0	10.596	0.319	3.382	-1.86
15	1.74477	0.03960	1055.6	542.0	10.500	0.318	3.343	-1.86
16	1.74571	0.03058	1055.9	541.8	10.493	0.320	3.355	-1.86
17	1.74114	0.06356	1053.4	541.8	10.437	0.320	3.342	-1.86
18	1.73037	0.12440	1046.8	542.6	9.957	0.327	3.260	-1.86
19	1.72075	0.10588	1041.5	552.7	12.277	0.311	3.820	-2.58

DATE OF RUN 8/12/1983
ENGINE TESTED MODEL TF30 W/OAFTER BURNER

TEST PT.	MDOT PRI	MDOT SEC	P STAG	T STAG	PTOT/ PCELL	PEXH/ PTOT	PEXH/ PCELL	CB TIP POSIT.
1	0.69419	0.00000	800.6	535.5	2.526	0.509	1.287	-4.47
2	0.69554	0.00000	802.3	535.7	2.925	0.467	1.366	-4.70
3	0.69415	0.00000	802.1	535.8	3.372	0.427	1.440	-4.47
4	0.80256	0.00000	931.8	537.1	3.184	0.441	1.403	-4.32
5	0.80265	0.00000	931.1	537.2	3.200	0.441	1.410	-4.71
6	0.80381	0.00000	931.8	536.4	3.851	0.386	1.486	-3.96
7	0.80539	0.00000	932.9	536.2	3.967	0.387	1.534	-4.19
8	0.80300	0.00000	930.3	536.0	3.957	0.387	1.531	-4.32
9	0.80409	0.00000	931.8	536.1	4.742	0.358	1.698	-4.45
10	0.90612	0.00000	1054.4	538.3	3.853	0.388	1.494	-4.05
11	0.90578	0.00000	1054.0	538.2	4.059	0.388	1.574	-4.36
12	0.90785	0.00000	1056.6	539.1	5.252	0.340	1.784	-4.38
13	0.90584	0.00000	1055.8	541.4	7.287	0.285	2.076	-4.15
14	1.02939	0.00000	1185.1	522.6	4.829	0.343	1.658	-4.40
15	1.02501	0.00000	1187.7	523.8	6.733	0.296	1.991	-4.06
16	1.02470	0.00000	1189.2	524.5	5.963	0.292	2.033	-4.34
17	1.02014	0.00000	1188.4	526.5	9.806	0.250	2.452	-4.14
18	1.02098	0.00000	1190.0	527.0	9.747	0.244	2.382	-4.14
19	1.02115	0.02659	1190.3	527.2	9.710	0.252	2.445	-4.14
20	1.02046	0.05986	1189.9	527.5	10.093	0.249	2.513	-4.14
21	1.02088	0.05112	1190.9	527.8	10.145	0.247	2.503	-4.14
22	1.01754	0.11344	1186.8	529.1	8.944	0.249	2.226	-4.14
23	1.01839	0.06676	1188.3	532.1	9.277	0.253	2.350	-4.14
24	1.01529	0.07095	1185.9	542.2	9.130	0.255	2.329	-4.30

DATE OF RUN 8/12/1983
ENGINE TESTED MODEL F404 WO/AFTER BURNER

TEST PT.	MDOT PRI	MDOT SEC	P STAG	T STAG	PTOT/ PCELL	PEXH/ PTOT	PEXH/ PCELL	CB TIP POSIT.
1	0.29001	0.00000	804.4	533.1	2.213	0.495	1.095	-4.40
2	0.29051	0.00000	805.3	533.2	2.397	0.476	1.141	-4.28
3	0.29143	0.00000	806.2	533.1	2.779	0.415	1.154	-4.40
4	0.34212	0.00000	950.8	533.1	2.690	0.423	1.138	-4.43
5	0.34280	0.00000	954.2	533.3	3.114	0.384	1.197	-4.43
6	0.33984	0.00000	946.9	533.3	3.635	0.336	1.221	-4.21
7	0.38573	0.00000	1080.9	534.7	3.187	0.374	1.193	-4.55
8	0.39310	0.00000	1100.2	534.2	3.755	0.314	1.180	-4.13
9	0.38553	0.00000	1077.4	533.9	5.007	0.276	1.380	-4.71
10	0.42895	0.00000	1209.1	535.9	3.570	0.345	1.233	-4.30
11	0.42440	0.00000	1197.3	536.5	4.640	0.284	1.319	-4.32
12	0.42828	0.00000	1209.7	537.3	5.382	0.225	1.434	-4.37
13	0.43022	0.00000	1215.8	537.5	6.609	0.244	1.615	-4.37
14	0.42833	0.04168	1210.9	538.1	5.415	0.233	1.496	-4.37
15	0.42886	0.05087	1213.0	538.5	6.516	0.230	1.497	-4.37
16	0.42846	0.05580	1212.6	538.7	6.445	0.228	1.471	-4.37
17	0.42814	0.07603	1211.8	539.2	6.369	0.231	1.473	-4.37
18	0.42662	0.07587	1207.7	540.7	6.079	0.235	1.429	-4.37
19	0.42647	0.05137	1207.6	547.4	6.106	0.230	1.403	-4.47

TABLE V

Engine Data; F404 and TF30

Engine	Maximum Thrust (lbf)	Stages	MDOT (lbm/sec)	Compressor Press. Ratio
F404	16,000	3 Fan, 7 Comp.	140	25:1
TF30	20,900	16	242	19.8:1

APPENDIX A

DATA ACQUISITION INTERFACE TO DIGITAL MICROCOMPUTER

I. The Digital Equipment Corporation microcomputer system [Ref. 5] as donated to the NPS Mechanical Engineering Department was comprised of four VT103 terminals containing the LSI-11 microcomputer and two TU-58 cassette drives, four LA-34 line printers, and one RX02 eight inch dual disk drive. Two of the terminals and the dual disk drive were intended to be utilized as an integral part of this project. It was intended that one of the terminals, with printer, would be interfaced to the Hewlett Packard bus at TPL. It would be used to control the bus (specifically, the HP-3495A scanner and HP-3455 Digital Voltmeter), collect the raw data from these instruments and mass store the data on cassette tapes, with selected data output to the line printer for monitoring during the test runs. The cassette tapes would then be transported to the Mechnical Engineering Microcomputer Laboratory, loaded into the tape drives of the second VT103 terminal and copied onto floppy disks for backup storage. Next a modem would have been utilized to transfer the data, under program control, to the IBM 3033.

II. Following unpacking, assembly, and installation of hardware the final requirement for an operable system was installation of software. The software included with the

grant consisted of utility programs, device drivers, system subroutine library, and an assembly language compiler. This software was distributed on seven cassette tapes and four dual-sided floppy disks. The floppy disks were the vehicle of choice for building the system, being orders of magnitude faster than the cassette tapes. The LSI-11 microcomputer uses the DIGITAL "RT-11" operating system described in [Ref. 6]. Following lengthy initial study of these instruction manuals and with frequent reference to them, the command syntax was mastered and proficiency was gained in file manipulation and use of the utility programs. The first major order of business was to make backup copies of the software distribution disks for safekeeping. System volumes were then built and tested for both floppy disk and cassette tape. Subsequently the software for installation of the higher level Fortran and Basic languages became available. These two languages with their attendant libraries, compilers, and interpreters were then installed on the RT-11 operating system and tested. The system volumes were modified to include these languages.

III. Most modern instruments are based on digital logic circuits and hence are amenable to interconnection on a bus with control and monitoring by one or several digital computers. To facilitate this type of interconnection using machines of different manufacturers, some type of standardization is necessary. This standard has been provided by

the Institute of Electrical and Electronics Engineers (IEEE) [Ref. 7] in the form of standardized bus connectors and intercommunication by means of standardized logic or "hand-shake" signals. All the instruments at TPL conform to this standard. To allow the LSI-11 microcomputer to communicate with and control these instruments using the IEEE standards, purchase of an additional circuit board (IBV11-A) was required. This circuit board was purchased from DIGITAL and was subsequently received. Unfortunately, the IBV11-A was not accompanied by any software. The instruction manual [Ref. 8] did include two very sketchy outlines of assembly language routines used for communication to and from the IBV11-A interface. The IBV11-A was installed in the VT103 terminal and a test devised wherein a Fortran program and assembly language subroutine were written directing a HP-5150A Thermal Printer to output a string of ASCII characters. This test never succeeded. Attempts to examine the memory registers assigned to the IBV11-A resulted in the microcomputer sending a message that the IBV11-A did not exist. This was confirmed by Mr. Bernard Hayes, a DIGITAL representative, who then advised that the IBV11-A was malfunctioning and should be returned for repair under warranty, which has been done.

APPENDIX B

SCALING OF MODELS

Design of a subscale altitude test facility to approximate the salient features of the parent facility at the Naval Air Propulsion Center was governed by a multiplicity of interwoven factors. The underlayment for the design was the motive air supply; compressed air from an Allis-Chalmers twelve-stage axial compressor (Figure 2). The dictates of the air supply qualified several engines from the family of engines tested by NAPC as candidates for scaled testing. The candidate engines elected, as listed in Table V were, from a first cut, the most likely to give a broad representation of existing test frames suitable for comparative analysis with alternative ejector-diffuser geometries. Two after burning engines were elected to span the operating range of the test facility from zero induced secondary flow to five (5) percent secondary flow. The choice of engines provided the vital ingredient upon which scaling of the facility could proceed.

Scaling to achieve Mach number similitude was elected consistent with past studies by Merkli [Ref. 10] and Bevilaqua and Combs [Ref. 11]. The geometry of a scale model may easily match the prototype but simultaneous matching of Mach and Reynolds numbers is impossible. A match in Mach number will present a model with a smaller

Reynolds number. A match of Reynolds numbers induces a higher Mach number in the model. Noting that large Reynolds numbers, consistent with fully turbulent flow, are characteristic of the prototype, any variations in Reynolds number would affect scaling only if a shift to less than fully turbulent flow was created. At a projected mass flow rate for the model of .5 lbm/s, a simple calculation results in a Reynolds number in excess of 1X10**6 thus relegating Reynolds effects to second order. It bears observation, however, that any flow phenomena which are sensitive to Reynolds number such as separation and reattachment will not result in agreement between model and prototype. Any improvement in diffusion which results from a geometric change must address this consideration.

Once Mach number had been established as the scaling parameter, the cold flow model carried with it a significant scaling bonus. Mach number is inherently insensitive to thermal effects since temperature appears as a dependent variable in both the stream and sonic velocities which comprise the ratio. In the context of this study, an order of magnitude difference between cold flow and hot flow temperatures will fail to elevate Reynolds effects beyond second order. At worst, an error within the range of computational accuracy is anticipated due to temperature extremes between model and prototype with the model outperforming the prototype. Work conducted by Welch [Ref. 12] with subsonic

exhaust stack eductors using Mach number scaling shows deviations of less than 1% between hot and cold flow model test results. An order of magnitude in temperatures variation occurs in these studies.

The TF30AB, having the largest throat area, governed the compressor-engine match. One dimensional isentropic nozzle flow theory for choking specifies mass flow will obey the following expression:

$$\dot{m} = \frac{.532\ Po}{\sqrt{To}}$$

The available air supply had the capacity to deliver 2.65 atmospheres and 12.0 lbm/sec at 600 degrees R. 2.65 atmospheres would be the maximum achievable ratio of Pt to Pex under atmospheric conditions in the nozzle exit. This ratio was below the desired test range but could be boosted by utilizing an exhaust eductor to lower Pex at the expense of air flow to drive the apparatus.

A survey of ejectors previously driven by this compressor revealed one design with a convergent-divergent nozzle operating with half an atmosphere back pressure and capable of pumping 2.0 lbm/sec with the exhaust eductor drawing 8.85 lbm/sec. The total flow of 10.85 lbm/sec was well within the capability of the compressor, and 2.0 lbm/sec was chosen as the design mass flow rate for an expected Pt/Pex equal to 5.70. For 2.0 lbm/sec at 2.65 atmospheres and 600 degrees R, a throat diameter (d*) was

computed to be 1.735 inches. A conservative design of 1.675 inches was chosen for d* which resulted in an A* = 2.204 in**2 and mass flow equal to 1.863 lbm/sec.

The TF30 has an actual throat area of 7.5 ft**2 and a diameter of 3.09 feet. Dividing this by the throat of the model, a scaling factor of 22.139 is derived. Full scale drawings of the test cell and diffuser assemblies to be modelled were scaled using this factor.

APPENDIX C

CALCULATION OF SECOND THROAT AREAS

A computer program was written to calculate the least distance between the centerbody and the diffuser wall along with the corresponding annular cross sectional area available to air flow through the ejector-diffuser. As seen in Figure 53 the zero or stowed position of the centerbody tip is in a plane normal to the centerline of the ejector-diffuser and passing through the point where the diffuser transitions from a right circular cylinder to a right circular frustrum of a cone. The program accepts the single signed argument of tip position (inches) and returns, in 0.1 inch increments of the x-axis, the closest distance (inches) and annular cross sectional area (in**2). The centerbody surface is divided into four conical segments and one cylindrical segment. Each segment has a different half-angle, with a separate subroutine (D1 through D5) written for each. The ejector-diffuser is separated into two zones; 1 and 4. As the program steps through the 0.1 in. increments along the x-axis, it determines which conical segment of the centerbody it is on and in which zone of the ejector-diffuser's geometry it is in. If it is in zone 1, the least distance is calculated normal to the diffuser wall, and if it is in zone 4 the least distance is calculated

normal to the surface of the centerbody. A plot of cross sectional area versus tip position is shown in Figure 11.

APPENDIX D

SYSTEM STARTUP PROCEDURE

The Allis-Chalmers compressor was maintained and operated by TPL personnel. Twenty minutes of prelubrication was required on the compressor prior to start followed by approximately twenty minutes of warmup before the compressor was ready to assume the load of supplying air to the experimental apparatus. During this time it was prudent to accomplish the following checks and tasks:

1. Examine all pressure taps, tubing, and connections to pressure scanner port manifold and the two dedicated pressure transducers.

2. Turn on thermocouple ice point reference and examine all thermocouples for broken wires or loose connections.

3. Hand test all PVC couplings for tightness and check to see that the primary and secondary root valves are open.

4. Turn on and test the centerbody drive mechanism to ensure full travel in both directions.

5. Turn on the HP-9830A Calculator and printer, HP-9867B Mass Memory Storage Unit, pressure scanner multiplexer (S/V MUX) HP-3495A Scanner, HP-3455 Digital Voltmeter, pressure scanner control power supply and the three separate digital voltmeters used for monitoring centerbody

drive voltage, engine test cell pressure, and exhaust chamber pressure.

6. Load the program "VIBTEM" (Table I) into the memory of the HP-9830A calculator. Run the program once to ensure there are no anomalous readings from any thermocouple or pressure tap.

7. Read and record atmospheric pressure from the Wallace & Tiernan gage.

The following miscellaneous instruments were utilized during test runs:

Barometric Pressure (in. Hg)------Wallace & Tiernan, model FA139
Centerbody Position (volts)-------Keithley DMM, model 168
Exhaust Chamber Press (in. H_2O)---Calif. Inst. Corp. DMM, series 8300
Test Cell Pressure (in. Hg)-------Calif. Inst. Corp. DMM, model 51

APPENDIX E

VIBRATION AND HEATING OF CENTERBODY AND DIFFUSER WALL

During the preliminary trial runs of the test apparatus, it was noted that, with the TF30 nonafterburning model installed and maximum total pressure being delivered, there was a severe rumbling vibration of the entire apparatus accompanied by a pronounced heating of the centerbody and ejector-diffuser wall. The extent of the heating was such that it was not possible to keep one's hand in contact with the diffuser. Prior to assembly of the test system modules the centerbody surface had been coated with machinist's blue dye. The centerbody tip (first conical segment) experienced higher temperatures than the remainder of the centerbody, as evidenced by the blue dye having been burned off the entire first segment. Observation of the centerbody through the plexiglass window while this phenomenon was occurring revealed that the centerbody was whipping violently and appeared to be the cause of the vibration. Heating of the diffuser wall was noted to be much less when the centerbody was vibrating at a minimal level. It was theorized that the inordinate heating at high vibration levels was due to an effect other than normal frictional heating caused by the boundary layer. It was decided to instrument the centerbody

and diffuser walls with thermocouples to allow more concrete quantification of any temperature rise.

The apparatus was disassembled for modification at which time it was noted that the welds on two of the centerbody shaft support spider arms were cracked completely through. The spider was repaired by welding on six small gussets (Figure 9), one on either side of each arm. Slots were milled in the surface of the centerbody, eight type T thermocouples were epoxied into the slots (Figure 7) and the epoxy was dressed flush with the surface of the centerbody. Ten type-T thermocouples were installed equally spaced along the length of the ejector-diffuser walls (Figure 48). Only eight of the thermocouples were subsequently used due to limitations of the data acquisition wiring at TPL.

Data on the frequency and amplitude of the centerbody vibration was also desired. Determination of the type of transducer necessitated preliminary calculation of the system's fundamental frequency. The centerbody was modelled as a cantilevered beam (supported at the spider) with a concentrated tip mass. Using Rayleigh's method as given in Thomson [Ref. 9] the fundamental frequency:

$$\omega_1 = \left[\frac{3EI}{(M + \frac{33}{140} M_s)\ell^3}\right]^{0.5}$$

where ω_1 is the fundamental frequency and using 30 x 10**6 lbf/in**2 for E (Young's Modulus) of the steel shaft, 0.015532 in**4 for I (moment of inertia of the .75 inch

diameter shaft, 14.889 lbm for M (mass of the centerbody), 0.7566 lbm for Ms (mass of the shaft), and 12.537 inches for 1 (distance from spider to centroid of shaft and centerbody) the resulting ω_1 = 134.81 rad/sec or 21.46 Hz.

Knowing the fundamental or natural frequency of the system it was decided to use self temperature compensating strain gages as transducers. Two pairs of Vishay Measurements Group, Inc. EA-06-250BG-120 strain gages were installed on the centerbody support shaft immediately adjacent to the centerbody in two perpendicular planes (vertical and horizontal). The voltage signals from the gages were fed into two Ellis Associates BAM-1 Bridge Amplifiers and then to a HP-3582A Spectrum Analyzer. With the centerbody and spider installed the centerbody was displaced in steps by means of a small hydraulic jack. Displacement was read with a dial indicator and plotted versus voltage output of the strain gages to obtain a calibration curve for the amplitude readings of the spectrum analyzer.

Following these modifications the apparatus was run with the same engine (TF30NAB) that had been installed when the heating phenomenon had occurred earlier. Temperatures were collected with the same data acquisition system as discussed in Chapter II. Amplitude and frequency were displayed for both the horizontal and vertical planes on the HP-3582A Spectrum Analyzer and were plotted on a HP-7035B X-Y Recorder. For the TF30NAB at the maximum total pressure, minimum exhaust pressure, and centerbody at point of highest

vibration, a temperature distribution profile for the centerbody and diffuser wall are shown in Figure 49 along with plots of the horizontal and vertical amplitude and frequency in Figures 50 and 51. Maximum vibration was produced with the centerbody inserted 2.25 inches from the reference position. The natural frequency and amplitude corresponding to these test conditions were 24.4 Hz and .24 inches, respectively (amplitude measured from the static position to point of maximum displacement).

The heavy rumbling vibration could not be reproduced nor was the heating, as judged by the touch test, nearly as severe as it had been in the earlier runs. Examination of the temperature gradients along the centerbody and diffuser wall showed that the temperature never exceeded the total temperature at the inlet to the engine model. Part of the reason that the temperature distribution is spread out is due to the high thermal conductivity of the model, which was fabricated from aluminum. The diffuser had also had locking pins (Figure 48) installed which could be driven through the diffuser wall to contact the centerbody and fix it rigidly. When this was done there was not a significant change in the temperature profiles or gradients (Figure 52), which tends to discount the possibility that the heating noted on these instrumented runs was due to any vibration of the shock systems. It is believed that the conditions of the run where the extraordinary vibration and heating were noticed

were unable to be recreated due to the centerbody and its support system having a much higher spring constant following the addition of the six new gussets. Secondarily, a new shaft bushing was installed in the spider following its repair in order to regain proper alignment of the centerbody with the diffuser centerline. The clearance of the centerbody shaft to the new bushing was different, also affecting the spring constant.

LIST OF REFERENCES

1. Arnold Engineering Development Center, Report AEDC-TR-73-198, Diffuser Studies by D. Taylor, February, 1974.

2. American Society of Mechanical Engineers Supplement on Instruments and Apparatus, Flow Measurement, 1959.

3. Molloy, J. W., Ejector-Diffuser Design, Engineer's Thesis, Naval Postgraduate School, September, 1983.

4. Geopfarth, R. N., Development of a Device for the Incorporation of Multiple Scanivalves into a Computer-Controlled Data System, M.S. Thesis, Naval Postgraduate School, March, 1979.

5. Digital Equipment Corporation, Worldwide Educational Grant Program Configuration Guide, 1982.

6. Digital Equipment Corporation, RT-11 V04 Instruction Manuals, Volumes 1A, 1B, 2A, 2B, 3A, 3B, 1981.

7. Institute of Electrical and Electronics Engineers, IEEE Standard Digital Interface for Programmable Instrumentation (488-1975), 1975

8. Digital Equipment Corporation, IBV11-A LSI-11/Instrument Bus Interface User's Manual, 1977.

9. Thomson, W. T., Theory of Vibration with Applications, Prentice-Hall, Inc., 1981.

10. Merkli, P. E., "Pressure Recovery in Rectangular Constant Area Supersonic Diffusers," AIAA Journal Vol. 14, No. 2, p. 168-172, September 1974.

11. Bevilaqua, P. M. and Combs, C. P., Theory and Practice of Ejector Scaling, Paper at Ejector Workshop for Aerospace Applications, Dayton, Ohio, August, 1981.

12. Welch, D. R., Hot Flow Testing of Multiple Nozzle Exhaust Eductor Systems, Engineer's Thesis, Naval Postgraduate School, September, 1978.

INITIAL DISTRIBUTION LIST

		No. Copies
1.	Defense Technical Information Center Cameron Station Alexandria, Virginia 22314	2
2.	Library, Code 0142 Naval Postgraduate School Monterey, California 93943	2
3.	Department Chairman, Code 69 Department of Mechanical Engineering Naval Postgraduate School Monterey, California 93943	1
4.	Professor Paul F. Pucci, Code 69Pc Department of Mechanical Engineering Naval Postgraduate School Monterey, California 93943	2
5.	Associate Professor R. P. Schreeve, Code 67Sf Department of Aeronautics Naval Postgraduate School Monterey, California 93943	1
6.	Mr. J. E. Hammer, Code 67 Department of Aeronautics Naval Postgraduate School Monterey, California 93943	1
7.	Commanding Officer Attention: Mr. Vito Truglio Naval Air Propulsion Center Trenton, New Jersey 08628	3
8.	CDR J. W. Molloy, USN 1253 Elm Road Baltimore, Maryland 21412	1
9.	LCDR T. H. Walsh, USCG 1908 Carriage Drive Walnut Creek, California 94598	2

END

FILMED

12-83

DTIC